A dissertation entitled

IONIC INTERACTIONS OF FATTY ACID MONOLAYERS AT THE AIR/WATER INTERFACE

submitted to the Graduate School of the
University of Wisconsin-Madison
in partial fulfillment of the requirements for the
degree of Doctor of Philosophy

by

Mehran Yazdanian

Degree to be awarded: December 19___ May 19___ August 19 90

Approved by Dissertation Readers:

George Zografi
Major Professor

July 6, 1990
Date of Examination

Dean, Graduate School

IONIC INTERACTIONS OF FATTY ACID MONOLAYERS AT THE AIR/WATER INTERFACE

by

MEHRAN YAZDANIAN

A thesis submitted in partial fulfillment of
the requirements for the degree of

Doctor of Philosophy
(Pharmacy)

at the
UNIVERSITY OF WISCONSIN-MADISON
1990

IONIC INTERACTIONS OF FATTY ACID MONOLAYERS AT THE AIR/WATER INTERFACE

Mehran Yazdanian
Under the supervision of Professor George Zografi
at the University of Wisconsin-Madison

The focus of this study is on the role played by divalent cations in determining various properties of fatty acids spread as monolayers at the air/water interface, and the possible implications of such properties for their role in the formation of Langmuir-Blodgett (LB) films. The fatty acids studied were saturated fatty acids of various chain length with particular emphasis on stearic acid. The thermodynamic, electrical, and optical properties of these monolayer were measured in terms of surface pressure, Π, surface potential, ΔV, and ellipsometric phase angle, $\delta\Delta$, respectively, over the pH range of 2.0-6.0, where these films exhibit sufficient stability over longer periods of time, and where significant changes in the degree of ionization of the fatty acids occur. The effects of two groups of cations, Mg^{2+}, Ca^{2+}, Ba^{2+}, and Co^{2+}, Cd^{2+}, Pb^{2+}, as a function of pH, cation concentration, and types of anionic counter-ions have been studied. The major effect of these ions within each group follow their states of hydration and their general chemical reactivity. Surface potential measurements at constant area occupied per molecule reveal particularly interesting results, wherein, Co^{2+}, Cd^{2+}, and Pb^{2+}, in increasing order, cause the surface potential to become significantly negative, and Mg^{2+}, Ca^{2+}, and Ba^{2+}, in increasing order, cause the surface potential to become more positive. In both groups, differences in

concentration dependence and in apparent saturation level with increasing concentration are noted.

Ellipsometric phase angle, $\delta\Delta$, was found to be linearly dependent on hydrocarbon chain length, whereas the magnitude of $\delta\Delta$ was found to reflect changes in the refractive index of the fatty acid carboxyl group caused by association with divalent ions. The order of such effects was shown to be $Pb^{2+}>Cd^{2+}>Co^{2+}\approx Ba^{2+}\approx Ca^{2+}\approx Mg^{2+}\approx Na^{+}$ at pH 6.0. In the case of Cd^{2+} and Pb^{2+} significant changes in $\delta\Delta$ with respect to pH and concentration were also observed, in good agreement with ΔV measurements. Moreover, for these ions significant effects on ΔV due to the presence of some anionic counter-ions have been observed. These results have been analyzed and interpreted in the context of earlier suggested models for divalent cation effects on LB film formation, whereby some cations appear to interact with two fatty acids while others exhibit a 1:1 stoichiometry.

The electrocapillary wave diffraction technique was used for the first time to investigate the rheological properties of stearic acid monolayers in the presence of various divalent ions. Rheological parameters of the fatty acid monolayer were shown to depend on the type of the metal ion and the pH of the subphase solution. Cd^{2+} and Pb^{2+} showed the most extreme effects on the surface elasticity and surface viscosity of stearic acid monolayers relative to the other metal ions including Na^{+}.

APPROVED

George Zografi

George Zografi
Professor

Date July 6, 1990

TO MY PARENTS

ACKNOWLEDGEMENTS

I am grateful for the scientific insight and pedagogical guidance provided by Prof. George Zografi for completion of this thesis. I express my gratitude for the support provided by Prof. Hyuk Yu. I am grateful to Dr. Mahn Won Kim for the use of the ellipsometry apparatus and helpful discussions. I thank Prof. Kenneth Connors for his guidance in stability constant computations. I am indebted to Randy Skarlupka for assistance in the ECWD measurements.

I express my sincere appreciation to all the fellow students in both Zografi and Yu groups for their help and assistance in completion of this project, in particular, to Jayne Hastedt for assistance in the SYSTAT calculations.

Acknowledgement is made to the donors of the Petroleum Research Fund, administered by the American Chemical Society for support of this research.

Finally I thank my companion for the past few years, Karen Mangasarian, for making this experience bearable.

TABLE OF CONTENTS

Page

TITLE PAGE i

ABSTRACT ii

DEDICATION iv

ACKNOWLEDGEMENTS v

TABLE OF CONTENTS vi

LIST OF FIGURES ix

LIST OF TABLES xv

INTRODUCTION 1

Historical Background and Development 1

Langmuir-Blodgett Films 4

Insoluble Monolayers 7

Scope 7

Surface Pressure 9

Surface Potential 11

Effect of pH on Fatty Acid Monolayers 14

Metal Ion-Fatty Acid Interactions 17

Surface Ellipsometry 20

Rheological Properties of Monolayers 24

Background 24

The Measurement of Dynamic Rheological Parameters 27

Rheological Measurements of Fatty Acids 31

STATEMENT OF THE PROBLEM 34

EXPERIMENTAL

Materials....36

Preparation of Solutions....37

Methods....38

Measurement of Surface Pressure....38

Measurement of Surface Potential....39

Surface Ellipsometry Measurement....40

Stability Constant Determination from Potentiometric Titrations....44

Measurement of Viscoelasticity....45

Appararus....45

The Generation of Capillary Waves....47

RESULTS....54

Measurements of Surface Pressure....54

The Effect of pH....54

The Effect of Divalent Ion Concentration....59

The Effect of Anionic Counter-ions....59

The Effect of Polyamines....65

Studies with Arachidic Acid....65

Measurements of Surface Potential....72

The Determination of pK_a....72

Estimation of the Degree of Ionization....74

The Effect of pH....74

The Effect of Divalent Ion Concentration....84

The Effect of Anionic Counter-ions....84

The Effect of Polyamines 84

Studies with Arachidic Acid 87

Surface Ellipsometry Measurements 87

Calibration and the Effect of pH 87

The Effect of Divalent Ion Concentration 97

The Effect of Sodium Chloride Concentration 97

The Effect of Anionic Counter-ions 103

Potentiometric Titration 105

Stability Constant Computations 106

Measurements of Rheological Properties 119

The Effect of pH 124

The Effect of Divalent Cations 124

pH Dependence in the Presence of Pb^{2+} 137

The Dependence of ε_l *and* $\omega\kappa$ *on frequency* 137

Static Elasticity 142

DISCUSSION 147

Surface Pressure, Surface Potential, and Surface Ellipsometry ... 147

Rheological Measurements 156

CONCLUSIONS 166

REFERENCES 169

LIST OF FIGURES

Figure	Title	Page
1	The formation of Langmuir-Blodgett films.	5-6
2	Structure of stearic acid and its schematic orientation at the air/water interface.	8
3	Surface pressure vs. area phase diagram.	10
4	The three layer capacitor model for monolayers at the air/water interface.	12
5	Schematic representation of the reflection of polarized light from monolayer covered surface treated as consisting of three distinct layers.	22
6	Possible motions of the molecules in a monolayer at the interface.	25-26
7	Block diagram of ellipsometry instrument.	41-42
8	A block diagram of the instrument setup for the electro-capillary wave diffraction measurement.	46
9	A schematic diagram of the process used to generate and detect capillary waves.	48
10	Plot of phase difference vs. radial distance x from the needle tip.	52
11	Plot of wave amplitude vs. radial distance x from the needle tip.	53
12	Π-A isotherms of stearic acid in the presence of 0.01M NaCl at pH 2.0 to 6.0.	55
13	Π-A isotherms of stearic acid in the presence of 0.01M NaCl and 1mM divalent cations, μ=0.01M and pH 5.0.	56
14	Π-A isotherms of stearic acid in the presence of 0.01M	

NaCl and 1mM divalent cations, μ=0.01M and pH 6.0. 57

15 Π-A isotherms of stearic acid in the presence of 1mM $PbCl_2$, μ=0.01M and various pH values. 58

16 Π-A isotherms of stearic acid in the presence of 1mM $CdCl_2$, μ=0.01M and various pH values. 60

17 Π-A isotherms of stearic acid in the presence of various $CaCl_2$ concentrations, μ=0.01M and pH 6.0....61

18 Π-A isotherms of stearic acid in the presence of various $CoCl_2$ concentrations, μ=0.01M and pH 6.0. 62

19 Π-A isotherms of stearic acid in the presence of various $CdCl_2$ concentrations, μ=0.01M and pH 6.0. 63

20 Π-A isotherms of stearic acid in the presence of various $PbCl_2$ concentrations, μ=0.01M and pH 6.0....64

21 Π-A isotherms of stearic acid in the presence of various 0.01M sodium salts of various counter-ions at pH 6.0....66

22 Π-A isotherms of stearic acid in the presence of 1mM salts of cadmium, μ=0.01M and pH 6.0. 67

23 Π-A isotherms of stearic acid in the presence of 1mM salts of barium, μ=0.01M and pH 6.0....68

24 Π-A isotherms of stearic acid in the presence of 1mM spermine and spermidine, μ=0.01M and pH 6.0 in comparison with 0.01M NaCl. 69

25 Π-A isotherms of arachidic acid in the presence of 0.01M NaCl at pH 2.0 to 6.0. 70

26 Π-A isotherms of arachidic acid in the presence of 0.01M NaCl and 1mM $BaCl_2$ and $CdCl_2$ concentrations, μ=0.01M and pH 6.0. 71

27 Surface potential vs. pH for stearic acid at 20$Å^2$/molecule and 25° C....75

28 Curve fitting of ΔV vs. pH for stearic and arachidic acids in the range of pH 2.0 to 6.0 with fourth and third order polynomials respectively. 77

29 Plot of change of pK_a^s with α for stearic acid. 78

30 Plot of change of pK_a^s with α for arachidic acid. 79

31 Simulation of α vs. pH(subphase) using Gouy-Chapman equations assuming pK_a^s=5.4 at T=25° C, C=0.01M, z=1, and different A (area occupied per molecule). 80

32 Simulation of α vs. pH(subphase) using Gouy-Chapman equations assuming pK_a^s=5.4 at T=25° C, z=2, A= 20Å^2/molecule, and various concentration of ions.....81

33 Simulation of α vs. pH(subphase) using Gouy-Chapman equations assuming pK_a^s=5.4 at A=20Å^2/molecule, T=25° C, and 0.001M univalent (M+) and divalent(M++) ions. 82

34 Concentration dependence of surface potential of stearic acid monolayers at 20Å^2/molecule, 25° C, and pH 6.0.....85

35 The chain length dependence of $\delta\Delta$, (ϕ_o=64.1±0.1°). 89

36 The chain length dependence of $\delta\Delta$, (ϕ_o=61.8±0.1°). 90

37 The pH dependence of $\delta\Delta$ in the presence of 1mM $PbCl_2$ and $CdCl_2$, μ=0.01M, and ϕ_o=61.8±0.1°. 94

38 Π-A isotherm of stearic acid in the presence of 1mM $PbCl_2$, μ=0.01M, at pH 2.0 to 6.0, measured by the horizontal float method. 95-96

39 The concentration dependence of $\delta\Delta$ in the presence of $PbCl_2$ at pH 6.0, μ=0.01M, and ϕ_o=61.8±0.1° 98

40 Π-A isotherm of stearic acid in the presence of various $PbCl_2$ concentrations, μ=0.01M, at pH 6.0, measured by the horizontal float method.....99-100

41 Titration of 0.1M acetic acid with 0.1M NaOH in the presence of 0.03M NaCl and 0.01M $BaCl_2$, $CdCl_2$, and $PbCl_2$ at μ=0.03M. 107

42 Enlarged portion of the early section of the titration curve of 0.1M acetic acid with 0.1M NaOH in the presence of 0.03M NaCl and 0.01M $BaCl_2$, $CdCl_2$, and $PbCl_2$ at μ=0.03M. 108

43 Titration of 0.1M acetic acid with 0.1M NaOH in the presence of 0.03M NaCl and 0.1M $BaCl_2$ and $CdCl_2$ at μ=0.03M. 109

44 Enlarged portion of the early section of the titration curve of 0.1M acetic acid with 0.1M NaOH in the presence of 0.03M NaCl and 0.1M $BaCl_2$ and $CdCl_2$, at μ=0.03M...110

45 Titration of 0.1M acetic acid with 0.1M NaOH in the absence and presence of various concentrations of $CdCl_2$. 111

46 Enlarged portion of the early section of the titration curve of 0.1M acetic acid with 0.1M NaOH in the absence and presence of various concentrations of $CdCl_2$. 112

47 The linear plot from equation 64 for the calculation of the stability constants in the presence of 0.01M $CdCl_2$. 116

48 The linear plot from equation 64 for the calculation of the stability constants in the presence of 0.01M $PbCl_2$. 117

49 Surface elasticity vs. frequency for stearic acid in the presence of 0.01M HCl at pH 2.0 and different areas occupied per molecule. 121

50 Surface viscosity vs. frequency for stearic acid in the presence of 0.01M HCl at pH 2.0 and different areas occupied per molecule. 122

51 Viscous loss modulus vs. frequency for stearic acid in the

presence of 0.01M HCl at pH 2.0 and different areas occupied per molecule. 123

52 Surface elasticity vs. frequency for stearic acid in the presence of 0.01M HCl at pH 2.0 and 0.01M NaCl at pH 6.0 at 20.5Å^2/molecule. 125

53 Surface viscosity vs. frequency for stearic acid in the presence of 0.01M HCl at pH 2.0 and 0.01M NaCl at pH 6.0 at 20.5Å^2/molecule. 126

54 Viscous loss modulus vs. frequency for stearic acid in the presence of 0.01M HCl at pH 2.0 and 0.01M NaCl at pH 6.0 at 20.5Å^2/molecule. 127

55 Surface elasticity vs. frequency for stearic acid in the presence of 1mM chloride salts of magnesium, calcium, and barium relative to that of 0.01M sodium chloride at pH 6.0 and μ=0.01M. 128

56 Surface viscosity vs. frequency for stearic acid in the presence of 1mM chloride salts of magnesium, calcium, and barium relative to that of 0.01M sodium chloride at pH 6.0 and μ=0.01M. 129

57 Viscous loss modulus vs. frequency for stearic acid in the presence of 1mM chloride salts of magnesium, calcium, and barium relative to that of 0.01M sodium chloride at pH 6.0 and μ=0.01M. 130

58 Surface elasticity vs. frequency for stearic acid in the presence of 1mM chloride salts of cobalt and cadmium relative to that of 0.01M sodium chloride at pH 6.0 and μ=0.01M. 131

59 Surface viscosity vs. frequency for stearic acid in the presence of 1mM chloride salts of cobalt and cadmium relative to that of 0.01M sodium chloride at pH 6.0 and μ=0.01M. 132

60 Viscous loss modulus vs. frequency for stearic acid in the presence of 1mM chloride salts of cobalt and cadmium relative to that of 0.01M sodium chloride at pH 6.0 and μ=0.01M. 133

61 Surface elasticity vs. frequency for stearic acid in the presence of 1mM chloride salts of all divalent ions relative to that of 0.01M sodium chloride at pH 6.0 and μ=0.01M. 134

62 Surface viscosity vs. frequency for stearic acid in the presence of 1mM chloride salts of all divalent ions relative to that of 0.01M sodium chloride at pH 6.0 and μ=0.01M. 135

63 Viscous loss modulus vs. frequency for stearic acid in the presence of 1mM chloride salts of all divalent ions relative to that of 0.01M sodium chloride at pH 6.0 and μ=0.01M. 136

64 Surface elasticity vs. frequency for stearic acid in the presence of 1mM lead chloride at pH 6.0 and μ=0.01M. ...138

65 Surface viscosity vs. frequency for stearic acid in the presence of 1mM lead chloride at pH 6.0 and μ=0.01M. ...139

66 Viscous loss modulus vs. frequency for stearic acid in the presence of 1mM lead chloride at pH 6.0 and μ=0.01M. ...140

67 Lead concentration dependence of δΔ and ΔV, at pH 6.0 and μ=0.01M. 154

68 Loss tangent vs. frequency for stearic acid in the presence of sodium and alkaline earth metals at pH 6.0 and μ=0.01M. 158

69 Loss tangent vs. frequency for stearic acid in the presence of Na^+, Co^{2+}, Cd^{2+}, and Pb^{2+} at pH 6.0 and μ=0.01M...160

70 Loss tangent vs. frequency for stearic acid in the presence of 1mM PbCl2, μ=0.01M, at various pH values.....162

LIST OF TABLES

Table	Title	Page
I	Surface potential as a function of pH at 20Å^2/molecule and μ=0.01M.	76
II	Surface potential as a function of pH at 20Å^2/molecule, 1mM divalent cation, and μ=0.01M.	83
III	Effect of anionic counter-ions on the surface potential of fatty acids at pH 6.0, 20Å^2/molecule, and μ=0.01M.	86
IV	Phase angle ($\delta\Delta$) of stearic acid in the presence of 0.01M NaCl and 1mM divalent cations at pH 6.0, μ=0.01M, and ϕ_o=61.8±0.1°.	93
V	Phase angle ($\delta\Delta$) of stearic acid in the presence of varying concentrations of $CdCl_2$, at pH 5.5±0.2, and ϕ_o=64.1±0.1°.	101
VI	Phase angle ($\delta\Delta$) of stearic acid in the presence of varying concentrations of NaCl at pH 6.0, μ=0.01M, and ϕ_o=61.8±0.1°.	102
VII	Phase angle ($\delta\Delta$) of stearic acid in the presence of various cations and anionic counter-ions at pH 6.0, μ=0.01M, and ϕ_o=61.8±0.1°.	104
VIII	The change in pK_a and pK_a' of acetic acid with change in the type and concentration of salt solutions.	113
IX	The stability constants of acetic acid, K_1 and K_2, with 0.01M $CdCl_2$ and $PbCl_2$ calculated by the least square linear fit and nonlinear regression.	118
X	ε_{st} and ε^0 in the presence of various metal ions at different pH values.	145
XI	The surface shear viscosity, η_s, values measured by	

different experimental methods in comparison to k from ECWD. 146

XII Number of Pb^{2+} ions in the subphase at different concentration relative to the number of stearic acid molecules ($1.660x10^{17}$) spread at 20$Å^2$/molecule 153

XIII Loss tangent values as a function of frequency for stearic acid in the presence of sodium and alkaline earth metals at pH 6.0 and μ=0.01M.....159

XIV Loss tangent values as a function of frequency for stearic acid in the presence of Na^+, Co^{2+}, Cd^{2+}, and Pb^{2+} at pH 6.0 and μ=0.01M. 161

XV Loss tangent values as a function of frequency for stearic acid in the presence of 1mM $PbCl_2$, μ=0.01M, at various pH values. 163

INTRODUCTION

This study is focused on the role played by divalent cations in determining various properties of long chain fatty acids, spread as monolayers at the air/water interface, i.e. thermodynamic state, electrical, optical, and rheological, and the possible implications of such properties for the formation of Langmuir-Blodgett films. Therefore, background information followed by detailed descriptions of both Langmuir-Blodgett films and spread monolayers is provided.

Historical Background and Development

The earliest account on the behaviour of oil spread on water can be found in the writings of the Babylonians in the eighteenth century BC (Tabor, 1980). The first scientific report on the calming effect of oil on surface waves was written by Benjamin Franklin (Franklin, 1774). The reduction in the surface tension of water by a spread oil film was first observed by Lord Rayleigh (Lord Rayleigh, 1890). Modern monolayer studies were pioneered by Agnes Pockels in the late nineteenth century (Pockels, 1891, Giles and Forrester, 1971), with her many inventions that today have become standard tools and techniques in the monolayer field. These include the design of a trough equipped with a barrier to control the area of the spread film and the use of volatile solvents to help spreading and quantifying the amount of insoluble material per unit area on the surface. Using Pockels' methods, Lord Rayleigh proposed that spread films of castor oil were monomolecular and consisted of rigid spherical molecules

(Lord Rayleigh, 1899). Hardy showed that only polar compounds spread on water and postulated that these molecules are oriented at the interface (Hardy, 1912, 1913). Devaux and Marcelin used simple experimental methods to demonstrate the existence of monomolecular films (Devaux, 1913, Marcelin, 1914). In 1917, Langmuir and Harkins independently provided experimental support for the ideas of molecular orientation at the surfaces and recognized that monolayer films are formed due to the amphiphilic nature of the molecules (Langmuir, 1917, Harkins, 1917). Langmuir developed a more elaborate film balance and trough which enabled him to analyze monolayer properties more quantitatively in terms of molecular structure and arrangement. For example, he demonstrated that at closest packing fatty acids occupy the same cross sectional area regardless of their chain lengths (Langmuir, 1917). Moreover, in fatty acid monolayers at the air/water interface, he showed that the arrangement and orientations of molecules were related to their hydrophilic and hydrophobic characters.

Langmuir reported the transfer of fatty acid molecules spread at the air/water interface as monolayers onto solid substrates as early as 1920 (Langmuir, 1920). Several years later Blodgett refined the technique (Blodgett, 1934) and showed that the presence of small concentrations of divalent cations permitted the sequential transfer of monolayers from alkaline subphases onto solid substrates, such as glass or metal plates, as multilayers (Blodgett, 1935). These built-up assemblies of monolayers are now commonly referred to as Langmuir-Blodgett (LB) films. A summary

of the pioneering experiments of Langmuir and Blodgett on LB films of a wide variety of compounds is given by Gaines (Gaines, 1983).

The initial interest in LB films, as seen by Langmuir and Blodgett, was in the use of reflected interference colours from stepped multilayers as a basis for gauging thicknesses and possible applications as anti-reflection coatings. In the 1960s, the construction of precise macromolecular structures from monolayers and successful experiments on the optical properties of monolayer assemblies and energy transfer in multilayers gave a new impetus to the study of LB films (Drexhage et al., 1963, Kuhn, 1968, 1972). Hence, it became conceivable that the Langmuir and Blodgett method of multilayer formation could afford a multitude of variants and a specific chemistry which in turn would allow the building and *in situ* modification of molecular assemblies to give them the required properties. The recent resurgence of activity in the field of monolayers and LB films is based mainly on this promise, and the suggestion of possible applications of organic thin films in sensors, electrical devices, and as models for mimicking the structure and function of biological membranes (Barraud et al., 1980, Roberts, 1983, Swalen, 1987, Barraud, 1988, Kuhn, 1989). Recently, the fabrication of single layers of inorganic semiconductors (Ruaudel-Teixeir et al., 1986) and glucose-sensing ultra thin membranes (Okahata et al., 1988) have been reported as pioneering examples of such applications.

The future of LB film research lies in the use of model systems in chemistry and physics in order to investigate processes which depend on the exact molecular structure and architecture. This in turn can be used for

the development of sensing and information-processing devices, inspired by biological systems, and modeling of biological functions for better understanding of biological processes.

Langmuir-Blodgett Films

Langmuir-Blodgett (LB) films are highly ordered arrays of surface active compounds extending out as multimolecular layers on solid substrates. The formation of LB films is illustrated in Figure 1. When a solid substrate is raised through a fatty acid film, the molecules adhere to the plate and orient with their hydrocarbon portions stretched outwards. Consequently, the surface of such a film-coated plate becomes very hydrophobic and a second layer can be deposited back-to-back upon dipping the plate back into the film-covered surface. Successive dipping in and out of the monolayer-covered liquid, at a constant rate, temperature, and surface pressure, results in deposition of as many as three hundred layers onto the plate, as measured by means of interference fringes (Blodgett, 1934, 1935).

A very crucial step in the deposition of LB films onto solids is insuring the stability and homogeneity of the monolayer at the air-water interface (Gaines, 1980, Mingins, 1987, Pethica, 1987). Much of the early work on the stability of fatty acid monolayers in the presence of counterions was carried out with metals such as barium, cadmium, and calcium (Blodgett, 1935, Langmuir and Blodgett, 1937, Langmuir and Schaefer, 1936, 1937, Myers and Harkins , 1937). The addition of these divalent cations to the subphase appears to increase both shear resistance and cohesion of the monolayer.

Figure 1. The formation of Langmuir-Blodgett films. Multilayers are formed on a solid substrate by successive folding back and forth of a monolayer.

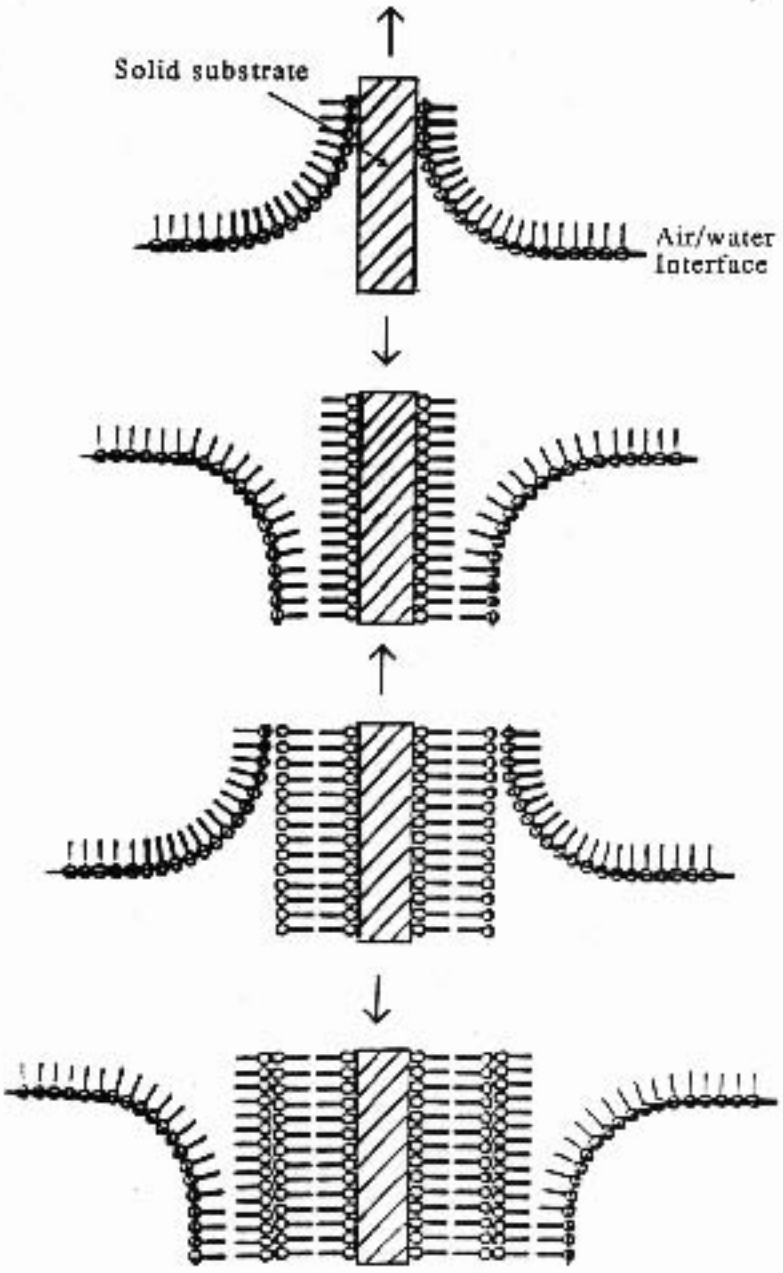
Solid substrate
Air/water
Interface

and to facilitate its transfer to form multilayers. The subphase pH value which determines the extent of ionization of the monolayer, along with the type and the amount of cations present in the subphase are the three most significant factors determining the stability of the monolayer and hence LB films. This stability also depends on other factors, including temperature, nature of the buffers used, presence of other ions and impurities, and the chain length of the fatty acid.

Insoluble Monolayers

Scope

Long-chain fatty acids, fatty acid derivatives, proteins, and many natural or synthetic polymers exhibiting amphiphilic structures, can be spread on aqueous surfaces to form monolayers. They tend to minimize free energy by orienting at the air/liquid interface with their hydrophobic portions directed toward the air and their polar functional groups immersed in the subphase. The structure of stearic acid, a long chain saturated fatty acid, is shown in Figure 2. The extensive studies of these amphiphilic compounds have been directed at measurement of shapes and packing of molecules, intermolecular interactions and forces, and phase behaviour (Cheesman, 1954, Dervichian, 1958, Berejich, 1964, Gaines, 1966, Adamson, 1982, Vold and Vold, 1983, Hiemenz, 1986). They have provided the basis for the understanding of many biological problems such as membrane structure and function, various orientational dependent phenomena such as micelle formation, stability of emulsions and foams in pharmaceutical systems, and the stability of LB films.

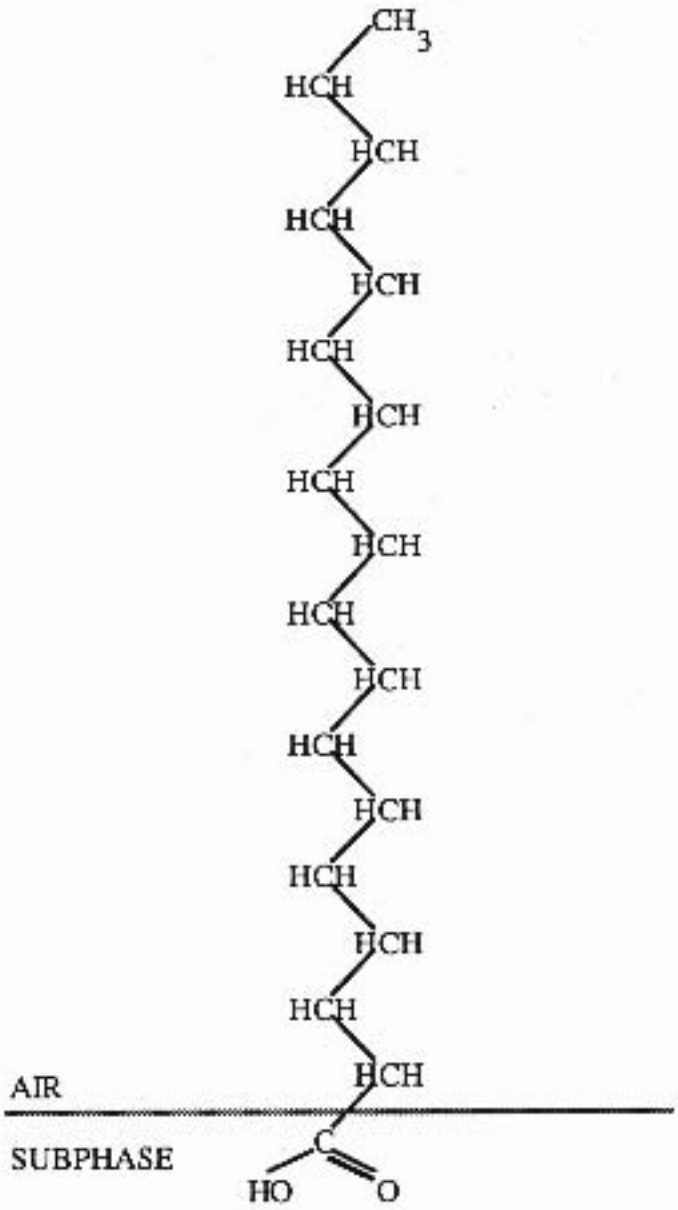

Figure 2. Structure of stearic acid and its schematic orientation at the air/water interface.

Surface Pressure

The major feature of the monolayer technique is that film forming materials can be placed on the surface as a single molecular layer and be brought to any surface concentration, Γ, i.e. number of molecules per unit area, up to the closest packing of the molecules (the collapse point). The difference between the surface tension of the clean surface, γ_0, and that of the monolayer-covered surface, γ, gives rise to a two-dimensional surface pressure, Π, where:

$$\Pi = \gamma_0 - \gamma \qquad (1)$$

From the relationship between the surface pressure, Π, and the area, A, (where A is the reciprocal of the surface concentration) occupied on the liquid surface by the molecules of the film a two-dimensional pressure-area (Π-A) phase diagram can be constructed in a manner analogous to a three-dimensional pressure-volume (P-V) phase diagram (Figure 3). After being spread, the molecules of a monomolecular film can be compressed and caused to undergo a number of phase transformations. These different phases can be considered to be two dimensional analogues of gases, liquids, and solids. They reflect different degrees of order or freedom resulting from intermolecular forces in the monolayer and between the monolayer and the underlying solution. Detailed discussions of the nature of such surface phases and phase equilibria of monolayers in general have been reported (Gaines, 1966).

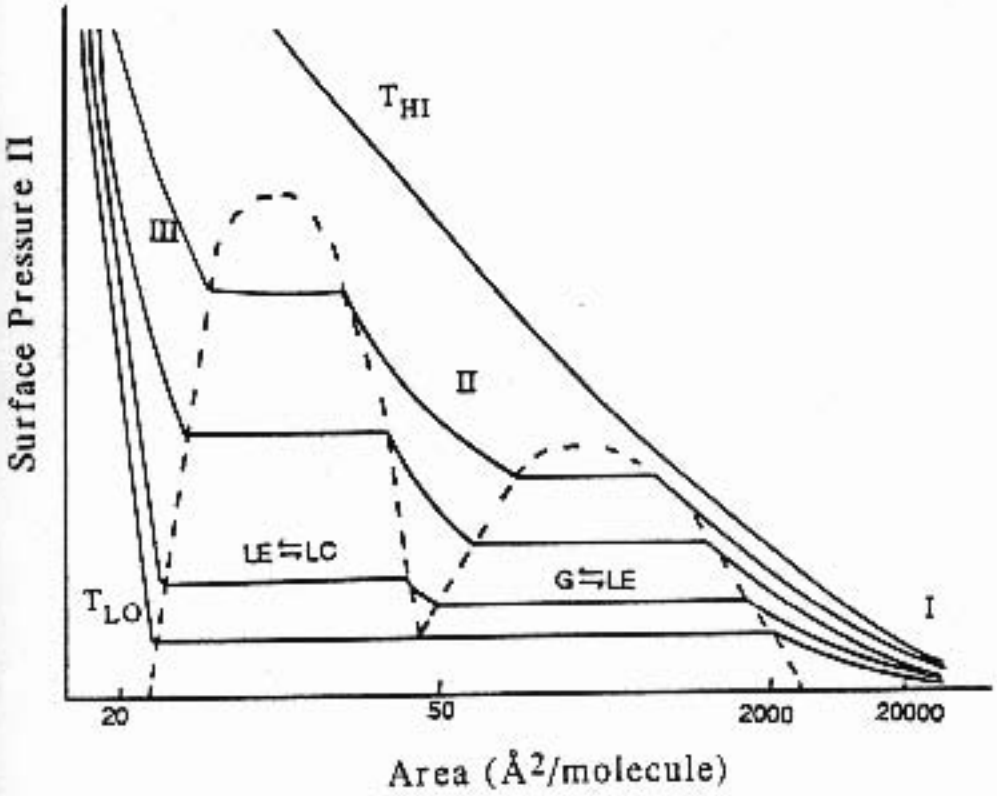

Figure 3. Surface pressure vs. area phase diagram. The scale is nonlinear in area. The single phase regions are I. gaseous (G), II. liquid expanded (LE), and III. liquid condensed (LC). The coexistence regions are indicated by dashed lines. T_{HI} and T_{LO} indicate high and low temperatures respectively.

Surface Potential

Amphiphilic molecules when spread at the air/water interface, orient with the hydrophilic end toward the water and the hydrophobic end away from it. The monolayer can then be treated as a uniform assembly of molecular dipoles, which results in the polarization of the layer. The potential difference commonly called surface potential, ΔV, results from the component of polarization, P_n, normal to the plane of the film. P_n can be defined in terms of dipole moment per unit volume by analogy with a parallel-plate capacitor as (Oliveira et al., 1989)

$$P_n=\varepsilon\varepsilon_o\Delta V/d=\mu/Ad \qquad (2)$$

where ε is the permittivity of the monolayer, ε_o is the permittivity in vacuum, A is the area per molecule, d is the thickness of the film, and μ is an overall effective surface dipole moment normal to the interface. Equation 2 yields the Helmholtz equation for the surface potential of an unionized monolayer (Schulman and Hughes, 1932)

$$\Delta V=\mu/\varepsilon\varepsilon_o\ A. \qquad (3)$$

Davies made improvements to the Helmholtz equation by considering the monolayer as a three layer capacitor where the dipole moments of each layer contribute to ΔV (Davies, 1963). The presence of a monolayer at the interface results in the polarization of water molecules and this is represented by the dipole moment μ_3 in the aqueous subphase layer (Figure 4). The polar head group and hydrophobic tail of the molecule constitute the other layers and are represented by dipole moments μ_2 and

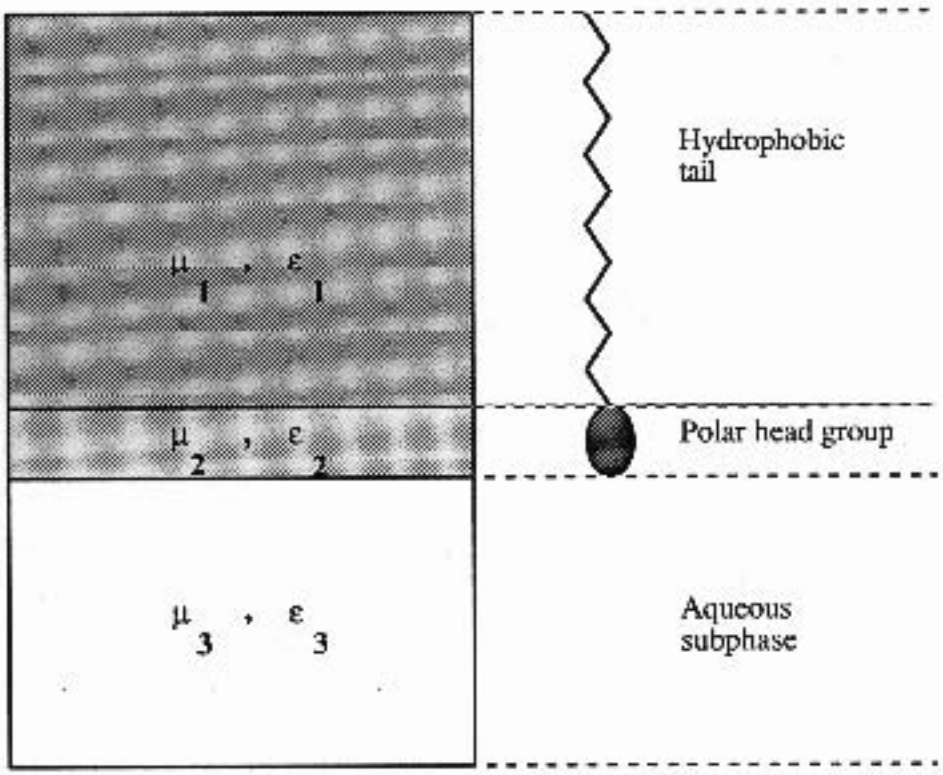

Figure 4. The three layer capacitor model for monolayers at the air/water interface. The local permittivity of each layer determines the extent of the contribution of the dipole moment to the surface potential.

μ_1. Further improvements were made by Demchak and Fort who took into account the different permittivities of the layers (Demchak and Fort, 1974). Equation 3 can then be rewritten as

$$\Delta V=(\mu_1/\varepsilon_1+\mu_2/\varepsilon_2+\mu_3/\varepsilon_3)/\varepsilon_o\ A \qquad (4)$$

where ε_1, ε_2, and ε_3 are the permittivities of the hydrophobic, hydrophilic, and aqueous layers respectively. Moreover, for ionized monolayers the term ΔV includes the electrostatic potential ψ_0 of the Gouy-Chapman electrical double layer such that

$$\Delta V=(\mu_1/\varepsilon_1+\mu_2/\varepsilon_2+\mu_3/\varepsilon_3)/\varepsilon_o\ A + \psi_o. \qquad (5)$$

The simplest method of assigning the contribution of dipole moments and electrostatic potential to the surface potential for ionizable monolayers, however, as suggested by Vogel and Möbius, appears to be dividing μ into two parts, μ_α and μ^ω, in the Helmholtz equation (Vogel and Möbius, 1989)

$$\Delta V=\mu_\alpha + \mu^\omega \qquad (6)$$

Here, μ_α represents the contribution of dipole charges caused by the intrinsic dipole moment of the polar group, the reorientation of water dipoles at the interface, and the presence of any ionized groups at the interface. The term μ^ω is defined as the apparent dipole moment due to the hydrophobic part of the monolayer, including that of the terminal CH_3 groups.

Effect of pH on Fatty Acid Monolayers

For long-chain fatty acids the intermolecular forces in a monolayer can be divided into two parts; the attraction or repulsion between polar head-groups, and the van der Waals interaction between the hydrocarbon chains. Ionization of a fatty acid monolayer generally affects the head group interaction, giving rise to increased repulsive energies and a more expanded monolayer.

Likewise, the extent of ionization of a fatty acid monolayer will affect the degree of metal ion binding to the monolayer and, hence, ultimately the properties of LB films. The degree of ionization of a monolayer is directly related to the bulk pH and the electrical properties of the interface. The potential difference between bulk solution and surface, ψ_o, caused by the ionization of the carboxylic head groups produces a difference in the bulk and surface pH, which leads to an apparent difference in pK_a between the surface and bulk. To account for this difference, the hydrogen ion concentration at the surface can be expressed by a Boltzmann distribution (Gouy, 1910):

$$[H^+]_s=[H^+]_b \exp(-e\psi_o/\underline{k}T) \qquad (7)$$

and hence;

$$pH_s=pH_b+e\psi_o/\underline{k}T \qquad (8)$$

where e stands for charge of an electron, $\underline{k}$ for the Boltzmann constant, T for the absolute temperature, and b and s refer to bulk and surface phases. The exact value of the pH at the surface is unknown, since the value of ψ_0

cannot be directly measured. However, it can be calculated approximately by the Gouy-Chapman equation for the diffuse double layer (Gouy, 1910, Chapman, 1913). The Gouy-Chapman (GC) model is essentially a variation of the Poisson-Boltzmann equation based on the assumption that the surface is made up of uniform single point charges, with charge density σ per cm^2. The model, hence, is a very simple one that relies heavily on the ideality of the system. In real systems, however, the ion size effects, the energies of interaction and polarization of the ions, and the dependence of the dielectric constant on the local field strength must also be taken into consideration (Bolt, 1955, Davies, 1963, Gaines, 1966, Levine and Outhwaite, 1977). Variations of the GC theory, made by appending new expressions via elaborate mathematical means to account for the shortcomings of the theory have been proven to be less than successful (For example see, Grahame, 1950, Bolt, 1955, Blum, 1977, Henderson and Blum, 1978, Torrie and Valleau, 1979, Carnie et al. 1981). Most intriguing, however, is the fact that all these investigations more or less share a common conclusion that for dilute electrolyte concentrations (<0.1M) and low surface charge densities (<0.2 C m^{-2}) the GC model is a very "reasonable" and adequate model for characterization of charged surfaces.

In the GC model ψ_o is given by (Gouy, 1910, Vewey and Overbeek, 1948)

$$\psi_o=(-2zkT/e)\ \sinh^{-1}\{\sigma/C^{1/2}(500\pi/DRT)^{1/2}\} \qquad (9)$$

In this equation z is the valence of an electrolyte, σ is the charge density (per cm^2), C is the concentration of electrolytes (molar), D is the dielectric

constant for water (78 at 25° C), and R is the gas constant. At 25° C, equation 9 simplifies to

$$\psi_o=(-2zkT/e)\ \sinh^{-1}(136\alpha/AC^{1/2}) \qquad (10)$$

where α is the degree of ionization and A is the area ($Å^2$/molecule).

If the intrinsic acidity constant at the surface for the acid HA is defined as

$$K_a^s=[H^+]_s[A^-]_s/[HA]_s \qquad (11)$$

and the apparent acidity constant as

$$K_{app}^s=[H^+]_b[A^-]_s/[HA]_s \qquad (12)$$

then using equation 8,

$$pK_a^s=pK_{app}^s+e\psi_o/kT \qquad (13)$$

where pK_a^s and pK_{app}^s are the intrinsic and the apparent pK_a values of the fatty acid at the surface.

On the basis of the Gouy-Chapman model and surface potential measurements as a function of pH, thus accounting for ψ_o, some investigators have found intrinsic pK_a values in the range of 5.0-5.6 (Betts and Pethica, 1956, Bagg et al., 1966, Buhaenko et al., 1988, Grundy et al., 1988), which is close to 4.8, the value of the pK_a for fatty acids dissolved in water (bulk). The shift in the pK_a relative to that in the bulk phase has been attributed to the differences between the heat of hydration of the fatty acid in bulk solution and at an interface (Betts and Pethica, 1956).

The presence of divalent cations in the subphase appears to decrease the difference between pK_a^s and pK_{app}^s . For example, Bagg et. al. (Bagg et al., 1964), reported a pK_{app}^s of 6.0 by infrared spectroscopy of skimmed monolayers and Matsubara et al. (Matsubara et al., 1964) reported a pK_{app}^s of about 6.4 by a radiotracer method (non-invasive) for stearic acid films on calcium containing substrates. These values are closer to the pK_a obtained in bulk solution and much lower than pK_{app}^s (in the range of 7.0-9.0) obtained in the absence of these ions (Joos, 1971, Egert-Charlier, 1978). This indicates that ψ_0 is considerably reduced in the presence of divalent cations such as calcium.

Metal Ion-Fatty Acid Interactions

The most critical factors determining the stability and properties of LB films formed from saturated fatty acids such as stearic and arachidic acids are the subphase pH value and the presence of divalent cations (Blodgett 1935, 1937, Langmuir and Schaefer 1936, 1937, Wolstenholme and Schulman, 1950, Spink and Sanders, 1955, Ellis and Pauley, 1963, Vogel et al. 1979b, 1980, Miyano et al. 1982, Shutt and Rickert, 1987, Laxhuber and Möhwald, 1984, Grundy et al., 1988, Petrov et. al., 1982, and Buhaenko et al., 1988, Kobayashi et al., 1988). Divalent metal ions such as Ca^{2+}, Ba^{2+}, Cd^{2+}, or Pb^{2+}, are believed to be important because of their ability to form 1:2 "disoaps" with ionized fatty acid, and indeed, a stoichiometry of one metal ion to two fatty acid molecules in LB films has been observed.(Blodgett, 1937, Ellis and Pauley, 1963, Petrov et. al., 1982, and Buhaenko et al., 1988, Kjaer et. al, 1989).

Studies with LB films have shown that different divalent ions under the same conditions, however, give films with different structure and properties (Vogel et al., 1979a, 1979b, Hasmonay et al., 1980, Kobayashi et al., 1988, Outka, et al., 1987, Rabe et al. 1988). Vogel et al., 1979b., for example, have shown, using infrared spectroscopy of LB films of stearic acid that the nature of the divalent cation dictates the type of binding with the fatty acid. In their study of barium and lead cations with stearic acid, it was concluded that barium ions interact with two fatty acids in each layer to form "disoaps" by neutralizing the charges on the fatty acids. However, in contrast to other studies, they suggested that the interaction of lead cations with the fatty acid in a multilayer was limited to one fatty acid per layer stabilized by the fatty acid in another layer. Outka et al, 1987 and Rabe et al, 1988, using X-ray spectroscopy with monolayers of calcium and cadmium arachidate transferred to a silicon Si (111) surface, concluded that the hydrocarbon chains of cadmium arachidate were oriented perpendicular to the surface, whereas with calcium arachidate they were tilted by 33°. Moreover, in the absence of metal ions the arachidic acid monolayer was not ordered at all. Furthermore, it was suggested by these authors that the hydrocarbon chain of cadmium arachidate is bonded to the surface via only one oxygen atom, while calcium arachidate is chelated with both oxygens on the surface. Such differences in LB films are not surprising, since differences between metal ions in aqueous solution related to their ionic size, degree of hydration, and Lewis acid/base character do exist (Pearson, 1963, 1967). For example, measurements of the forces acting between mica surfaces covered by

monolayers of docosanedioic acid (dicarboxylic fatty acids) at pH 6.0 have shown a decrease in double layer electrical repulsion and an increase in adhesion forces in the presence of $CdCl_2$ while these parameters remained unchanged in the presence of $CaCl_2$ (Berg and Claesson, 1989). Alkaline earth ions have the electronic configurations of rare gas cores, whereas the ions of cobalt, cadmium, and lead have those involving d and f orbitals, whereby they exhibit propensities for coordination complexing with a substantial covalent character. For example, the tendency to form complexes with polyuronates in aqueous solutions has been shown to be much greater for these ions than that of alkaline earth ions, which form weakly electrostatic bonds (Cesàro et al., 1988, Kohn, 1987).

There is significant evidence available in the literature to suggest that the physical state of the monolayer at the air-water interface is critical in determining the final state of LB films (Gaines, 1980, Pethica, 1987, Mingins and Owens, 1987). Metal ions in the subphase along with the degree of dissociation of fatty acids are expected to affect the nature of molecular packing and arrangement, which can play an important role in determining the resultant shear resistance of the film during transfer. Indeed, studies with fatty acid monolayers and various metal ions in the subphase have shown that, although all divalent ions cause greater condensation of such monolayers, transition metal ions behave very differently from other types of ions, e.g. cadmium ions have been shown to produce more stable and condensed monolayers than do magnesium, calcium, or barium ions (Hasmonay et al, 1980, Gordziel et al., 1982, Laxhuber and Möhwald, 1984, and Shutt and Rickert, 1987). Such differences generally have been attributed to the

differences in Lewis acid/base character, size, and states of hydration of these groups of ions. Based on their work with LB films, Vogel et al., 1980, have suggested that stearic acid as a monolayer at the air-water interface interacts 2:1 with barium ions through electrostatic attraction, whereas lead ions are able to form 1:1 complexes with the fatty acid, while also combining with a second ion from the subphase to complete charge neutralization. More recently, Itaya et al., 1989, have concluded that there exists a one to one interaction between cadmium ions and thiolate groups of octadecanethiol monolayers, whereas barium ions appear to coordinate with two thiolate groups of the same monolayer. However, the possibility of cadmium ions interacting with two ionized carboxylic groups cannot be entirely ruled out. For example, Kjaer et al., 1989, from X-ray studies of arachidic monolayers at the air/water interface, have concluded that through the binding of cadmium, water, and the carboxyl group a 2:1 stoichiometry is possible.

Surface Ellipsometry

Ellipsometry is an extremely sensitive, precise, and non-destructive technique for the analysis of the optical properties of monolayers. It is based on the principle that the monolayer covered surface changes the state of polarization of elliptically polarized light reflected by the interface. A brief summary of the theory underlying the applications of ellipsometry is presented here to provide for later discussions in this thesis.

An elliptically polarized light is "a light wave whose electric vector at fixed point in space traces the same ellipse in a regular repetitive fashion"

(Azzam and Bashara, 1977). The polarization state of this light beam is then characterized by the amplitude ratio of A_p/A_s and the phase difference δ_p-δ_s of the two components of the electric vector, E, parallel (p) and normal (s), to the plane of incidence (Bootsma and Meyer, 1968):

$$E_p=A_p \exp(i\delta_p) \quad \text{and} \quad E_s=A_s \exp(i\delta_s) \qquad (14)$$

The change in the polarization state due to reflection at an interface is defined as (Azzam and Bashara, 1977, de Feijter, 1978)

$$\tan\psi = (A_p^r/A_s^r)/(A_p^i/A_s^i) \qquad (15)$$

and

$$\Delta = (\delta_p^r-\delta_s^r)/(\delta_p^i-\delta_s^i) \qquad (16)$$

where $\tan\psi$ is the change in the amplitude ratio, Δ is the change in the phase difference due to reflection, and r and i denote the properties of the reflected and incident beams. The total effect caused by the reflection of the polarized beam can be written in terms of the overall amplitude reflection coefficients, R_p and R_s, which are related to the amplitude ratio, ψ, and the phase difference, Δ, between the orthogonal p and s electric vectors (Bootsma and Meyer, 1968):

$$R_p/R_s=(E_p^r/E_p^i)/(E_s^r/E_s^i)=\tan\psi \exp(i\Delta) \qquad (17)$$

R_p and R_s depend on the wavelength of light, λ, the angle of incidence, ϕ_0, and the optical properties of the reflecting system. R_p and R_s are given for the case where the surface is regarded as having three distinct layers as depicted in Figure 5, as:

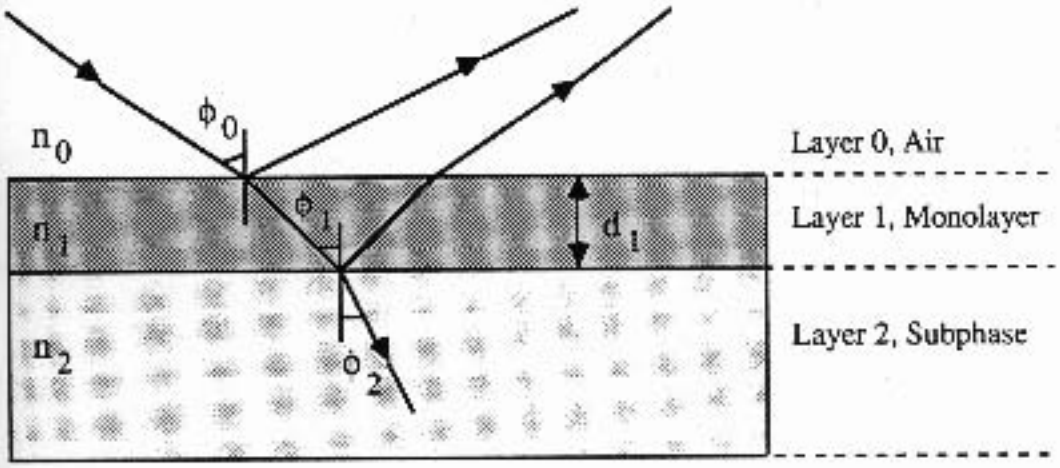

Figure 5. Schematic representation of the reflection of polarized light from monolayer covered surface treated as consisting of three distinct layers.

$$R=[r_{01}+r_{12}\exp(-i\Theta)]/[1+r_{01}r_{12}\exp(-i\Theta)] \quad (18)$$

where

$$\Theta=4pn_1d_1\cos\phi_1/\lambda \quad (19)$$

and n_1 is the average refractive index of the monolayer, d_1 is the film thickness, and ϕ_1 is the incident angle in the monolayer.

Equation 18 is valid for both p and s polarizations, and the Fresnel coefficients for the reflection between these layers are given as

$$r_p01=[n_1\cos o_0-n_0\cos\phi_1]/[n_1\cos\phi_0+n_0\cos\phi_1] \quad (20)$$

$$r_s01=[n_0\cos\phi_0-n_1\cos\phi_1]/[n_0\cos\phi_0+n_1\cos\phi_1] \quad (21)$$

for layers 0 and 1 and as

$$r_p12=[n_2\cos o_1-n_1\cos\phi_2]/[n_2\cos\phi_1+n_1\cos\phi_2] \quad (22)$$

$$r_s12=[n_1\cos o_1-n_2\cos\phi_2]/[n_1\cos\phi_1+n_2\cos\phi_2] \quad (23)$$

for layers 1 and 2, where n_0 and n_2 are the refractive indices of air and subphase and ϕ_0 and ϕ_2 are the incident angle at air and refracted angle in the subphase, respectively.

For monolayers such as fatty acids, with dimensions small compared to the wavelength of the light, the following expression (Drude approximation) has been derived (Drude, 1889a, 1889b, Bootsma and Meyer, 1968, den Engelsen, 1974a, 1974b):

$$\tan\psi'\exp(i\Delta')/\tan\psi\exp(i\Delta)=\{1-i[4\pi d_1\cos\phi_o\sin^2\phi_o n_2{}^2M /(1(n_2{}^2-n_o{}^2)(n_o{}^2\sin^2\phi_0-n_2{}^2\cos^2\phi_0))]\} \quad (24)$$

The monolayer covered surface and the clean water are represented by ψ', Δ' and ψ, Δ, respectively. The parameter M is defined as:

$$M=n_o^2+n_2^2-n_x^2-n_o^2n_2^2/n_z^2 \qquad (25)$$

where the anisotropy in the monolayer refractive index is defined by two indices: n_z, which is in the direction normal to the surface, and $n_x=n_y$, which are in the plane parallel to the surface.

Rheological Properties of Monolayers

Background

An examination of the relationship between stress, deformation, and the rate of deformation of the molecules at an interface constitutes the study of surface rheology. Monolayers are viscoelastic in nature; they exhibit both viscous (dissipative) and elastic (storage) forces when stressed.

Of the several different kinds of motion for the molecules in a monolayer suggested by Goodrich and Eliassen (Goodrich, 1962, Eliassen, 1963), the three modes of motion most relevant to the estimation of viscoelastic parameters are (Figure 6):

1. Transverse mode.
2. Compression mode.
3. Shear mode.

Each of these modes is defined by assuming a cylindrical portion of the monolayer at the interface to be symmetric about a direction. Also, each mode has an elastic and a viscous component associated with it. The elastic constant of the transverse mode, the motion normal to the interface, is the surface tension, γ, and the viscous constant is the transverse

Figure 6. Possible motions of the molecules in a monolayer at the interface. Cylinders represent cross sections of the monolayer.

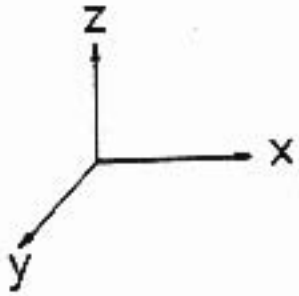

1. TRANSVERSE MODE

	Elastic Constant		Viscous Constant
	γ	;	μ_v

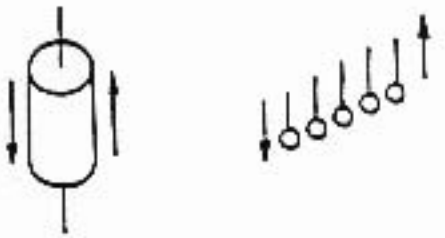

2. COMPRESSION MODE

	ϵ_d	;	η_d

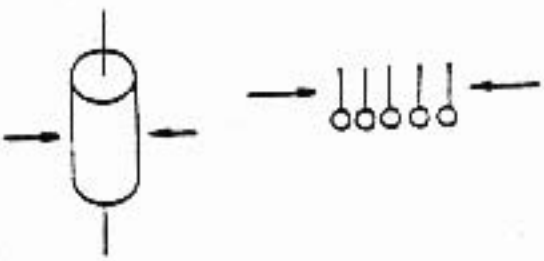

3. SHEAR MODE

	ϵ_s	;	η_s

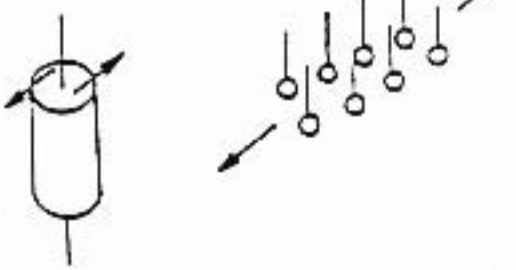

viscosity, μ_v. The viscoelastic constants for the compression and shear modes, the motions longitudinal to the interface, are the surface dilational elasticity (ε_d), surface dilational viscosity (η_d), surface shear elasticity (ε_s), and surface shear viscosity (η_s).

Since the stability of the monolayer at the air/water interface is of paramount importance in determining the final state of LB films, optimization of monolayer properties that would lead to better deposition and perhaps improve the deposition of monolayers that would not characteristically form LB films is essential. Such optimizations can be accomplished, for example, by controlling the rheological properties of the monolayer (Biddle et al., 1985, Mann et al., 1987). The two predominant stresses that a monolayer experiences during deposition are the tangential shearing stress and compressional stress (Buhaenko et al, 1988). However, in the monolayer state, the shearing stress due to in-plane displacement of the molecules in the monolayer becomes more significant than the compressional stress since the area of the monolayer is constant and the latter approaches zero (Buhaenko et al, 1988).

The Measurement of Dynamic Rheological Properties

Until fairly recently the focus of research with insoluble monolayers concerned with their mechanical properties has been on the measurement of shear viscosity, estimation of which for a given monolayer can vary with the nature of the measurement, e.g., the size and shape of the apparatus (Joly, 1964, 1972). It appears, however, that dilational elasticity and viscosity may be more important than their shear counterparts in many

processes involving the dynamic behaviour of monolayers (Lucassen-Reynders, 1981). Hence, shear viscosity measurements alone may not always be useful in assessing monolayer properties. The study of the damping of mechanically-induced surface waves addresses this problem to some extent by measuring both the dilational and shear moduli. In this technique the surface waves are formed by an external force; the wave characteristics are determined as a function of the stimulus and the moduli are deduced under the assumption that there is a linear response between the two (Mann et al., 1963, Lucassen, 1981). The disadvantages of this technique are: 1) the need to use surface waves of low frequency and large amplitude relative to their wavelength and, 2) the use of mechanical probes which alter the equilibrium conditions at the surface and hence result in a nonlinear viscoelastic region.

The surface light scattering (SLS) technique used with capillary waves is a non-invasive method of studying surface rheological parameters. It thus avoids the problems seen with mechanically-induced surface waves. Capillary waves are surface waves of small amplitude (≈4Å) thermally generated due to spontaneous density fluctuations at the surface and the restoring force of surface tension. The presence of a monolayer alters the pattern of liquid flow underneath the surface and consequently results in a higher rate of energy dissipation and a greater damping effect compared to that of the pure liquid surface. The alteration of these surface properties can then be expressed in terms of surface viscoelasticity, e.g. surface elasticity and surface viscosity, by means of an appropriate dispersion relation (Mann, 1985, Sano et al., 1986). SLS,

however, has a low limit of detection of surface viscosity (≈0.05 s.p.) and a small range of discrete wave vectors at high frequency range (=10 kHz), which in turn does not allow the detection of the small changes in the viscoelastic parameters of fatty acid monolayers caused by their interactions with metal ions in the subphase solution (Yazdanian, 1988).

The electrocapillary wave diffraction technique is a relatively new method for investigating surface rheological properties. This technique relies on the difference between the dielectric constants across an interface which allow fluid to rise into higher electric fields. Hence the term electrocapillarity (Jackson, 1962). This technique recently has been shown to be an effective method for generating capillary waves (Magerlein and Sanders 1976, Sohl et al., 1978, Nagarajan et al., 1982, Miyano et al, 1983, Stenvot and Langevin, 1988, Vogel and Möbius, 1989, Ito et al., 1990).

Capillary wave propagation characteristics can be described by a dispersion equation (Lucassen-Reynders and Lucassen, 1969) in the form

$$[i\eta(k^*+m)+i\eta'(k^*+m')+(\varepsilon^*k^{*2}/\omega)][i\eta(k^*+m)+i\eta'(k^*+m')+(\gamma^*k^{*2}/\omega) +(g(\rho-\rho')/\omega)-(\omega(\rho+\rho')/k^*)]]+[\eta^2(k^*-m)^2-\eta'^2(k^*-m)^2]=0 \qquad (26)$$

where $k^*=k-i\beta$, k is the spatial capillary wave vector, β is the spatial capillary wave damping coefficient, $i=\sqrt{-1}$, $m=[k^{*2}+(i\omega\rho/\eta)]^{1/2}$, $m'=[k^{*2}+(i\omega\rho/\eta)]^{1/2}$, ω is the angular frequency, η and η' are the shear viscosities of air and subphase solution, respectively, ρ and ρ' are the densities of air and subphase solution, respectively, and ε^* is the complex viscoelastic modulus given as

$$\varepsilon^* = \varepsilon_1 - i\omega\kappa \qquad (27)$$

Here, ε_l is the surface longitudinal elasticity and κ is the surface longitudinal viscosity. The latter two have both dilational and shear components. γ^* is the complex surface tension comprised of surface tension , γ, and transverse viscosity, μ_v, given as

$$\gamma^* = \gamma - i\omega\mu_v \qquad (28)$$

The use of the above dispersion equation in estimating the viscoelastic parameters will be discussed in the Experimental Section.

γ^* and ε^* are two dimensional complex elastic moduli analogous to the three dimensional complex elastic modulus, G*, which describes viscoelasticity due to periodic straining and is defined as

$$G^* = G' + i\omega G'' \qquad (29)$$

where G' describes the elastic or storage properties and G" describes the viscous or loss properties. A phase lag, δ, which exists between the stress and rate of strain is an important parameter that describes the relative contribution of elastic and viscous components in three dimensional systems; it is defined as

$$\tan\delta = \frac{G''}{G'} \qquad (30)$$

where $\tan\delta$ is the loss tangent, a measure of energy lost to energy stored in periodic straining. By analogy, in two dimensional systems $\tan\delta$ is equal to

$$\tan\delta = \frac{\omega\kappa}{\varepsilon} \quad \text{or} \quad \frac{\omega\mu}{\gamma} \qquad (31)$$

The response of a monolayer in terms of different values of δ has been suggested to be as follows; for $\delta<10°$, the monolayer is purely elastic, for $10° \leq \delta \leq 75°$ the monolayer is viscoelastic, and for $\delta>75°$ is purely viscous (Buhaenko et al., 1988).

Static Elastic Modulus

The static surface dilational (compressional) elasticity, ε_{st}, can be estimated directly from the Π-A isotherms. ε_{st} is an equilibrium quantity defined as (Gibbs, 1928):

$$\varepsilon_{st} = -A\left(\frac{d\Pi}{dA}\right) \qquad (32)$$

ε_{st} represents the elasticity of the monolayer at essentially zero frequency or infinite time.

Rheological Measurements of Fatty Acids

A review of the literature on the rheological properties of fatty acid monolayers reveals that surface viscosity and surface elasticity increase with increase in the temperature, surface pressure, and chain length of fatty acids. A closer examination, however, shows large discrepancies in the numerical values of the rheological parameters obtained (Boyd and Harkins, 1939, Motomura and Matuura, 1962, Jarvis, 1965, Enever and Pilpel, 1967, Pilpel and Enever, 1968, Neuman, 1975, Abraham et al., 1981, Buhaenko et al., 1985,

1988). This is due most likely to variations in the techniques used, experimental conditions, experimental apparatuses, and the purity of the materials used.

In spite of the importance of the rheological properties of fatty acid monolayers spread at the air/water interface, before and during transfer, in determining the characteristics and properties of the LB films, e.g. mechanical strength and proper molecular order, there is very little information on the effect of metal ions on the viscoelastic behaviour of monolayers (Mann et al., 1987). Consequently, to date, the interplay between the rheological properties of fatty acid monolayers and the presence of various metal ions, known to produce LB films of varying stability, has not been fully developed.

Shear viscosity measurements of stearic acid in the presence of calcium ions have been shown to be time dependent (Enever and Pilpel, 1967), and to increase with increase in concentration (Pilpel and Enever, 1968) and pH of the subphase solution (Neuman, 1975). Stearic acid monolayers in the presence of calcium and magnesium ions have been shown to have negligible shear moduli compared to trivalent ions, such as aluminum and iron(Abraham et al., 1981). Indeed, SLS studies of pentadecanoic acid monolayers in the presence of aluminum ions have shown much higher dynamic surface elasticities and surface viscosities than in the presence of divalent cations (Yazdanian, 1988). However, the presence of various hydroxycomplexes of aluminum and iron makes the interpretation of the measured values for these systems extremely difficult.

Most recently, Buhaenko et al, 1988, have determined the shear viscosity of docosanoic acid in the presence of cadmium ions by resonance rheometry and have analyzed their data in terms of LB film formation. Cadmium docosanoate monolayers at pH 5.6 and 6.0 with viscosities below 0.20 surface poise at 20 dyn/cm, deposit good LB films while those with viscosities above this value, e.g. cadmium docosanoate at pH 6.5, are poorly transferred and do not form good LB films (Buhaenko et al., 1988). These results appear to demonstrate the importance of rheological parameters in establishing the windows of operation for the formation of good LB films and the sensitivity of these parameters in turn to the subphase solution conditions such as pH.

STATEMENT OF THE PROBLEM

The long-range objective of this project is to further the understanding of physical chemical properties of spread monolayers at the air/water interface in the context of the effect they might have on the formation of LB films. A review of the literature reveals the significant role played by the metal ions and the pH of the subphase solution in the formation of LB films of desirable properties, e.g. proper mechanical strength and ordered molecular arrangement. To date, however, the interplay between these two factors and the stability and properties of fatty acid monolayers, has not been fully developed and understood. This is primarily due to the general limitation of the methods used, insufficient knowledge of the role of various metal ions relative to the degree of ionisation of the monolayer, and the uncertainty about the chemistry and solution state of the metal ions.

The specific objective of this work, therefore, is to study the effect of a series of divalent ions on the thermodynamic, electrical, optical, and rheological properties of fatty acid monolayers using surface pressure, surface potential, ellipsometry, and electrocapillary wave diffraction, respectively, in order to answer the following questions:

1. Why are divalent cations so important in the formation of LB films and why do some form better LB films under a given set of conditions?

2. What is the relationship between fatty acid monolayers and the type and concentration of the divalent cations in the subphase solution? What is the optimum pH of the subphase solution for these interactions? How does the degree of ionization of the monolayer change with the pH and the type and concentration of divalent ions? Of what chemical physical nature are the fatty acid divalent cation interactions?

3. Since the rheological behaviour of spread fatty acid monolayers appears to be a critical factor in the formation of LB films, how do different divalent cations in solutions of known pH affect the viscoelastic properties of such monolayers? How does the contribution of surface elasticity and surface viscosity vary depending on the type of cation present and how does it explain the type of lateral chain interaction and packing in a monolayer? Based on the viscoelastic behaviour of the monolayer in the presence of various ions, what predictions can be made for effective deposition of LB films?

EXPERIMENTAL

Materials

The water used as the subphase liquid in all experiments was the house-distilled water, first purified with a Millipore Milli-Q filtering system with two carbon and two ion-exchange stages and then distilled from an alkaline potassium permanganate solution and from a dilute sulfuric acid solution, respectively. The spreading solvent used to spread fatty acids was hexane (99.9%, spectrophotometric grade, Aldrich) either doubly distilled or used as received; both gave the same results. The purity of hexane was checked in either case by monitoring the change in the surface tension of water as the spread hexane evaporated from the surface. Hexane was judged pure when upon further compression of the surface with the barrier, no detectable change in the surface tension of water was observed. Pentadecanoic acid (C15), palmitic acid (C16), arachidic acid (C20) (Fluka Chemical Corp., Renekonkoma, NY), and stearic acid (C18) (Applied Sciences Labs., State College, PA) had a stated purity of >99%. They were recrystallized three times from hexane for further purification (Yazdanian, 1988). Docosanoic acid (C22) (98%) (Aldrich Chemical Co., Milwaukee, WI) was used in ellipsometry measurements as received. The compounds: $BaCl_2$(dihydrate,99+%), BaF_2 (99.99%), $CaCl_2$ (hexahydrate,99.99%), $CdCl_2$ (99.999%), CdF_2 (99.99%), CdI_2 (99.999%), $CoCl_2$ (Anhydrous,97%), $Co(SCN)_2$(98%) $MgCl_2$ (hexahydrate,99.999%), NaCl (99.99%), NaF (99.99%), NaI(99.99+%), NaSCN(98%), $PbCl_2$(99.999%), $Pb(SCN)_2$(99.5%), spermidine trihydrochlride (99%), and spermine tetrahydrochloride (98%)

were obtained from Aldrich Chemical Co. and used as received. BaI_2 (>97%) and sodium methanesulfonate (98%) were obtained from Fluka Chemical Corp. and used as received. Acetic acid (Volumetric standard, 0.100N) and sodium hydroxide (Volumetric standard, 0.1015N) were obtained from Aldrich. The volumetric standards were prepared from A.C.S. reagent grade compounds and standardized potentiometrically against N.B.S. reference material.

Preparation of Solutions

The ionic strength of all solutions was brought to 0.01M with NaCl, except when stated otherwise. The pH values of the subphase solutions from 2.0 to 6.0 were adjusted with dilute solutions of HCl and NaOH prepared from concentrated HCl (Hi-pure Chemical Inc., Nazareth, PA) and NaOH pellets (98.5%, Mallinckrodt Inc., Paris, KY), respectively. For surface potential measurements at higher pH values the following buffers were used: Tris (Ultrapure reagent, >99.9%, International Biotechnologies, Inc.)-HCl for pH 7.0-9.0, borax (sodium tetraborate, anhydrous, 99%, Aldrich)-HCl and borax-NaOH for pH 8.0-11.0, and KCl(99.99%, Aldrich) for pH 12.0. All the aforementioned fatty acids except pentadecanoic acid (Yazdanian, 1988) could be maintained as stable monolayers in the range of pH values from 2.0 to 6.0 over 6 to 8 hours without the use of buffers. Buffers were avoided since they could contribute to the surface pressure and surface potential. Moreover, this is the pH range most often reported in LB film studies. The change in the ionic strength of the solutions upon pH adjustments was less than 5% and the pH of solutions changed by less than 0.1 pH units during the time

(Model 2000, Cahn Co., Paramount, CA). The voltage output of the electrobalance was monitored by a chart recorder (Kipp & Zonen, Delft, Holland). The filter paper plates were washed extensively with triply distilled water and soaked in a beaker containing the subphase solution for at least an hour before each measurement. Since absolute surface tension of the subphase solutions before spreading the monolayer could not be measured accurately with filter paper plates, it was measured using platinum plates and found to be equal in each case to that of pure water at 25°C (Pallas and Pethica, 1985, 1989). Moreover, spread monolayer in the absence of divalent cations were compared with both the filter paper and platinum plates and shown to exhibit identical surface pressure-area isotherms. The monolayer was compressed by discontinuous stepwise compression to avoid overcompressing the monolayer (Sims and Zografi, 1972, Yazdanian, 1988). 15 to 20 minutes were allowed for solvent evaporation and surface temperature equilibration after each measurement. The length of the plate in the wet state was measured with a caliper right after each measurement to make accurate calculations of the surface pressure possible. The precision of the measurements was ± 0.1 dyne/cm.

Measurement of Surface Potential

Surface potential, ΔV, the Volta potential change at the air/water interface upon spreading an insoluble monolayer,

$$\Delta V = V_{(\text{monolayer})} - V_{(\text{subphase solution})} \qquad (33)$$

was measured by the ionizing electrode method (Gaines, 1966) using an ^{241}Am alpha radiation source connected to a digital pH/mV meter. The aqueous electrode was a standard (Ag/AgCl) pH reference electrode dipped into the subphase behind the movable barrier of the trough where no monolayer is present. The radioactive electrode ionizes the air above the monolayer so that it becomes conducting. The radioactive electrode was suspended 3 mm above the subphase surface to provide sufficient conductivity and to prevent leakage to other surfaces of the system, which would induce error (Gaines, 1967). The potential difference between the two electrodes, the radioactive electrode in the air above the monolayer and the reference electrode in the subphase solution, can then be measured directly. The reported surface potential values represent the average of at least five independent measurements with 95% confidence limit error of less than 5%.

Surface Ellipsometry Measurement

The ellipsometric measurements along with surface pressure measurements were carried out simultaneously on equipment housed in Dr. M.W. Kim's laboratory at the EXXON Research and Engineering Company.

The instrument design, shown schematically in Figure 7, was based on modulation ellipsometry principles(Azzam and Bashara, 1977). The ellipsometer was set on an optical table and the experiments were performed at a fixed incident angle in air (ϕ_o=61.8±0.1° or ϕ_o=64.1±0.1°, measured relative to the axis normal to the surface) using a 5 mW He-Ne

Figure 7. Block diagram of ellipsometry instrument.

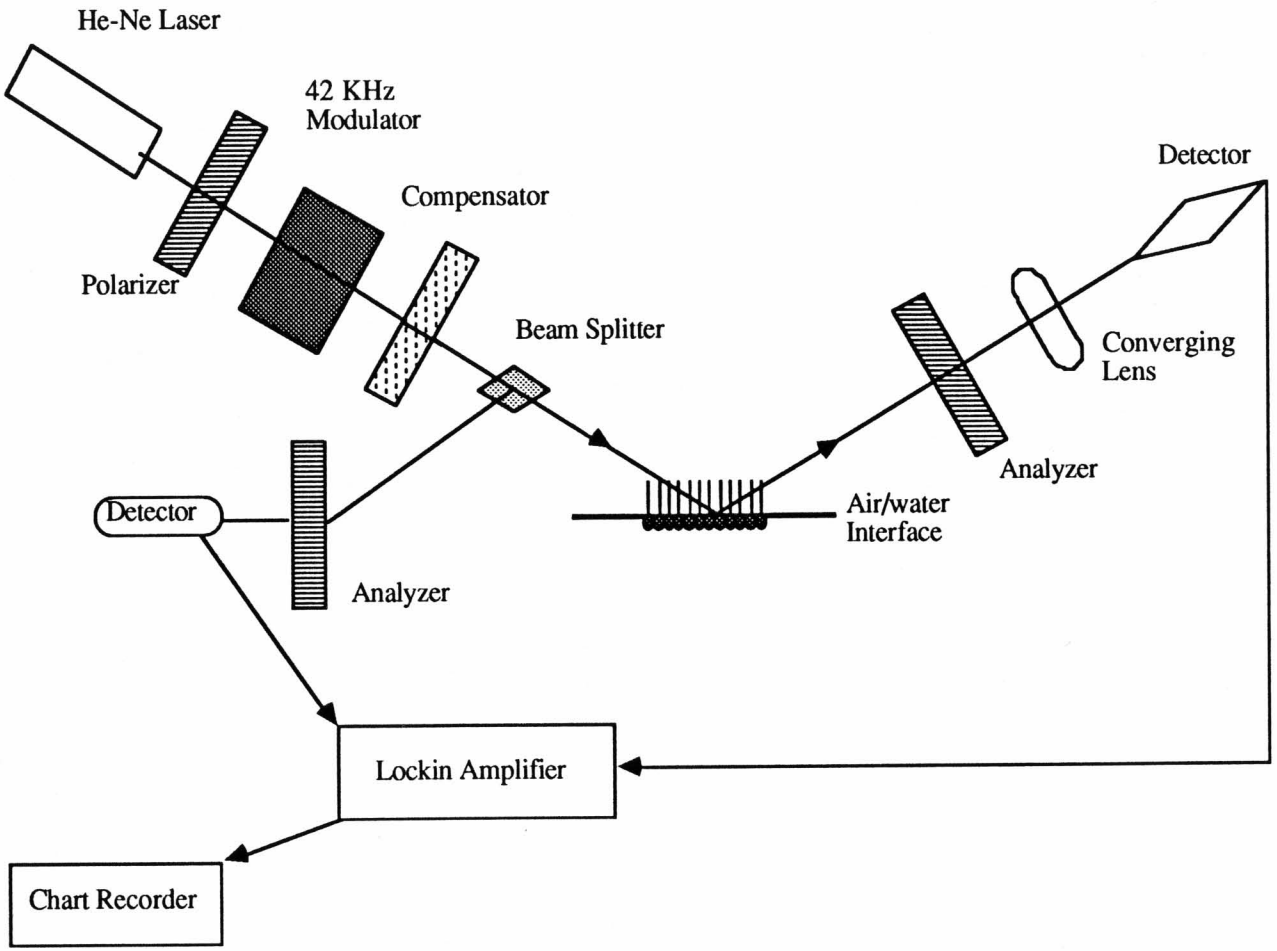
He-Ne Laser
42 KHz
Modulator
Compensator
Polarizer
Beam Splitter
Detector
Converging
Lens
Analyzer
Air/water
Interface
Detector
Analyzer
Lockin Amplifier
Chart Recorder

laser beam with λ=6328Å and a 1 mm beam diameter. The beam is polarized ($+\pi/2$) with a quarter wave plate (polarizer) and then passed through a photoelectric modulator (Hinds International, Portland, OR) which introduces a periodic phase shift between orthogonal amplitude components at a frequency of 42 kHz. The latter is the most important component of the ellipsometer in giving it the high sensitivity required at the air/water interface. The compensator is essentially a phase retarder that can be used to adjust the orthogonal p and s components, and to calibrate the alignment of the optics in the null angle measurements. Reflection from the surface causes additional phase shift and amplitude attenuation, and the phase shift relative to that of a reference beam is detected in the analog mode by locking into the modulation frequency.

The experimental quantity measured is the change in the ellipsometric phase angle $\delta\Delta$ defined as

$$\delta\Delta=\Delta'-\Delta \qquad (34)$$

The change in the amplitude attenuation for non-adsorbing substrates has been shown to be approximately zero and was not measured here (den Engelsen, 1974). Moreover, in our experiment absolute values of Δ' or Δ were not determined, only the difference (Rasing et al. 1985, Sauer et al., 1989, Kim et al., 1990).

The relationship between $\delta\Delta$ and the thickness d_1 is given by

$$\delta\Delta=\alpha d_1 \qquad (35)$$

where α is a proportionality constant that depends on the incident angle and the birefringent refractive indices and may be calculated from equation 24. For all the systems studied the $\delta\Delta$ values were found to be constant within experimental error between the surface pressures of 1-30 dyn/cm (or <24Å^2/molecule).

Surface pressure measurements were carried out simultaneously in an enclosed Langmuir trough (Lauda, Brinkman Inst. Co., Westbury, NY) with a maximum area of 700 cm^2. A thermostated water bath circulated water at 25.0±0.1°C through the coils under the trough in order to regulate the subphase temperature. The surface pressure was measured with a horizontal Teflon float as a strain gauge with an overall sensitivity of ±0.05 dyn/cm. The surface was aspirated before each run and was judged clean when a 30-fold compression produced a change of less than 0.05 dyn/cm. Monolayers were spread by delivering fatty acid solutions on the aqueous subphase with a Hamilton micrometer syringe. At least 15 minutes were allowed for the solvent to evaporate. The surface concentration was varied by a Teflon barrier moving at a rate of 0.5-0.6Å^2/molecule/min.

Stability Constant Determination from Potentiometric Titrations

Twenty five ml of volumetric standard solutions of acetic acid in the absence and presence of various concentrations of divalent cations were titrated in each experiment with volumetric standard solutions of sodium hydroxide delivered from a 50 ml burette. The change in the pH was monitored with a combination electrode connected to a pH meter.

Measurement of Visoelasticity

Apparatus

The electrocapillary wave diffraction (ECWD) technique was used to measure the viscoelastic properties of stearic acid in the presence of various metal ions using the apparatus shown in Figure 8. The sample cell was made of Teflon with a circular area of 80.1 cm^2 equipped with a quartz window on the cell wall to allow visual observation of the interface. The sample cell was placed in a heavy brass base and covered with a thick aluminum cover. A thermostated water bath circulated water at 25.0±0.1℃ through both the base and the cover. A mechanical knob in the middle of the cover allowed adjustment of the gap between a surgical needle placed in the middle of the cover and the interface. The distance between the needle tip and the interface was adjusted to less than 40μm, as measured by a cathetometer via visual observation through the cell window. The radius of curvature of the needle tip was estimated from electron micrographs to be around 10μm (Ito et al., 1990).

The generation of an oscillating electric field at the needle tip from the output of a frequency generator (Hewlett Packard, 3325Bm Synthesizer/Frequency generator), amplified ten times by a voltage amplifier (KEPKO, BOP 100-1M), allowed the formation of capillary waves on the surface. A 5-mW He-Ne laser beam (Melles Griot, 05-LHP-171) was directed normal to the interface through a beam splitter and a converging lens. The focal spot of the beam at the interface has been calculated to be about 120μm (Ito et al , 1990). The reflected beam from the interface was traced back to the beam splitter and then to a position

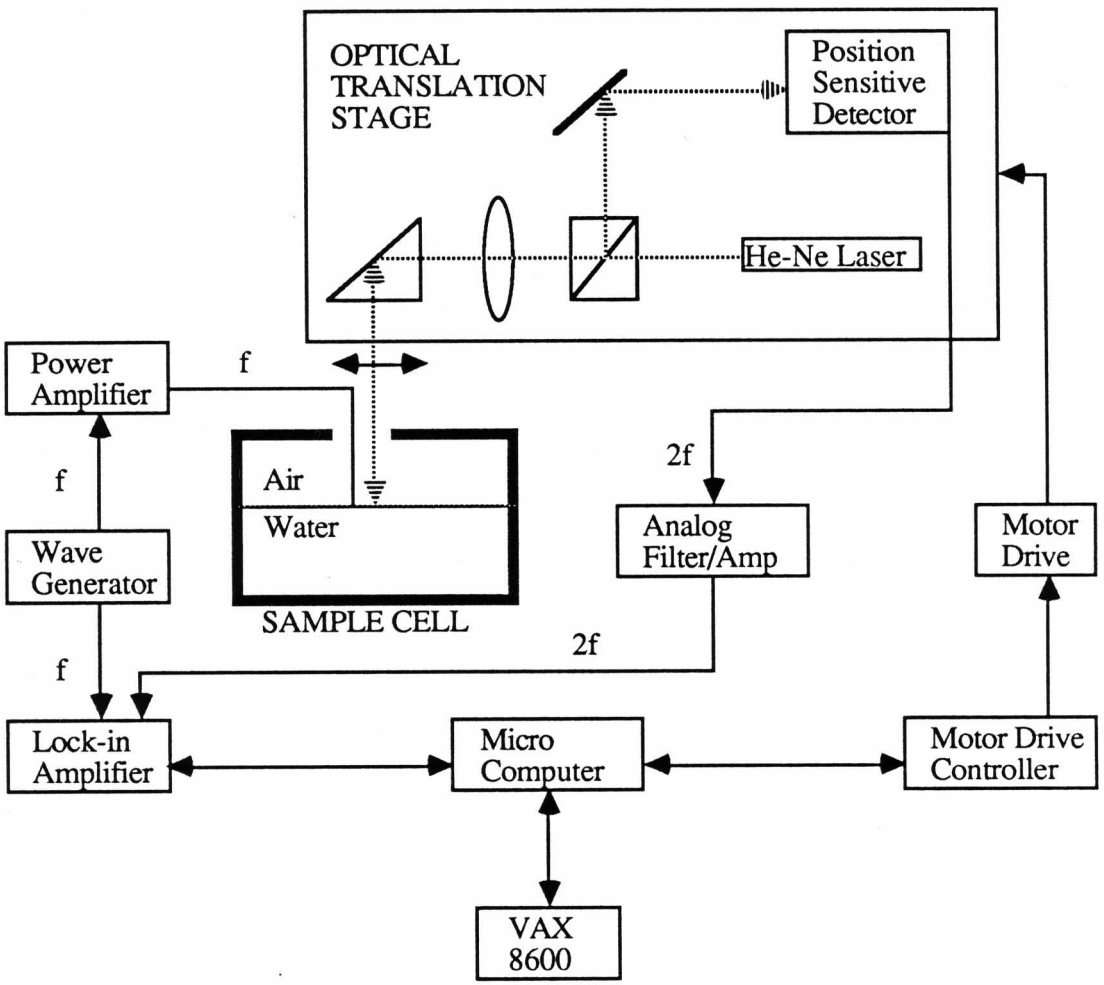

Figure 8. A block diagram of the instrument setup for the electrocapillary wave diffraction measurements.

sensitive detector (Hamamatsu, S1545). It was then fed into a lock-in amplifier (Stanford Research Systems, Inc.) together with the output of the same frequency generator, after passing through a frequency doubler, as the reference. A stepping motor (Superior Electric Co., Bristol, CT) and a microcomputer (IBM, PC) allowed the movement of the complete set of optics mounted on a translation stage. The whole apparatus was set on an optical table floating on a set of pneumatic isolation legs (Newport, Fountain Valley, CA) to minimize external vibrations.

The Generation of Capillary Waves

A sinusoidally varying voltage applied to a needle sets up an intense electric field in the gap between the needle and the liquid surface. Due to differences in the dielectric constants (the liquid having a larger dielectric constant than the air above) the liquid rises up to the needle (Figure 9). Surface tension and gravitation act as restoring forces of this rise, the latter being relatively unimportant and negligible in the range of capillary wavelengths (100-10000 cm^{-1}).

The harmonic external potential, V(t), applied to the tip of the needle is in the form

$$V(t)=V_0\cos(\omega t) \qquad (36)$$

where V_0 is the amplitude of the wave, ω is the angular frequency of the wave, and t is time. The time dependent part of the electric field, E(t), can be shown as (Sano, 1987)

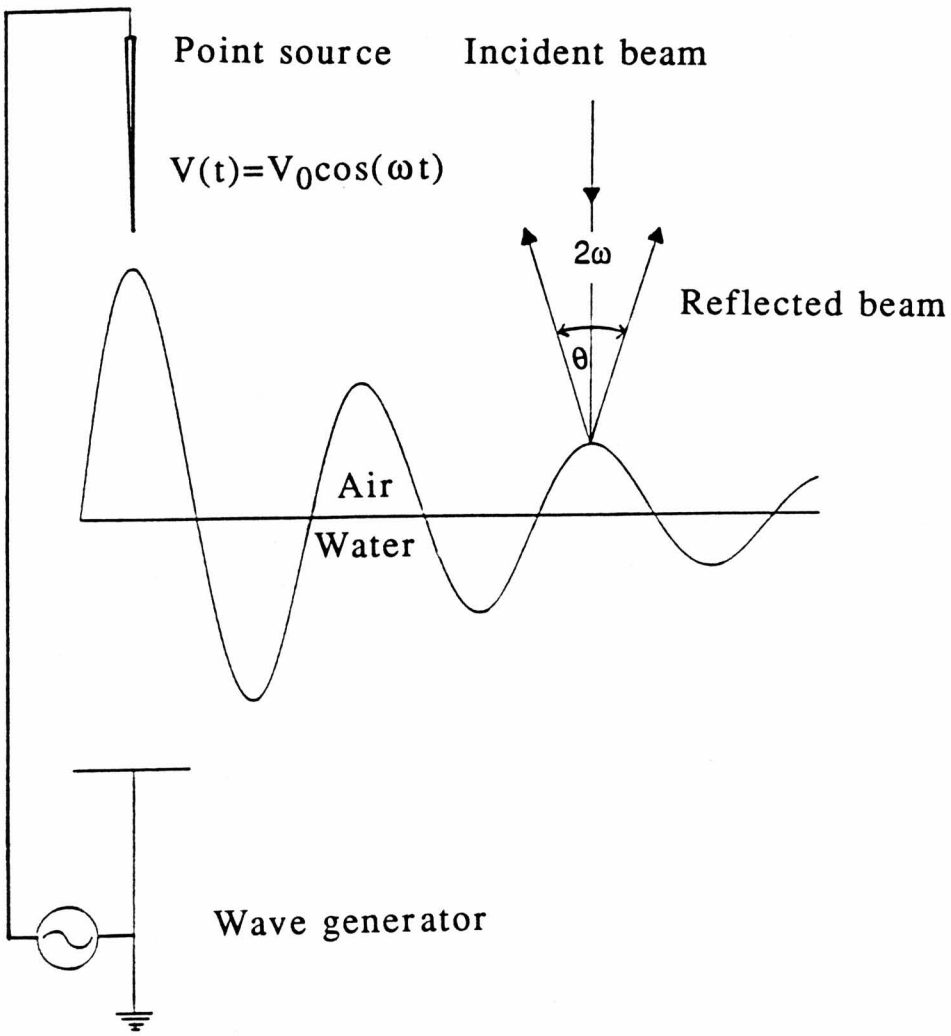

Figure 9. A schematic diagram of the process used to generate and detect capillary waves.

$$E(t) \propto V_0 \cos(\omega t) \qquad (37)$$

and the time dependence of the force, F(t), acting across the interface is given as (Ito et al., 1990)

$$F(t) = V_0^2(\varepsilon - \varepsilon_0)\cos(2\omega t) \qquad (38)$$

Where ε and ε_0 are the dielectric constants of the subphase solution and the air, respectively. Hence, the response of the surface to the applied potential of the frequency ω is the propagation of a capillary wave with twice the frequency 2ω, and of amplitude proportional to V_0^2.

The capillary waves generated are detected by monitoring the deflection of the focused laser beam from the surface. This reflected beam contains information on the capillary wave amplitude, attenuation, frequency, and wavelength since angular deflection, θ, of the beam due to reflection is given as (Sohl et al., 1982)

$$\theta = \theta_0 \exp(-\beta x)\sin(kx - \omega t) \qquad (39)$$

where

$$\theta_0 = 2\xi_0(\beta^2 + k^2), \qquad (40)$$

β is the spatial damping coefficient over radial distance x from the tip of the needle, k is the spatial wave vector, and ξ_0 is the displacement of the fluid in the z direction. A position sensitive detector (PSD) along with a lock-in amplifier are used to detect these deflections. Hence, the voltage output, S, from PSD is in the form (Sano, 1987)

$$S = S(x)\cos(kx + 2\omega t) \qquad (41)$$

where S(x) is the amplitude of the wave. The damping of the waves can be modeled by a zeroth order circular Bessel function and approximated by a Hankel function (exponential spatial decay) as (Ito et al., 1990, Skarlupka, 1990)

$$H_0(x) \propto x^{-1/2}\exp(-\beta x) \qquad (42)$$

where $H_0(x)$ is the Hankel constant. The phase difference and the wave amplitude are obtained by inputting the signals from equations 39 and 40 into the lock-in amplifier. Then

$$\text{Phase difference} = kx \qquad (43)$$

and

$$\text{Wave amplitude} = S(x) \propto x^{-1/2}\exp(-\beta x) \qquad (44)$$

In the course of each experiment, a series of phase differences and wave amplitudes at different distances x from the tip of the needle at various frequencies are obtained. The exact values of k and β are obtained from the slopes of plots of phase difference and natural logarithm of amplitude, $\ln[x^{1/2}S(x)]$, against x. Examples of such linear plots are shown in Figures 10 and 11 for five frequencies. The values of ε^* are calculated from k and β under the assumption that the transverse viscosity, μ_v, is negligible and therefore that $\gamma^*=\gamma$, where the static limit of the surface tension γ^* is that of γ in the low frequency limit and remains unchanged over the entire frequency range. Moreover, since the surface tension could not be measured simultaneously, the surface tensions used in the calculations were those obtained in Π-A measurements. The instrument

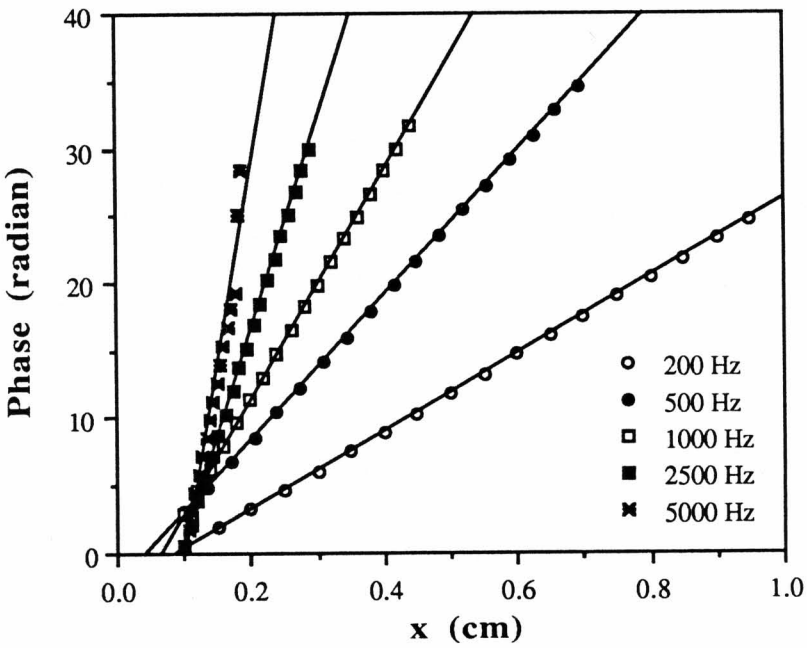

Figure 10. Plot of phase difference vs. radial distance x from the needle tip. The wave vector, k, is calculated from the slope of these lines.

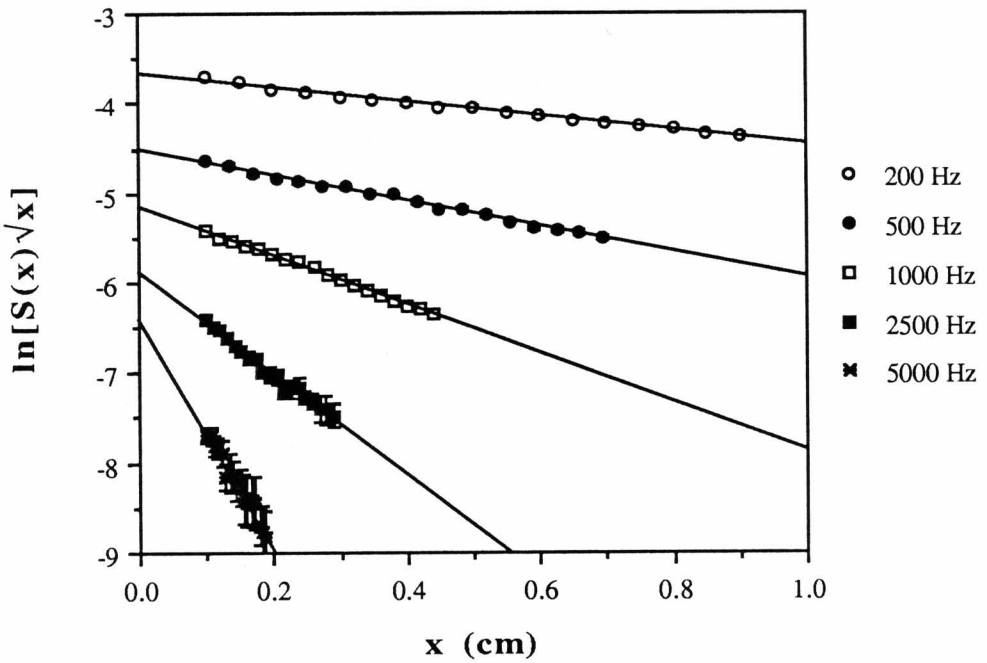

Figure 11. Plot of wave amplitude vs. distance x from the needle tip. The damping coefficient, β, is calculated from the slope of these lines.

was calibrated by determining the surface tension and viscosity of water and cyclohexane from the dispersion equation by assuming $\varepsilon^*=0$ (Ito et al., 1990).

RESULTS

Measurements of Surface Pressure

The effect of pH

The results of a pH change from 2.0 to 6.0 in the subphase solution on the Π-A isotherm of stearic acid in the presence of 0.01M NaCl are presented in Figure 12. The increase in the surface pressure for a given area is an indication of a slight expansion of the stearic acid monolayer caused by an increase in ionization and head group repulsion. The curves are drawn over the points merely to indicate the trends; they do not represent any statistical fitting. The effects of divalent cations on the isotherms at pH 5.0 are shown in Figure 13. There appears to be no change in the isotherms in the presence of 1mM concentrations of the chloride salts of cobalt, cadmium, and calcium at this pH. The presence of 1mM concentration of lead chloride, however, produced a significant decrease in surface pressure for a given area of the monolayer under identical conditions. At pH 6.0 the degree of ionization of stearic acid is significantly increased such that the effect of various ions on the Π-A isotherm becomes more apparent. This is shown in Figure 14. While Co^{2+} and all alkaline earth ions caused a slight condensation of the isotherm at this pH, cadmium and lead ions produced a significant condensing effect.

Figure 15 shows the great tendency of Pb^{2+} to interact with the monolayer over a wide range of subphase pH values. It appears that the limiting extent of the condensation effect is reached at pH 4.0, which is

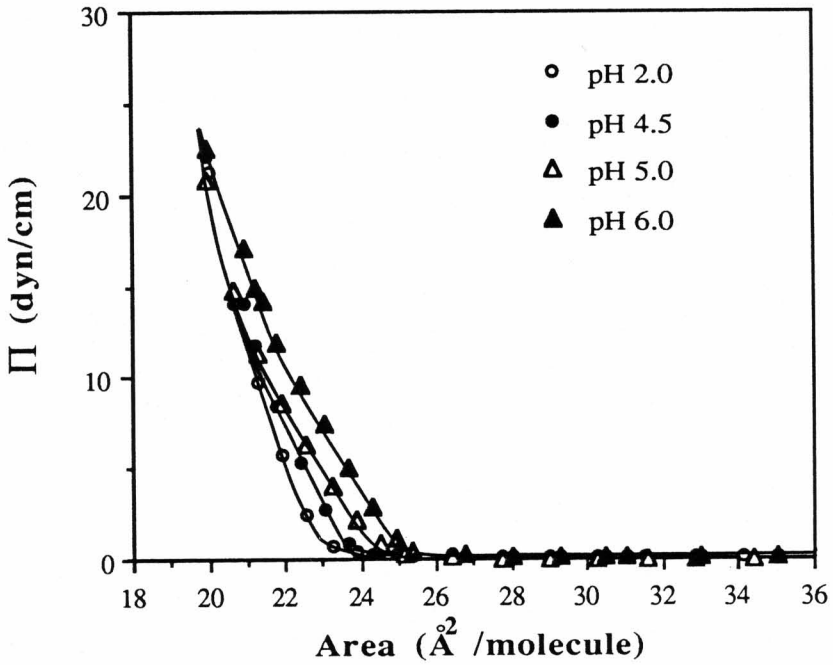

Figure 12. Π-A isotherms of stearic acid in the presence of 0.01M NaCl at pH 2.0 to 6.0.

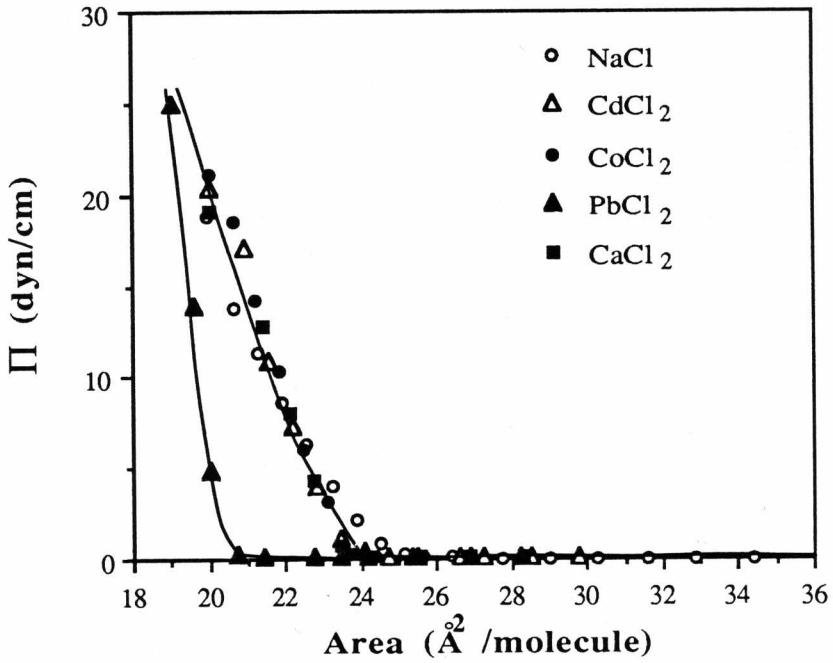

Figure 13. Π-A isotherms of stearic acid in the presence of 0.01M NaCl and 1mM divalent cations, μ=0.01M and pH 5.0.

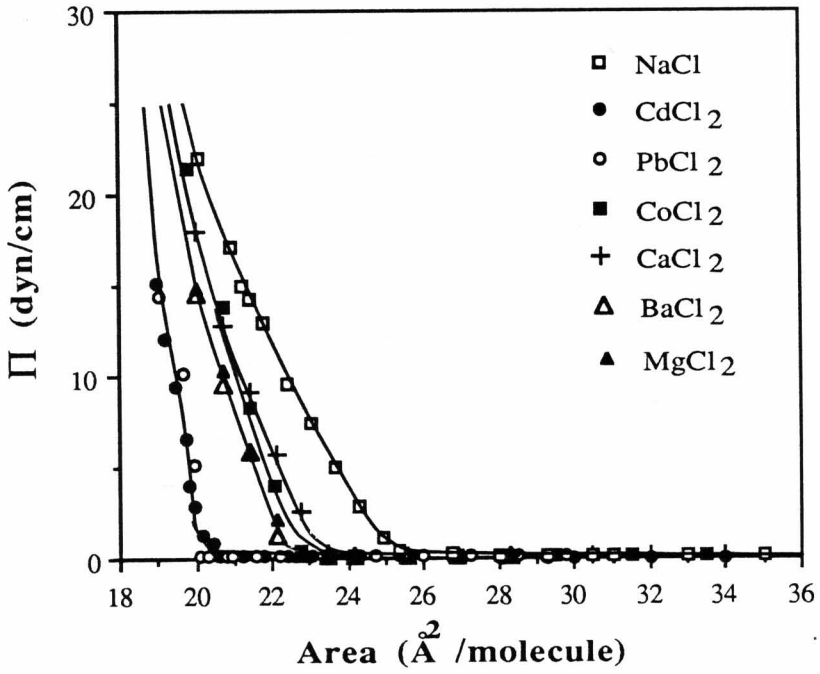

Figure 14. Π-A isotherms of stearic acid in the presence of 0.01M NaCl and 1mM divalent cations, μ=0.01M and pH 6.0.

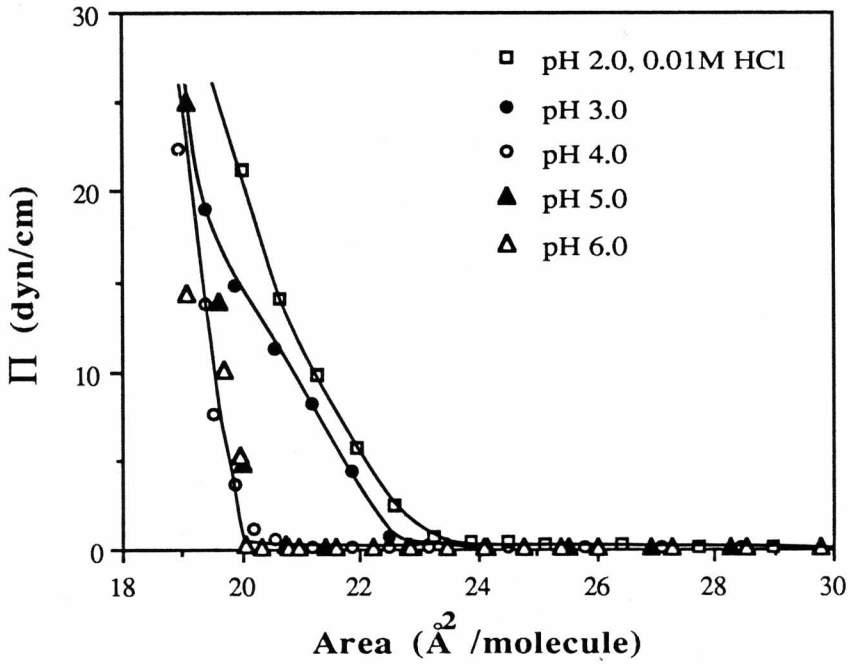

Figure 15. Π-A isotherms of stearic acid in presence of 1mM $PbCl_2$, μ=0.01M, and various pH values.

distinctly different from all other ions that have been examined. For example, Figure 16 shows that the condensation effect of Cd^{2+} on stearic acid monolayers is only in the range of pH 5.0 to 6.0, since the isotherm at pH 5.0 is identical to that in the presence of sodium ions.

The Effect of Divalent Ion Concentration

The extent of condensation of the stearic acid Π-A isotherms at pH 6.0 due to change in the concentration of Ca^{2+}, Co^{2+}, $Cd^{2+}$and Pb^{2+} at constant ionic strength, μ=0.01M, is shown in Figures 17-20. The effect of Co^{2+} and Ca^{2+} on the isotherms at this pH appears to be essentially independent of the concentration in the range of concentrations studied (0.25mM to 3.3mM) (Figures 17-18). These two ions appear to reach a saturation level and exert their maximum effect on the Π-A isotherm at 0.25mM. For cadmium ions, however, there is a gradual condensation of the isotherm as the concentration of divalent ions increases from 0.1mM to 3.3mM (Figure 19). Cadmium ions appear to fully condense the Π-A isotherm at >1.0mM. The presence of Pb^{2+} in the subphase solution results in an extreme condensation of the isotherms over a wide range of concentration from 0.005mM to 1.5mM at pH 6.0 with no apparent expansion even at the lowest concentration (Figure 20).

The Effect of Anionic Counter-ions

In the context of the models proposed for the interaction of divalent cations with fatty acids (See Introduction), where ions like Pb^{2+} and Cd^{2+} appear to interact via specific and strong bonds and alkaline earth metal interactions appear to be mainly ionic in nature, Π-A measurements in the presence of various anionic counter-ions were performed in order to

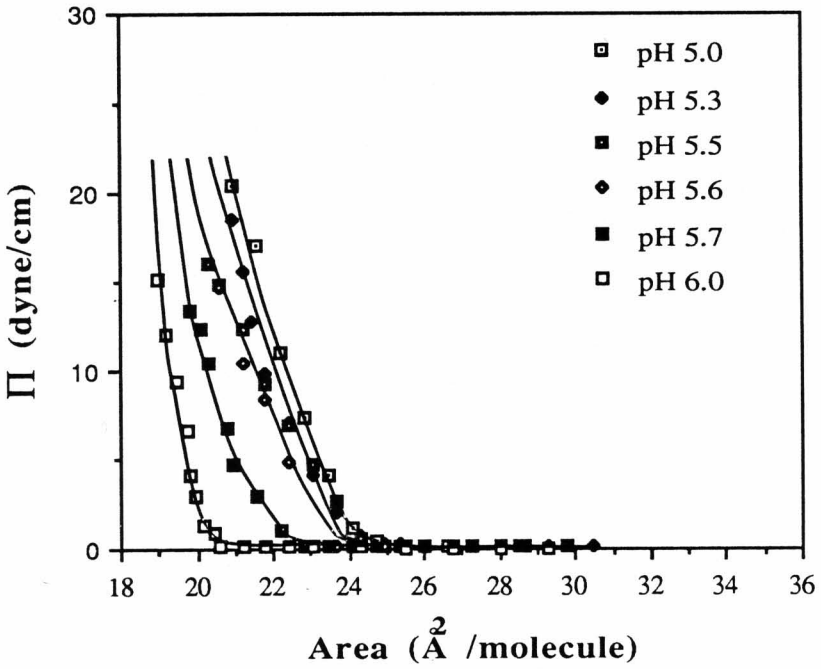

Figure 16. Π-A isotherms of stearic acid in presence of 1mM $CdCl_2$, μ=0.01M, and various pH values.

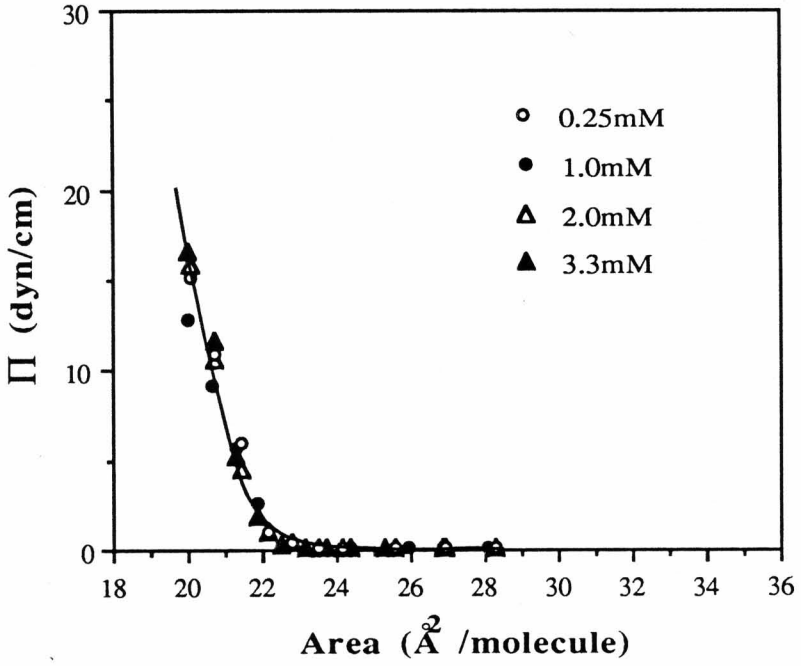

Figure 17. Π-A isotherms of stearic acid in presence of various $CaCl_2$ concentrations, μ=0.01M, and pH 6.0.

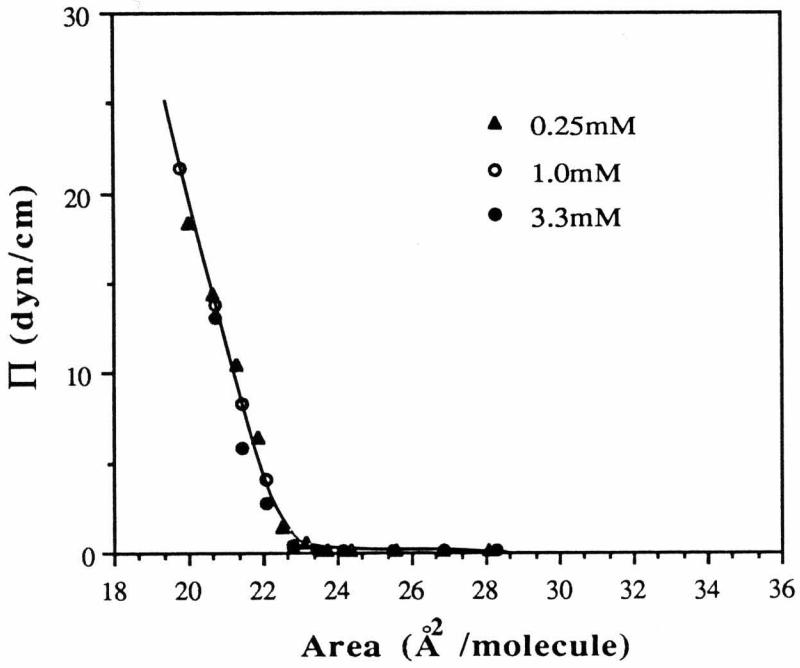

Figure 18. Π-A isotherms of stearic acid in presence of various $CoCl_2$ concentrations, μ=0.01M, and pH 6.0.

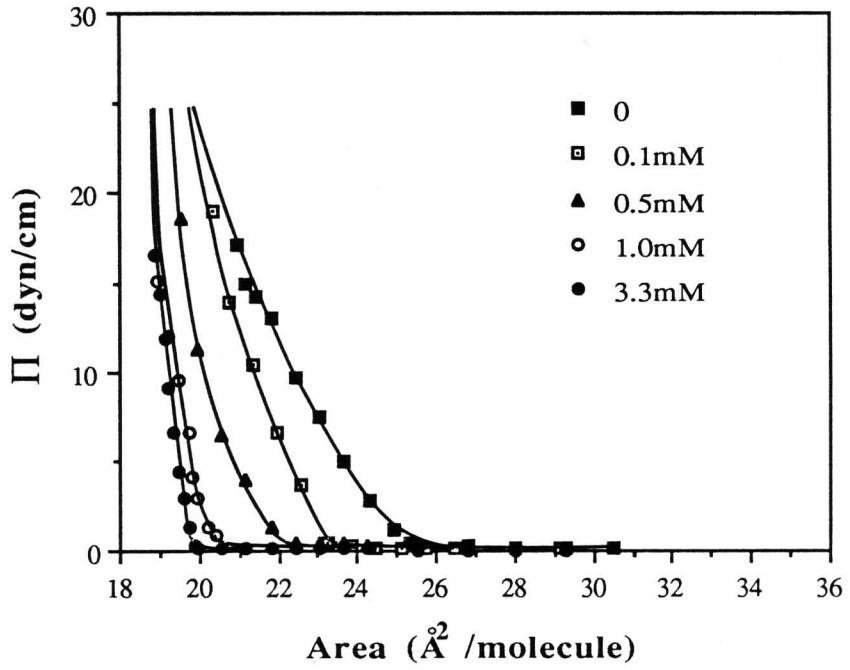

Figure 19. Π-A isotherms of stearic acid in presence of various $CdCl_2$ concentrations, μ=0.01M, and pH 6.0.

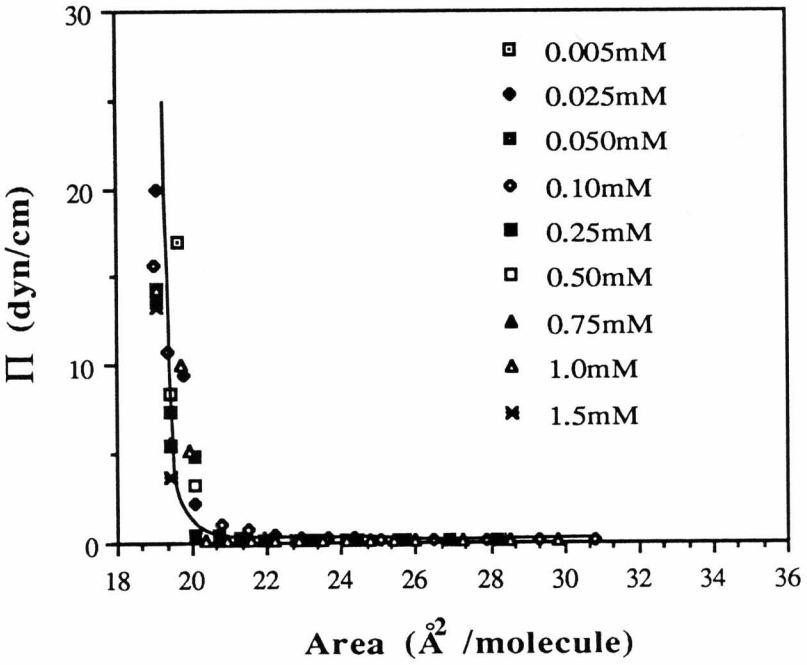

Figure 20. Π-A isotherms of stearic acid in presence of various $PbCl_2$ concentrations, μ=0.01M, and pH 6.0.

investigate their possible effect on this interaction. The counter-ions were chosen in the order of an increase in tendency to complex or to flocculate colloids. This order of effect is known as the Hofmeister series where the change occurs in the order $F^- > Cl^- > I^- > SCN^-$ (Mysels, 1967). Methanesulfonate ion was also chosen because of its large size and highly polarized structure. The presence of 0.01M sodium salts of fluoride, chloride, iodide, thiocyanate, and methanesulfonate ions appear to have no significant effect on the Π-A isotherms (Figure 21). Moreover, there are no significant differences in the isotherms due to these ions in the presence of divalent cations, i.e. Ba^{2+} and Cd^{2+} (Figures 22-23). In this regard, the Π-A measurements appear to be insensitive to any possible effects of the anionic counter-ions on the fatty acid-divalent cation interaction.

The Effect of Polyamines

Since all divalent ions caused some condensation of the stearic acid Π-A isotherms at pH 6.0 relative to sodium ions, the effect of the presence of polyamines such as spermine and spermidine, trivalent and tetravalent respectively, on the Π-A isotherms was investigated. The presence of these positively charged polyamines caused a slight condensation of the isotherm in a manner very similar to that caused by the alkaline earth ions. This is shown in Figure 24.

Studies with Arachidic Acid

Similar results, as are shown in Figures 12 and 14 with stearic acid, are seen in Figures 25 and 26 with arachidic acid though this fatty acid was not studied as comprehensively as in the former case. There appears

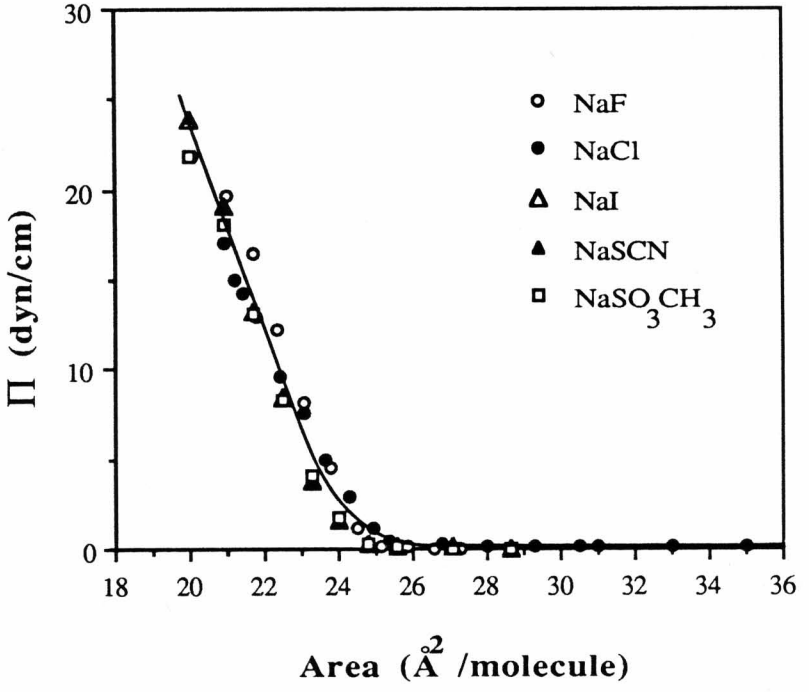

Figure 21. Π-A isotherms of stearic acid in presence of various 0.01M sodium salts of various counter-ions at pH 6.0.

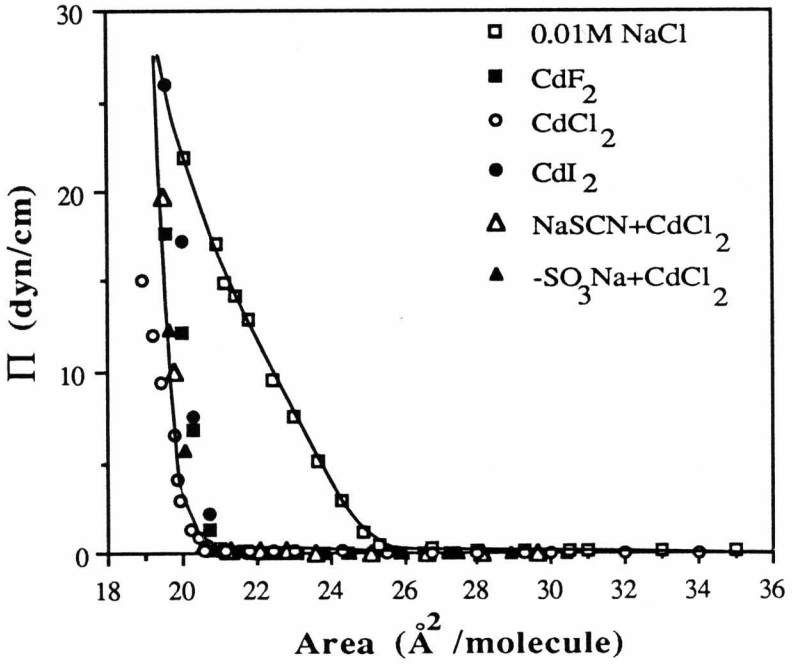

Figure 22. Π-A isotherms of stearic acid in presence of 1mM salts of cadmium , μ=0.01M, and pH 6.0.

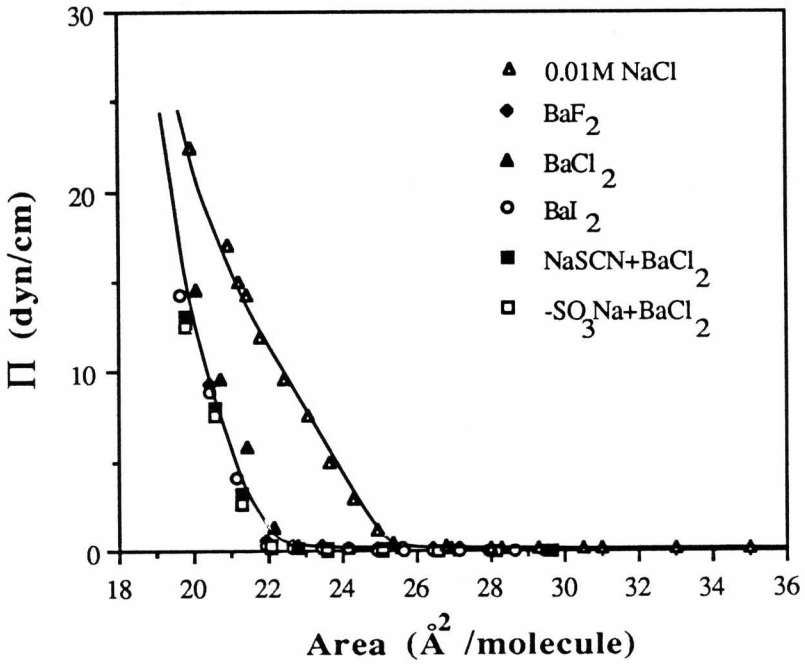

Figure 23. Π-A isotherms of stearic acid in presence of 1mM salts of barium, μ=0.01M, and pH 6.0.

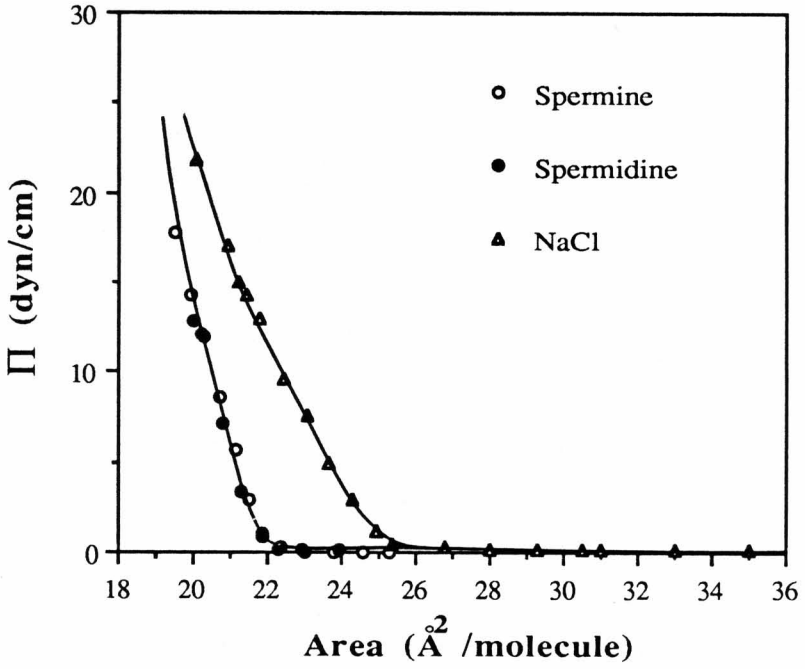

Figure 24. Π-A isotherms of stearic acid in presence of 1mM spermine and spermidine, μ=0.01, and pH 6.0 in comparison with 0.01M NaCl.

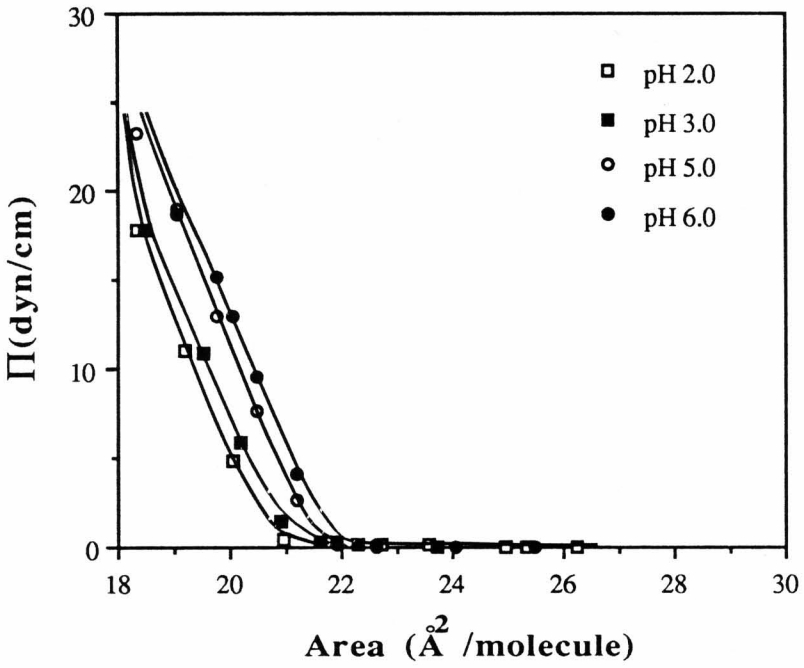

Figure 25. Π-A isotherms of arachidic acid in the presence of 0.01M NaCl at pH 2.0 to 6.0.

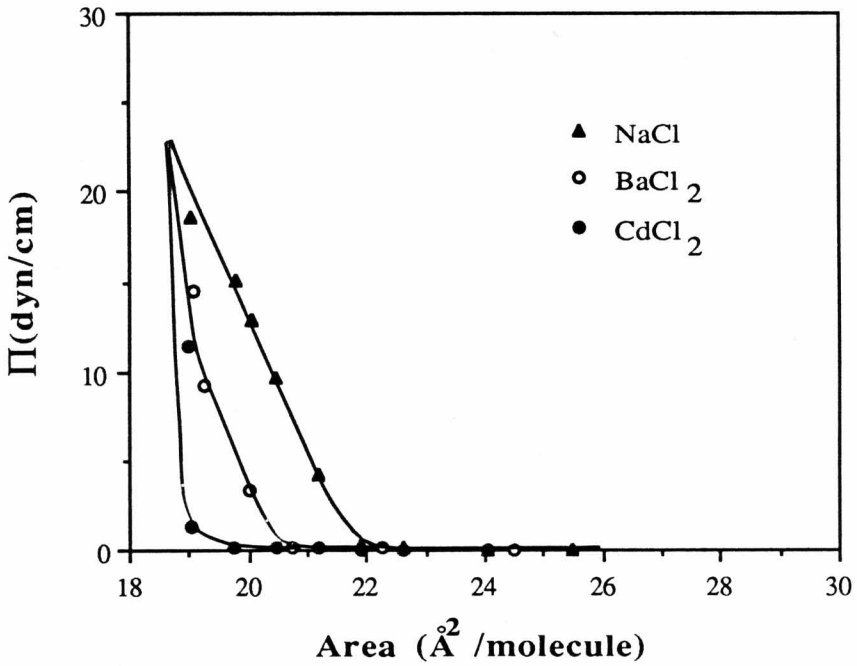

Figure 26. Π-A isotherms of arachidic acid in the presence of 0.01M NaCl and 1mM $BaCl_2$ and $CdCl_2$, μ=0.01M, and pH 6.0.

to be a slight expansion of the isotherms as the pH is raised from 2.0 to 6.0. Marked condensation effects at pH 6.0 in the presence of divalent ions are apparent; the effect of cadmium ion is much greater than barium ion, as expected.

Measurements of Surface Potential

The determination of pK_a

The surface potential of a partially charged monolayer is given as (Schulman and Hughes, 1932, Davies, 1963)

$$\Delta V=\frac{12\pi}{A}\{(1-\alpha)\mu_I+\mu_U\}+\psi_o \qquad (45)$$

where ΔV is the surface potential, A is the area occupied per molecule, α is the degree of ionisation, μ_I and μ_U are the surface dipole moments of the ionized and unionised groups, and ψ_o is the electrostatic potential at the interface. When α is low, μ_I and μ_U can be assumed to be constant with α and equation 43 can be written as (Betts and Pethica, 1956)

$$\left(\frac{\partial\Delta V}{\partial pH_s}\right)=\frac{12\pi}{A}(\mu_I-\mu_U)\left(\frac{\partial\alpha}{\partial pH_s}\right)+\left(\frac{\partial\psi_o}{\partial pH_s}\right) \qquad (46)$$

at constant area, concentration, and temperature. pH_S is the effective pH at the surface that can be given in terms of the Gouy-Chapman electrical double layer theory (equations 8 and 10) or by the Henderson-Hasselbalch equation for the ionisation of acids and bases as

$$pH_S=pK_a^S+z\ln[\alpha/(1-\alpha)] \qquad (47)$$

Equation 46 can be rewritten using equations 8,10, and 47 as

$$\left(\frac{\partial \Delta V}{\partial pH_s}\right) = -z\frac{12\pi}{A}(\mu_I - \mu_U)\alpha(1-\alpha)\left\{1+\frac{e}{kT}\left(\frac{\partial \psi_o}{\partial pH_s}\right)\right\} + \left(\frac{\partial \psi_o}{\partial pH_s}\right) \quad (48)$$

where

$$\left(\frac{\partial \psi_o}{\partial pH_s}\right) = \left(\frac{2kT}{e}\right)\left(\frac{1-\alpha}{2(1-\alpha)+\coth\frac{ze\psi_o}{kT}}\right) \quad (49)$$

and

$$\left(\frac{\partial \psi_o}{\partial pH_s}\right) = -z\alpha(1-\alpha)\left\{1+\frac{e}{kT}\left(\frac{\partial \psi_o}{\partial pH_s}\right)\right\} \quad (50)$$

Using the above equations surface potential data can be used to estimate pK_a^s as α approaches zero in the limit of low charge density where the Gouy-Chapman equations are most applicable.

The change in the surface potential, ΔV, with the subphase pH for stearic acid is shown in Figure 27. It can be seen that at very low pH values (2.0 to 4.0) the change in ΔV is very small. However, with further increase in pH there is a sharper decline in ΔV followed by a leveling off at the highest pH values. In this respect the ΔV-pH profile resembles a pH titration curve with an apparent pK_a of about 8.0. Table I shows values of ΔV at 20Å^2/molecule as a function of pH, from 2.0 to 6.0 for stearic and arachidic acids. These data are plotted in Figure 28 and curve-fitted with polynomial functions for determination of pK_a^s, since as mentioned before, no buffers were used in this range. Using equations 8,

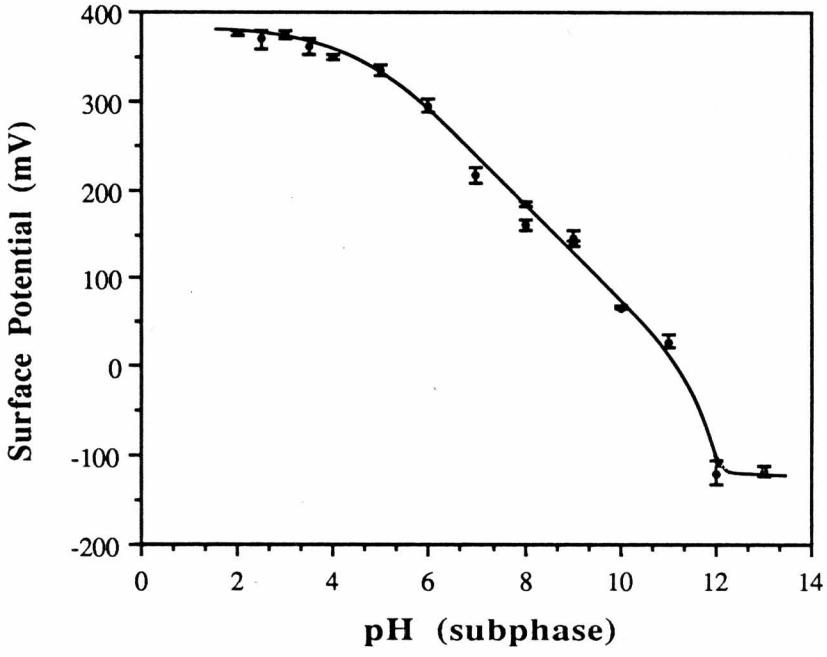

Figure 27. Surface potential vs. pH for stearic acid at 20Å2/molecule and 25° C.

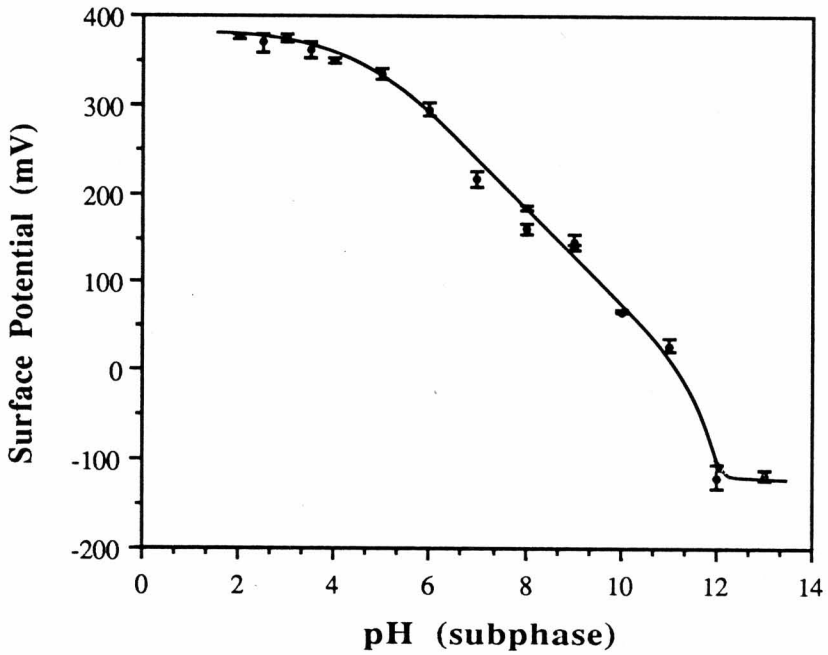

Figure 27. Surface potential vs. pH for stearic acid at 20Å^2/molecule and 25° C.

	Surface Potential (mV)	
pH	Stearic acid	Arachidic acid
2.0	375±5	383±9
3.0	373±9	373±6
4.0	350±4	351±5
5.0	330±9	316±6
6.0	293±8	280±5

Table I. Surface potential as a function of pH at 20$Å^2$/molecule and μ=0.01M. Error estimates are for 95% confidence limit intervals as calculated from Student's t-distribution.

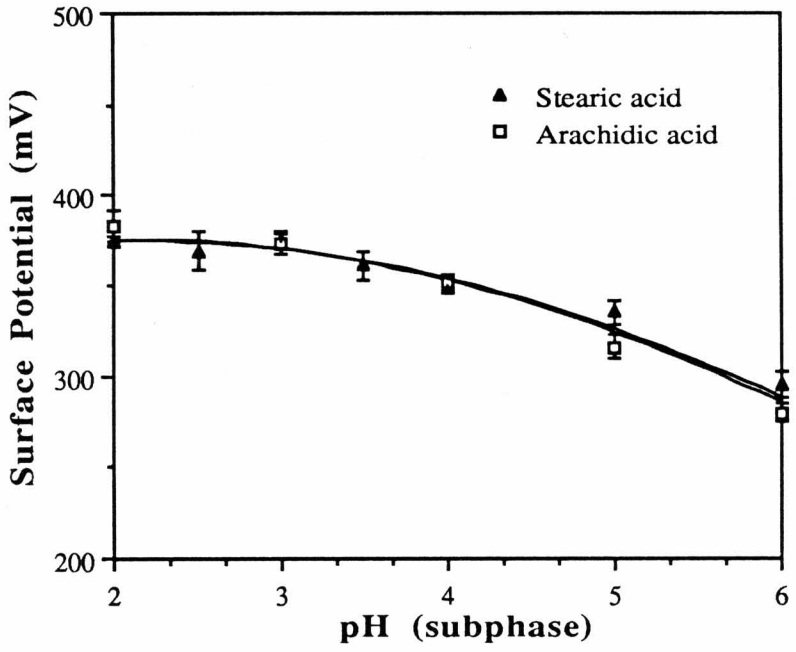

Figure 28. Curve fitting of ΔV vs. pH for stearic and arachidic acids in the range of pH 2.0 to 6.0 with fourth and third order polynomials respectively. The equations for the fit are $y=337.04+36.342x-9.4880x^2+0.3589x^3-0.004595x^4$ for stearic acid and $y=344.29=30.762x-8.1883x^2+0.22242x^3$ for arachidic acid. The correlation coefficients for both fits are 0.986.

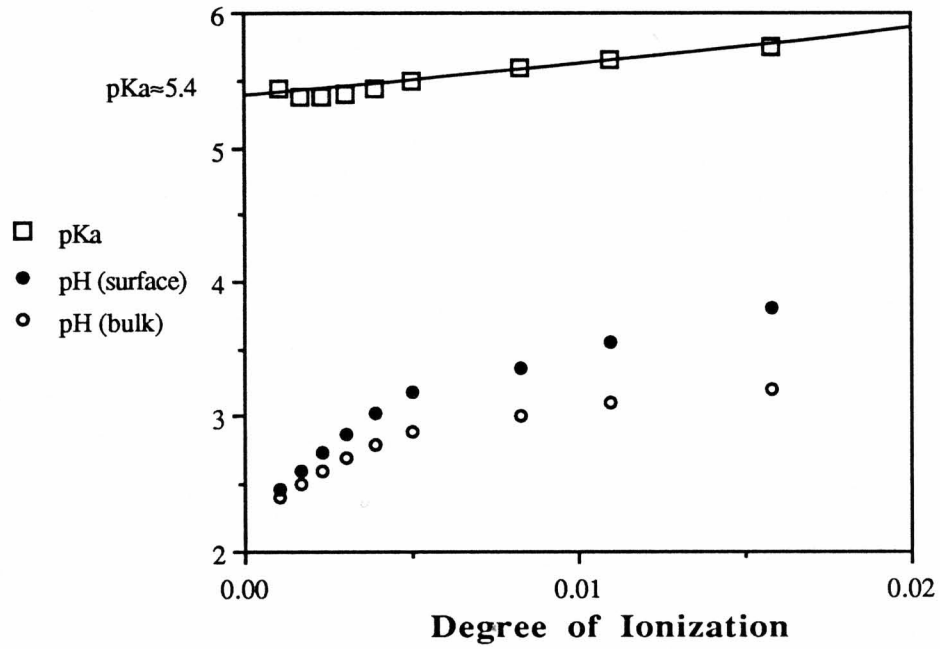

Figure 29. Plot of change of pK_a^s with α for stearic acid. Also shown are the changes in pH_s and pH_b with α. pK_a^s is estimated at $\alpha=0$ to be about 5.4.

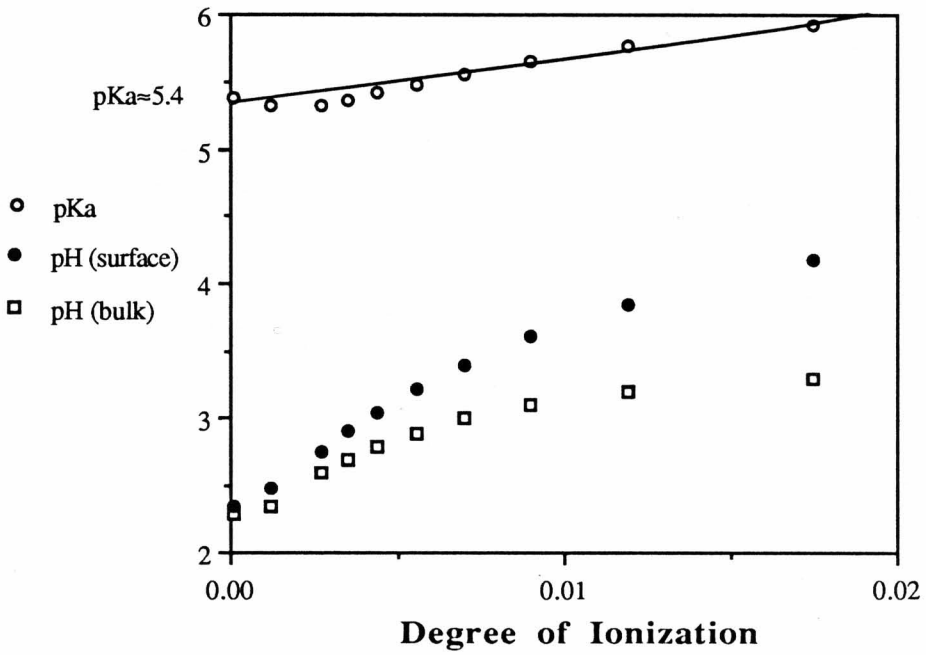

Figure 30. Plot of change of pK_a^s with α for arachidic acid. Also shown are the changes in pH_s and pH_b with α. pK_a^s is estimated at $\alpha=0$ to be about 5.4.

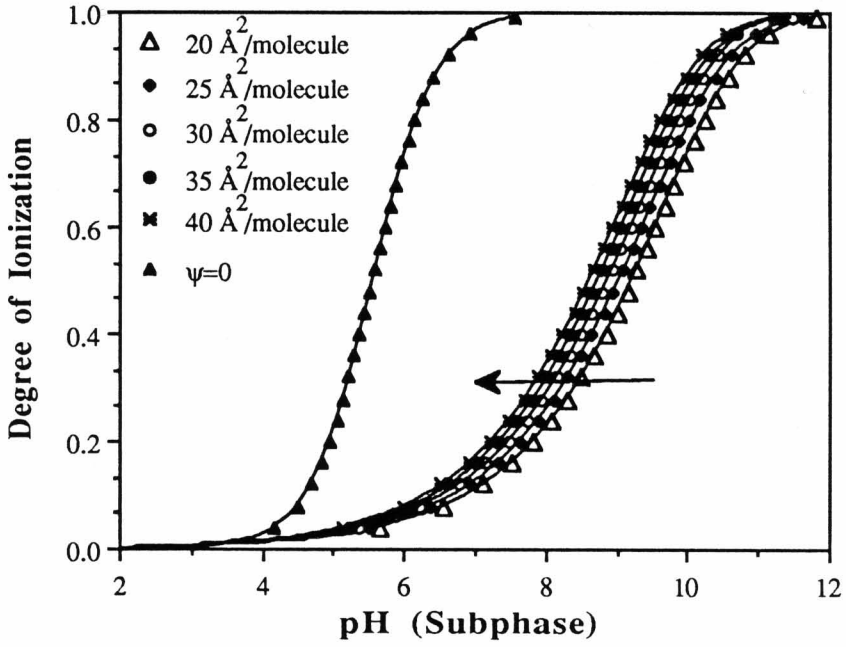

Figure 31. Simulation of α vs. pH(subphase) using Gouy-Chapman equations assuming $pK_a^s=5.4$ at T=25° C, C=0.01M, z=1, and different A (area occupied per molecule). $\psi=0$ represents the profile in the absence of an electrostatic potential due to the electrical double layers. The arrow is in drawn in the direction of larger areas ($Å^2$/molecule).

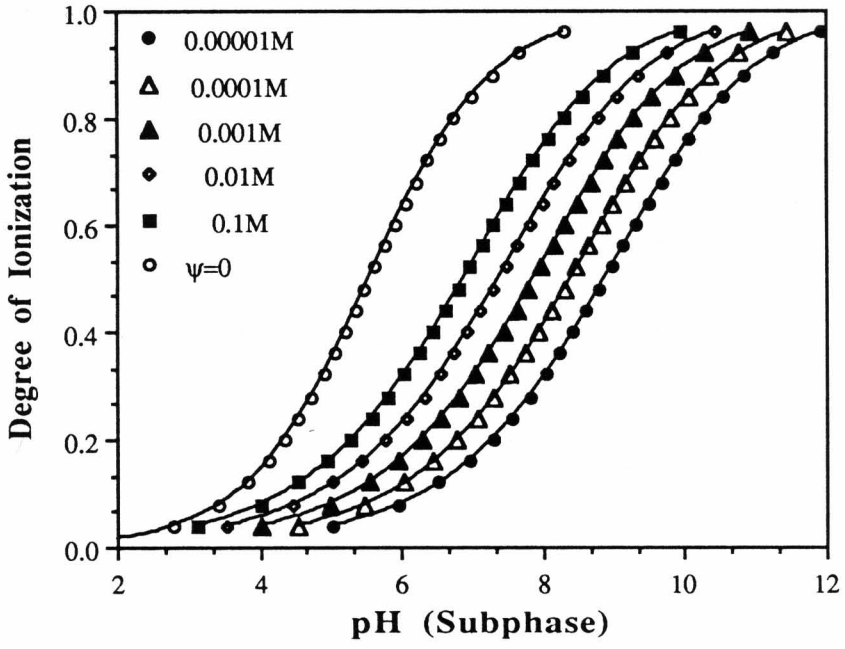

Figure 32. Simulation of α vs. pH(subphase) using Gouy-Chapman equations assuming $pK_a^s=5.4$ at T=25° C, z=2, A=20Å^2/molecule, and various concentrations of ions. $\psi=0$ represents the profile in the absence of an electrostatic potential due to the electrical double layers.

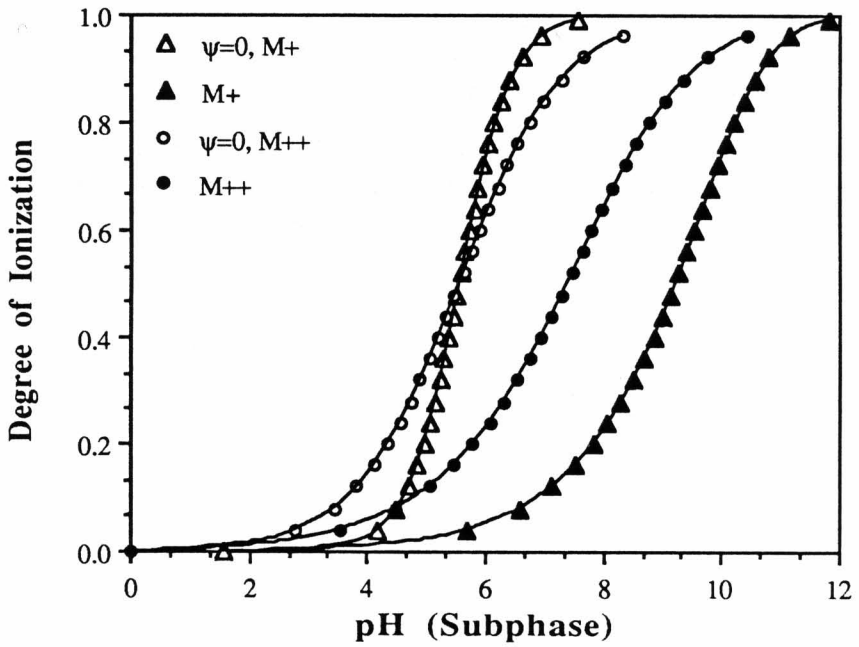

Figure 33. Simulation of α vs. pH(subphase) using Gouy-Chapman equations assuming pK_a^s=5.4 at A=20Å^2/molecule, T=25° C, and 0.001M univalent (M+) and divalent (M++) ions. ψ=0 represents the profile in the absence of an electrostatic potential due to the electrical double layers.

	Surface Potential (mV)			
	pH 3.0	pH 4.0	pH 5.0	pH 6.0
NaCl	375±12	350±3	335±8	293±8
$MgCl_2$	-	-	-	293±6
$CaCl_2$	-	-	328±8	291±11
$BaCl_2$	-	-	-	334±5
$CoCl_2$	-	-	330±6	274±4
$CdCl_2$	-	-	337±6	157±9
$PbCl_2$	373±8	345±9	212±7	154±12

Table II. Surface potential as a function of pH at 20$Å^2$/molecule, 1mM divalent cation, and μ=0.01M. Error estimates are for 95% confidence limit intervals as calculated from Student's t-distribution.

differences in ΔV in the absence or presence of various divalent ions except for Pb^{2+} which lowered ΔV. The effect of Pb^{2+} on ΔV diminished at pH ≤ 4.0.

The Effect of Divalent Ion Concentration

At pH 6.0, as shown in Figure 34, the surface potential of systems containing various divalent ions changed significantly depending on the type and concentration of each ion. The alkaline earth ions produced an increasingly more positive change in ΔV in the order of $Mg^{2+}<Ca^{2+}<Ba^{2+}$, whereas, the other ions produced an increasingly more negative ΔV in the order of $Co^{2+}<Cd^{2+}<Pb^{2+}$. In all cases the effect increases with increasing ion concentration to an apparent constant value.

The Effect of Anionic Counter-ions

The effects of various anionic counter-ions on surface potential at pH 6.0 and 20 $Å^2$/molecule are shown in Table III. Here, it can be seen that, whereas all the anionic counter-ions in the absence of divalent ions and in the presence of Ba^{2+} and Co^{2+} have no effect on ΔV, in the presence of Cd^{2+} and Pb^{2+} some counter-ions, e.g. iodide and thiocyanate, tend to make ΔV more positive. Such a counter-ion effect was not observed with the surface pressure measurements, described above.

The Effect of Polyamines

The presence of polyamines, e.g.. spermidine and spermine, did not alter ΔV significantly relative to Na^+, e.g. 294±6mV and 302±3mV respectively, even though there was a small condensing effect in terms of surface pressure. In some aspects, therefore, these polyamines with 3 or 4 charges per molecule behave somewhat like Mg^{2+}, but certainly not as

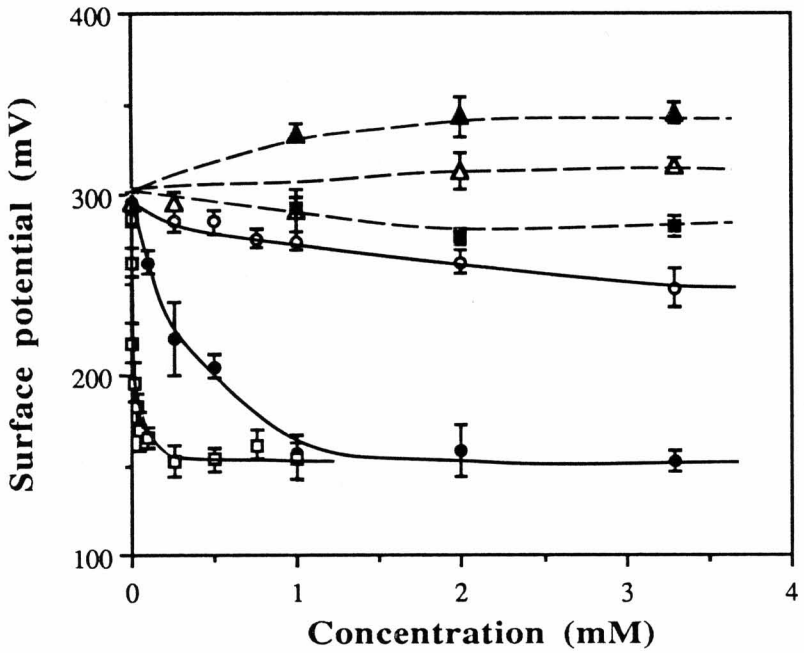

Figure 34. Concentration dependence of surface potential of stearic acid monolayers at 20 $Å^2$/molecule, 25°C, and pH 6.0: (▲) $BaCl_2$; (△) $CaCl_2$; (■) $MgCl_2$;(○) $CoCl_2$; (●) $CdCl_2$; (□) $PbCl_2$.

	Surface Potential (mV)				
	Na^+	Ba^{2+}	Cd^{2+}	Co^{2+}	Pb^{2+}
		Stearic Acid			
F^-	289±7	329±5	157±9	-	-
Cl^-	293±8	334±6	157±9	274±4	154±12
I^-	293±4	328±11	185±6	282±8[a]	-
SCN^-	288±10	329±10	214±6[b]	289±8[b]	194±9
$CH_3SO_3^-$	291±4	326±10[c]	162±8[c]	-	-
		Arachidic Acid			
Cl^-	280±5	327±7	174±4	-	-

Table III. Effect of anionic counter-ions on the surface potential of fatty acids, at pH 6.0, 20Å^2/molecule, and μ=0.01M.

a. 1mM chloride salt and excess NaI.

b. 1mM chloride salt and excess NaSCN.

c. 1mM chloride salt and excess CH_3SO_3Na.

Error estimates are for 95% confidence limit intervals as calculated from Student's t-distribution.

strongly as the other divalent ions. This would suggest that the effects of Cd^{2+} and Pb^{2+}, particularly, are due to more than an electrostatic interaction with the fatty acid.

Studies with Arachidic Acid

Similar results, with just a few selected ions as is shown in Table III with stearic acid, are seen with arachidic acid. At pH 6.0, Ba^{2+} appears to increase ΔV whereas Cd^{2+} results in a significant decrease in ΔV, as expected.

Surface Ellipsometry Measurements

Calibration and The Effect of pH

In order to calibrate the ellipsometry set-up, the changes in $\delta\Delta$ with respect to chain length and ionic environment were first examined. The values of $\delta\Delta$ vs. carbon number are reported under two sets of conditions: i) C15, C16, C18, and C22 spread on 10mM HCl, pH 2.0 and 1mM $PbCl_2$, and $CdCl_2$ on water (pH 5.5±0.2) at ϕ_o=64.1±0.1°; and ii) C18, C20, and C22 spread on 10mM HCl, pH 2.0 and 1mM $PbCl_2$, μ=0.01 (with NaCl), pH 6.0, at ϕ_o=61.8±0.1°. These data are plotted in Figures 35 and 36. As seen in these figures the change in $\delta\Delta$ in each case is linearly dependent on the chain length of the fatty acids. For the purpose of calibration the following scheme was followed. The change in $\delta\Delta$, $\delta(\delta\Delta)$, with respect to change in chain length (carbon number) of two fatty acids, C18 and C20, is τ=0.075 at ϕ_o=61.8±0.1°. This can be converted to a change in the actual length of these two fatty acids obtained from the literature, 24.5Å for C18 (Blodgett and Langmuir, 1937) and 27.1Å for C20

(Kjaer et al., 1988), by a constant, Λ=0.615. Another constant, Λ', can be calculated in order to calculate $\delta(\delta\Delta)$ in terms of carbon-carbon length of a fatty acid hydrocarbon chain. Λ' is calculated to be =0.0595, using C—C of 1.54Å and a tetrahedral bond angle of 109.5° (Karplus and Porter, 1970). Comparing Λ and Λ' , it can be seen that they are in good agreement, hence, the experimental $\delta\Delta$ values appear to reflect the actual length of the fatty acids.

Plots of $\Delta\delta$ vs. chain length (carbon number) give slopes which are identical within experimental error for fatty acid monolayers on 10mM HCl, pH 2.0 and 1mM $PbCl_2$ and $CdCl_2$ on water (pH 5.5) at ϕ_o=64.1±0.1° (Figure 35)and on 10mM HCl, pH 2.0 and 1mM $PbCl_2$, μ=0.01 (with NaCl), pH 6.0, at ϕ_o=61.8±0.1° (Figure 36). The intercept of about nine carbons for HCl is consistent with previous results (den Engelsen and de Koning, 1974). A number of factors could contribute to this unexpectedly low intercept including water structure in the head-group region, water penetration into the monolayer, or refractive index anisotropy. Negative values of $\delta\Delta$ for chain lengths less than nine are not physically reasonable, and due to fatty acid stability problems with smaller chain lengths, it is not known whether the linear extrapolation to $\delta\Delta$=0 is valid.

Comparing the intercepts of these plots, it can be seen that the magnitude of $\delta\Delta$ increases in the order of HCl, $CdCl_2$ and $PbCl_2$. Indeed, the relative effect of various metal ions at the same concentration on $\delta\Delta$ appears to follow the extent of their interaction with the carboxylate group. Pb^{2+} and Cd^{2+} compared to the other ions studied have shown the

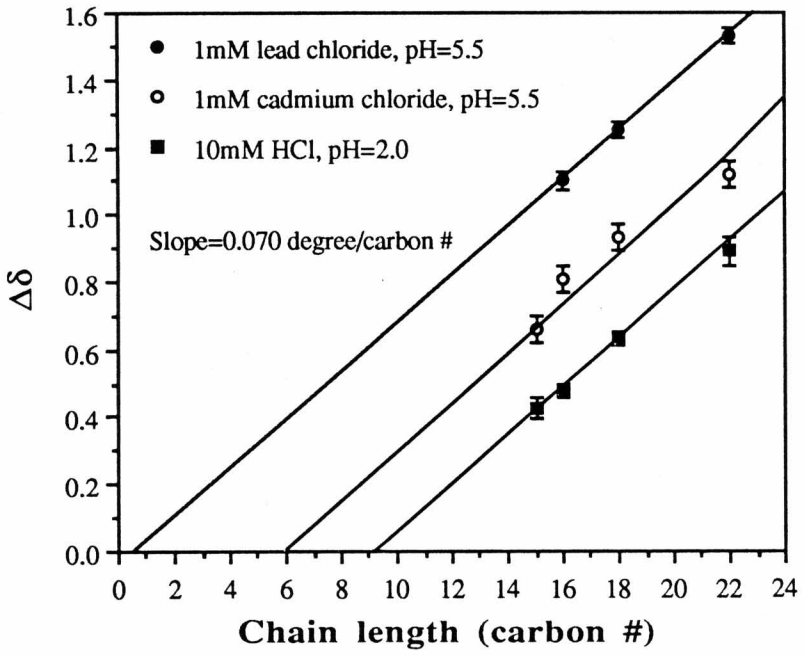

Figure 35. The chain length dependence of $\delta\Delta$, (ϕ_o=64.1±0.1°).

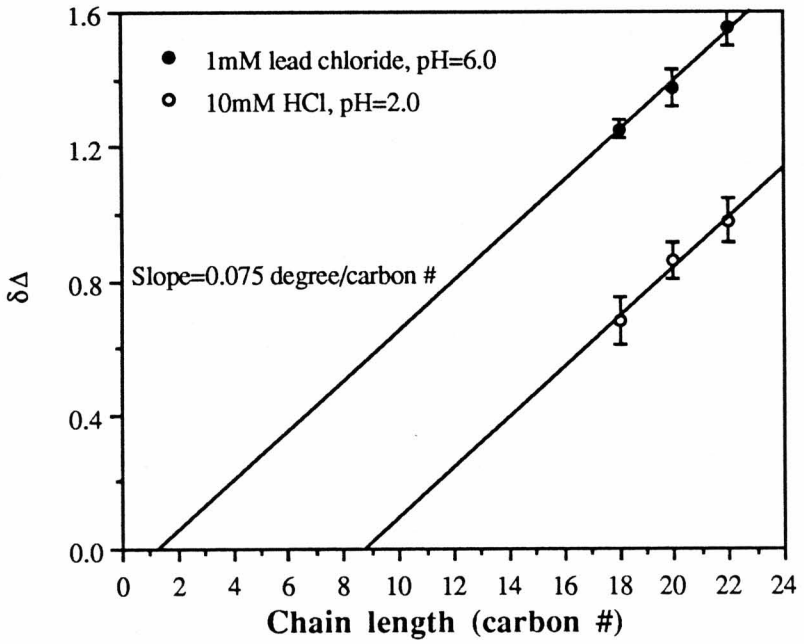

Figure 36. The chain length dependence of $\delta\Delta$, (ϕ_o=61.8±0.1°).

most significant effects with respect to condensation of the Π-A isotherms and change in surface potential values at pH 6.0 and μ=0.01. These two ions also show the most extreme effects on $\delta\Delta$ values, perhaps due to their strong interaction with the carboxylic acid group.

Regardless of the intercepts, the values of $\delta\Delta$ in Figures 35-36 increase because of a change in hydrocarbon chain thickness for a given ionic environment. Since it has been shown that the fatty acid monolayers with and without Cd^{2+} have the same thickness (Grundy et al. 1988), and the slopes of the lines, τ, in Figures 35-36 are shown to be constant irrespective of the ionic environment, the change in the magnitude of $\delta\Delta$ is attributed to the change in surface optical properties caused by the particular carboxylate-metal ion interaction. This is consistent with a two-layer model, where the bottom layer consists of head groups and the top one of hydrocarbon chains. In this regard, the Drude equation (equation 35), derived based on the assumption of a single layer on the surface, does not apply here and may be modified empirically to

$$\delta\Delta=\alpha d_1+\beta \qquad (51)$$

where β is a constant (intercept) that depends on the type of metal ion-carboxylate interaction, to account for the two-layer model. The thickness of a specified fatty acid can, in principle, be calculated by calculating α using estimated values of the refractive index and the slope of the $\delta\Delta$ vs. chain length plots. Unfortunately, refractive index anisotropy causes this approach to be ambiguous. For example, Kim et al., have shown that the chain length dependence of $\delta\Delta$ is consistent with some anisotropic

refractive indices reported in the literature for LB films while deviating considerably with others (Kim et al., 1990). Consequently, the thicknesses for specific fatty acids in the presence of various metal ions are not calculated since there are too many experimental variables required to determine unique values of the anisotropic refractive indices.

Table IV lists the values of $\delta\Delta$ in the presence of 1mM concentrations of various cations at pH 6.0 and μ=0.01M. In the presence of 0.01M NaCl at pH 6.0 the value of $\delta\Delta$ is the same within experimental error as that in the presence of 0.01M HCl at pH 2.0. The presence of 1mM chloride salts of magnesium, calcium, barium, and cobalt also does not appear to significantly change the value of $\delta\Delta$. However, $\delta\Delta$ values change in the presence of 1mM chloride salts of cadmium and lead, the latter having the most significant effect.

The change in $\delta\Delta$ with change in pH in the presence of Pb^{2+} and Cd^{2+} is shown in Figure 37. Here, the effect of Pb^{2+} on $\delta\Delta$ is constant at pH 6.0 to 5.0 and decreases sharply between pH 5.0 and 3.0 with a half-way point of pH 4.0. At pH$\leq$3.0 the $\delta\Delta$ values in the presence of Pb^{2+} are the same as in the presence of Na^{+}. Simultaneous Π-A measurements showed extreme condensation at pH 4.0 to 6.0 and expansion at pH$\leq$3.0. This is shown in Figure 38.

Cd^{2+}, on the other hand, decreased $\delta\Delta$ from pH 6.0 to 5.0 and levelled off to a value similar to that in the presence of Na^{+} at pH < 5.0. This is consistent with the effect of Cd^{2+} on the surface pressure and surface potential (Figure 16 and Table II).

Salt	$\delta\Delta°$
NaCl	0.69±0.02
$MgCl_2$	0.72±0.02
$CaCl_2$	0.73±0.03
$BaCl_2$	0.71±0.10
$CoCl_2$	0.75±0.03
$CdCl_2$	0.87±0.01
$PbCl_2$	1.25±0.02

Table IV. Phase angle ($\delta\Delta$) of stearic acid in the presence of 0.01M NaCl and 1mM divalent cations at pH=6.0, μ=0.01M, and ϕ_o=61.8±0.1°. Error estimates are for 95% confidence limit intervals as calculated from Student's t-distribution.

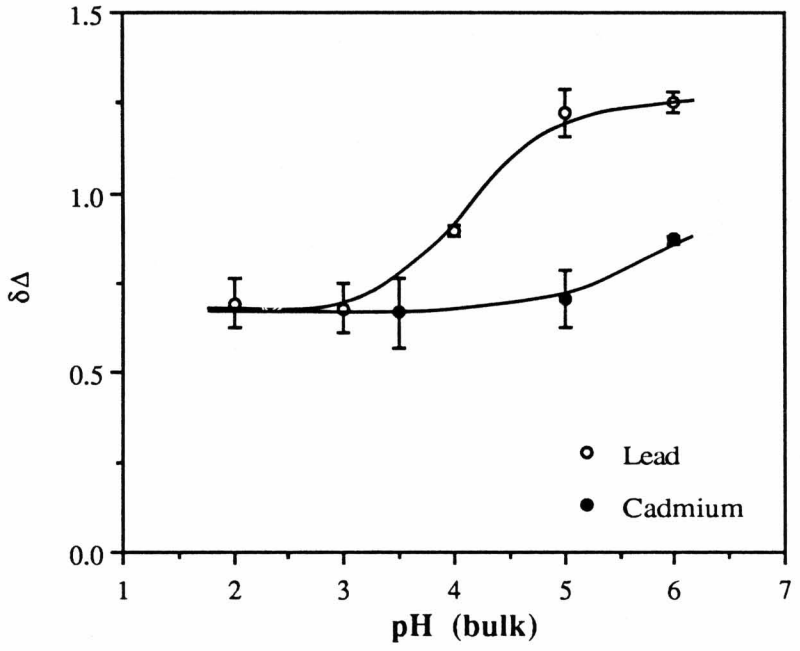

Figure 37. The pH dependence of $\delta\Delta$ in the presence of 1mM $PbCl_2$ and $CdCl_2$, μ=0.01M, and ϕ_o=61.8° ±0.1.

Figure 38. Π-A isotherms of stearic acid in the presence of 1mM $PbCl_2$, μ=0.01M, at pH 2.0 to 6.0, measured by the horizontal float method.

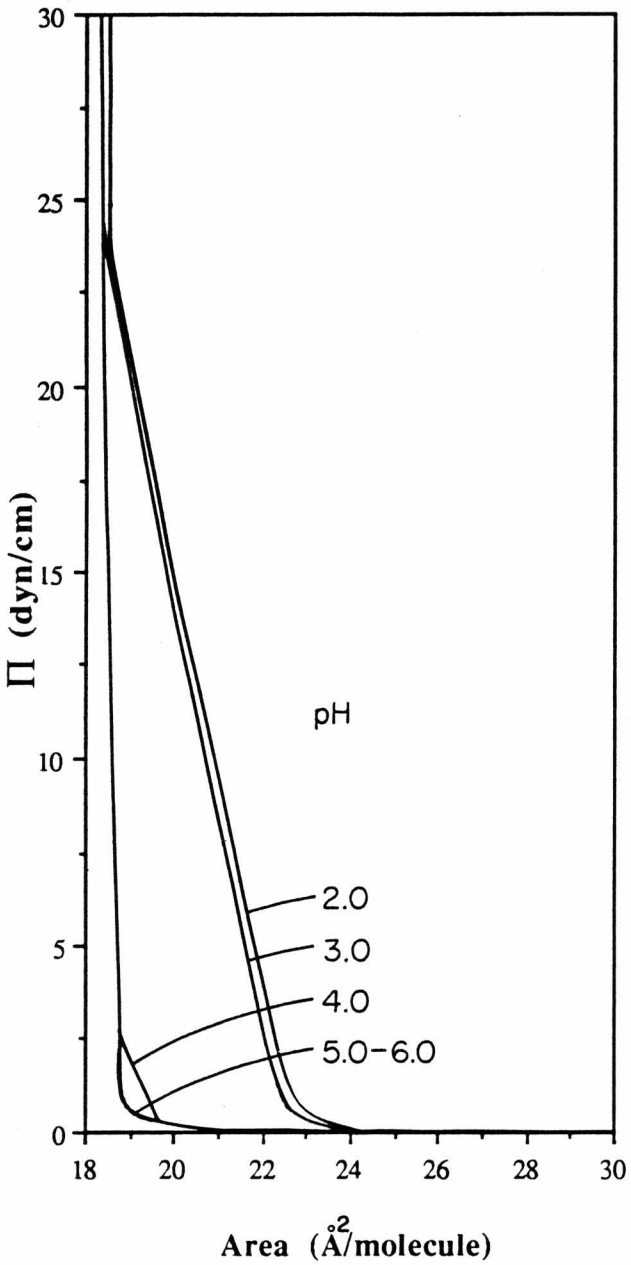
30
25
20
15
10
5
0
Π (dyn/cm)
pH
2.0
3.0
4.0
5.0-6.0
18
20
22
24
26
28
30
Area (Å²/molecule)

The Effect of Divalent Ion Concentration

Figure 39 shows the profile of change in $\delta\Delta$ with concentration over a wide range of $PbCl_2$ concentrations. It can be seen that the $\delta\Delta$ values show a marked dependence on the subphase $PbCl_2$ concentrations. The values for $\delta\Delta$ are fairly constant from 1.0 to 0.1mM and start to decrease at 0.01mM and level off at 0.0005mM to a value equal to that in the absence of Pb^{2+}. Simultaneous Π-A measurements showed extreme condensation up to 0.00125mM. The isotherms gradually expanded with further reduction in Pb^{2+} concentration towards that which occurs in the absence of Pb^{2+} at pH 6.0 (Figure 40).

The concentration range where Cd^{2+} is effective in altering $\delta\Delta$ is between 0.1mM and 1mM. These results, tabulated in Table V are consistent with the effect of Cd^{2+} on the Π-A isotherms as is seen in Figure 19.

The Effect of Sodium Chloride Concentration

$\delta\Delta$ appears to be very sensitive to the overall composition of cations at the surface. This can be seen by the change in $\delta\Delta$ under constant Cd^{2+} concentration and different Na^+ concentrations (Table VI). Cd^{2+} has the most significant effect on $\delta\Delta$ in the absence of Na^+. Increasing the Na^+ concentration and hence the ionic strength of the subphase solution appears to diminish the effect of Cd^{2+} as measured by a gradual decrease in $\delta\Delta$ down to a saturation concentration of about 7mM NaCl, above which $\delta\Delta$ remained constant. The value of $\delta\Delta$ at this saturation level is higher than that in the presence of Na^+ alone at pH 6.0. Moreover, the Π-A isotherms exhibited total condensation at all concentrations. These results

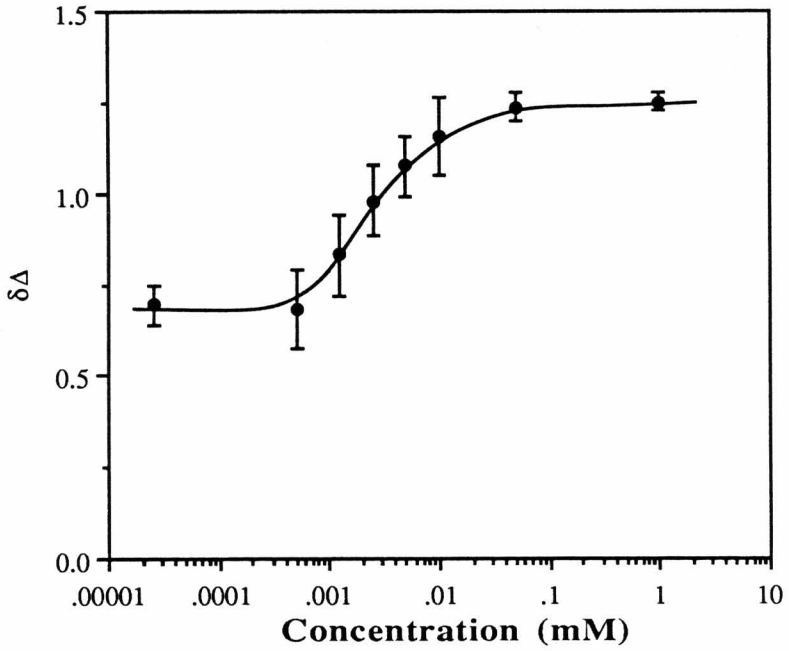

Figure 39. The concentration dependence of $\delta\Delta$ in the presence of $PbCl_2$, at pH 6.0, μ=0.01M, and ϕ_o=61.8±0.1°.

Figure 40. Π-A isotherms of stearic acid in the presence of various $PbCl_2$ concentrations, μ=0.01M, and pH 6.0, measured by the horizontal float method.

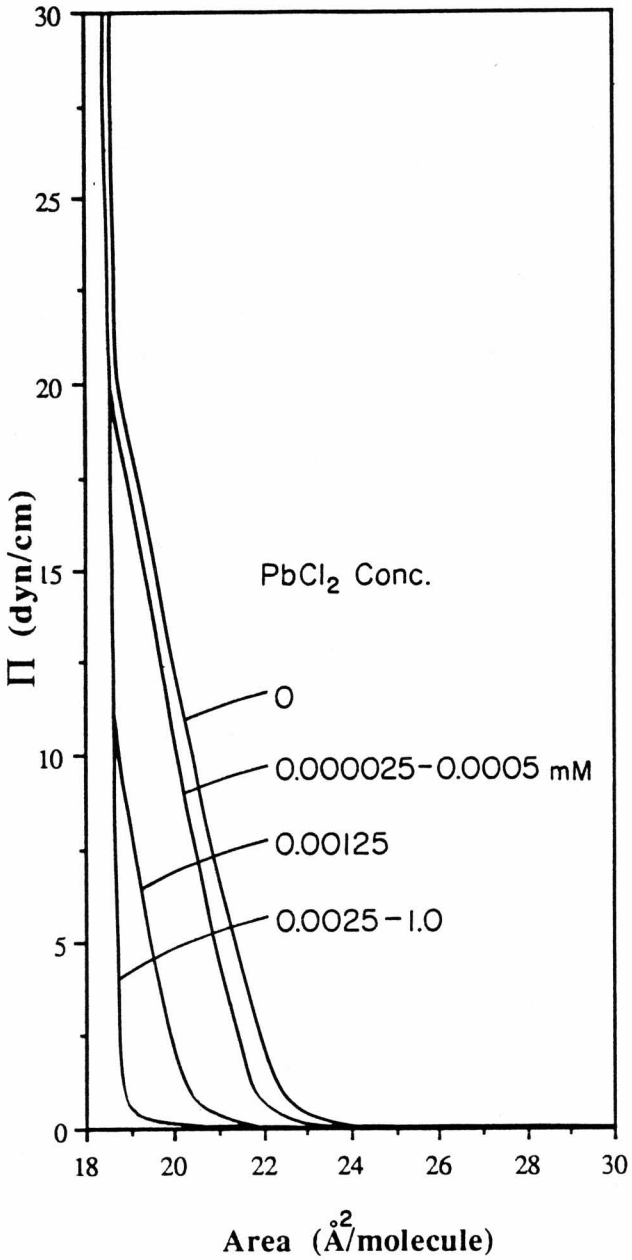
30
25
20
15
10
5
0
Π (dyn/cm)
PbCl2 Conc.
0
0.000025-0.0005 mM
0.00125
0.0025-1.0
18
20
22
24
26
28
30
Area (Å2/molecule)

$CdCl_2$(mM)	δΔ°
0.0	0.63±0.04
0.1	0.78±0.04
0.2	0.89±0.04
0.5	0.85±0.03
1.0	0.93±0.02
10.0	0.95±0.03

Table V. Phase angle (δΔ) of stearic acid in the presence of varying concentrations of $CdCl_2$, at pH 5.5±0.2, and ϕ_o=64.1±0.1°. Error estimates are for 95% confidence limit intervals as calculated from Student's t-distribution.

$CdCl_2$(mM)	NaCl(mM)	μ(M)	δΔ°
1.0	0.0	0.003	0.98±0.01
1.0	2.0	0.005	0.95±0.03
1.0	5.0	0.008	0.90±0.03
1.0	7.0	0.010	0.87±0.01
1.0	20.0	0.023	0.86±0.04

Table VI. Phase angle (δΔ) of stearic acid in the presence of 1mM $CdCl_2$ and varying concentrations of NaCl at pH 6.0 and ϕ_o=61.8±0.1°. Error estimates are for 95% confidence limit intervals as calculated from Student's t-distribution.

may be explained by attributing the initial decrease in $\delta\Delta$ to the ionic or electrostatic interaction of Na^+ with the unbound, "cadmium free" fatty acids at the surface as the concentration of these ions at the surface increases while Cd^{2+} concentration remains constant. At Na^+ concentrations above 7mM when all the surface "free sites" are occupied there is no more decrease in $\delta\Delta$ since Cd^{2+} is tightly bound and cannot be replaced.

The Effect of Anionic Counter-ions

It was shown in the last section that the surface potential measurements allowed the distinction of the effects caused by the presence of various anionic-counter-ions on the fatty acid-divalent ion interaction. For example, iodide and thiocyanate ions, in that order, were most effective in changing surface potential, whereas, fluoride and methanesulfonate ions had no effects. In this context, chloride, iodide, and thiocyanate ions were chosen to be studied by surface ellipsometry. The effect of these ions on $\delta\Delta$ at pH 6.0, μ=0.01M, and constant metal ion concentration is listed in Table VII. It can be seen that $\delta\Delta$ does not appear to be as sensitive as ΔV to the effects of these anionic counter-ions on the fatty acid-divalent ion interactions.

Anions \ Cations	Na^+	Ba^{2+}	Cd^{2+}	Pb^{2+}
	$\delta\Delta°$			
Cl-	0.69±0.02	0.71±0.10	0.87±0.01	1.25±0.02
I-	0.71±0.04	0.69±0.08	0.91±0.04	-
SCN-	0.72±0.04	0.71±0.06	0.94±0.05	1.29±0.05

Table VII. Phase angle ($\delta\Delta$) of stearic acid in the presence of various cations and anionic counter-ions at pH=6.0, μ=0.01M, and ϕ_o=61.8±0.1°. Error estimates are for 95% confidence limit intervals as calculated from Student's t-distribution.

Potentiometric Titration

To better understand fatty acid-metal ion interactions at the fatty acid monolayer interface, it would be useful to know whether or not complexation described by stability constants occurs. There is an extreme variation in the stability constant values reported in the literature for carboxylic acid (e.g. acetate ion) metal ion complexes due to different experimental conditions used and different methods of determination (Sillen, 1971, Högfeldt, 1982). Also, almost all the measurements reported in the literature were done in non-aqueous solutions. Hence, it appeared essential to determine the stability constants for various divalent ions under the conditions of our surface studies. Due to the water insolubility of stearic and arachidic acids, acetic acid was chosen as a model compound to be potentiometrically titrated with sodium hydroxide. A shift in the pK_a of the acetic acid in the presence of divalent ions could then be used to estimate stability constants (Calvin and Wilson, 1945, Irving and Rossotti, 1953, 1954).

The curves for the titration of 0.1M acetic acid with 0.1M NaOH in the presence of various concentrations of chloride salts of sodium, barium, cadmium, and lead are shown in Figures (41-46). In each case the middle portion of the titration curve is enlarged to more clearly demonstrate the effect of these ions on the titration curve. It can be seen that the presence of Cd^{2+} and Pb^{2+}, under constant ionic strength, results in a shift in the plateau region of the titration curve to lower pH values relative to that in the presence of sodium ions. This is an indication that the apparent pK_a, pK_a', of the acetic acid is lowered. Moreover, this shift appears to be

concentration dependent; for example, the effect of cadmium ions on the pK_a at 0.1M concentration is most significant, whereas, at 0.001M there appears to be no effect (Figures 45-46). Titration of lead ions at concentrations of higher than 0.01M could not be made due to the diminishing solubility of the various possible lead salts (Baes and Mesmer, 1976). Barium ions appear to have no effect on the titration curve in the range of concentrations studied. The intrinsic pK_a along with the apparent pK_a' values due to metal ions are estimated from the shift in the titration curves and tabulated in Table VIII.

Stability Constant Computation

It has been shown that pH measurements made during an acid-base titration can be used to calculate the stability constants of metal-ligand complexes present in solution (Calvin and Wilson, 1945, Irving and Rossotti, 1953, 1954). In the acetic acid-divalent ion systems, it is assumed that two equilibria may exist where the metal ion, M, complexes with the acid, A, as

$$M^{2+} + A^- = MA^+ \qquad (52)$$

$$MA^+ + A^- = MA_2 \qquad (53)$$

and that the species MAOH and MOH^+ are absent. The dissociation of the acid is given as

$$HA = A^- + H^+ \qquad (54)$$

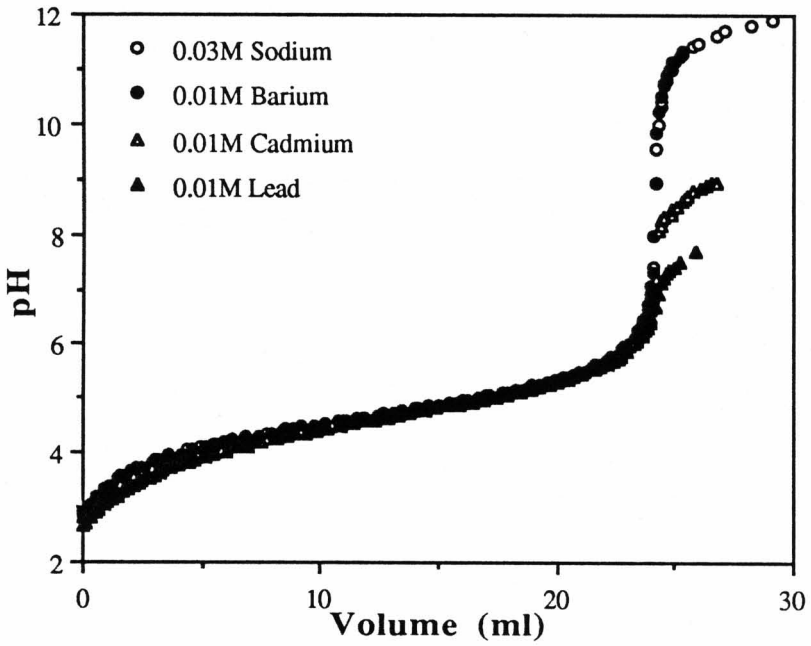

Figure 41. Titration of 0.1M acetic acid with 0.1M NaOH in the presence of 0.03M NaCl and 0.01M $BaCl_2$, $CdCl_2$, and $PbCl_2$ at μ=0.03M. The precipitation of cadmium and lead ions at higher pH values is marked by an early second plateau in the titration curve.

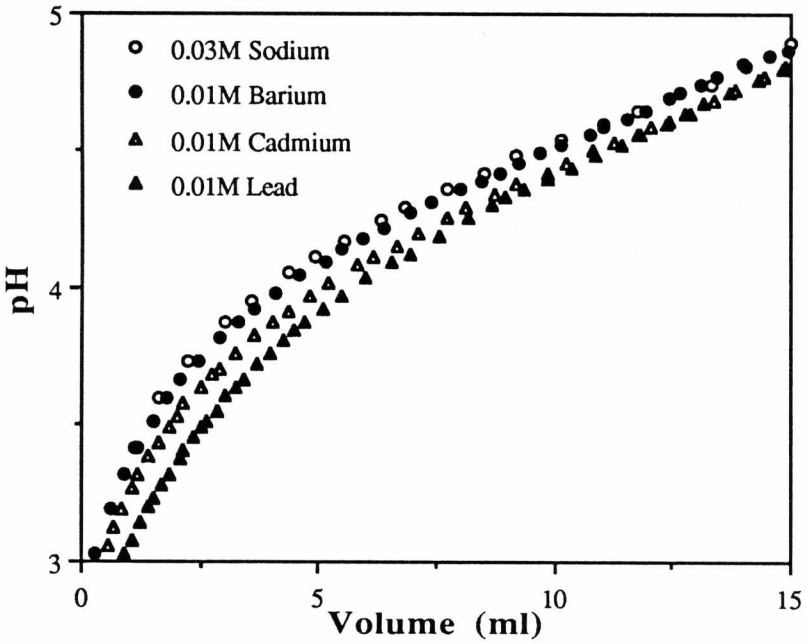

Figure 42. Enlarged portion of the early section of the titration curve of 0.1M acetic acid with 0.1M NaOH in the presence of 0.03M NaCl and 0.01M $BaCl_2$, $CdCl_2$, and $PbCl_2$ at μ=0.03M.

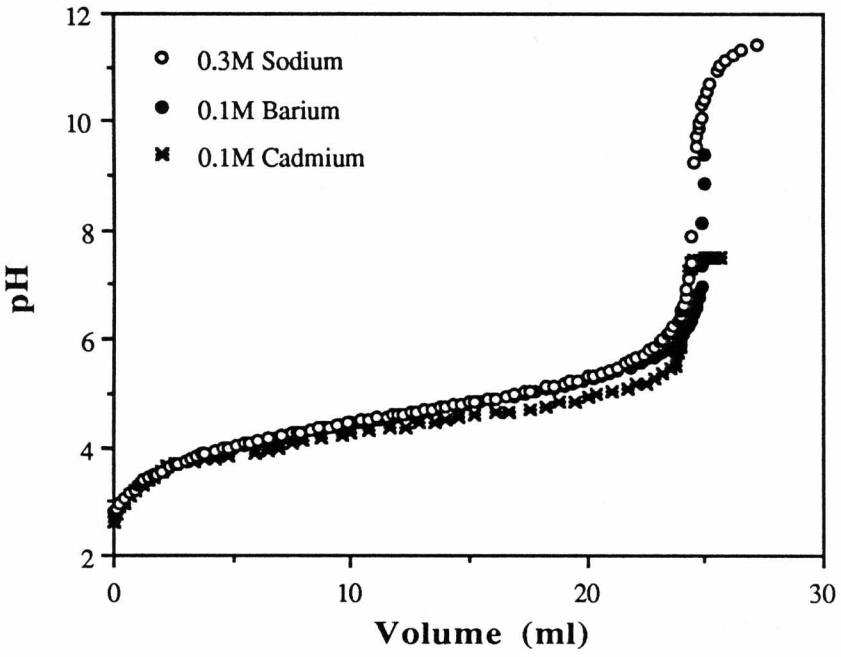

Figure 43. Titration of 0.1M acetic acid with 0.1M NaOH in the presence of 0.3M NaCl, 0.1M $BaCl_2$, and $CdCl_2$ at μ=0.03M. The precipitation of cadmium and barium ions at higher pH values is marked by an early second plateau in the titration curve.

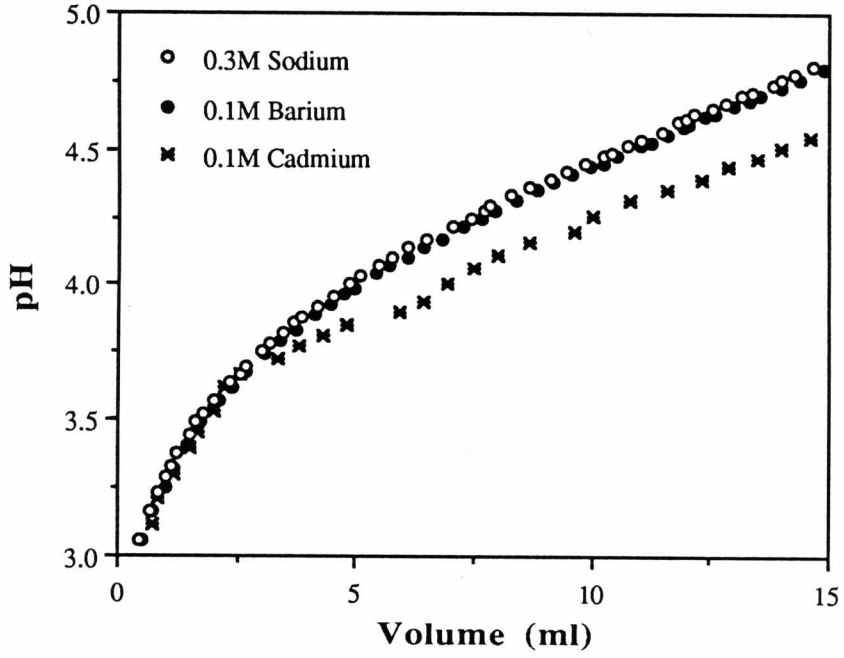

Figure 44. Enlarged portion of the early section of the titration curve of 0.1M acetic acid with 0.1M NaOH in the presence of 0.3M NaCl, 0.1M $BaCl_2$, and $CdCl_2$ at μ=0.03M.

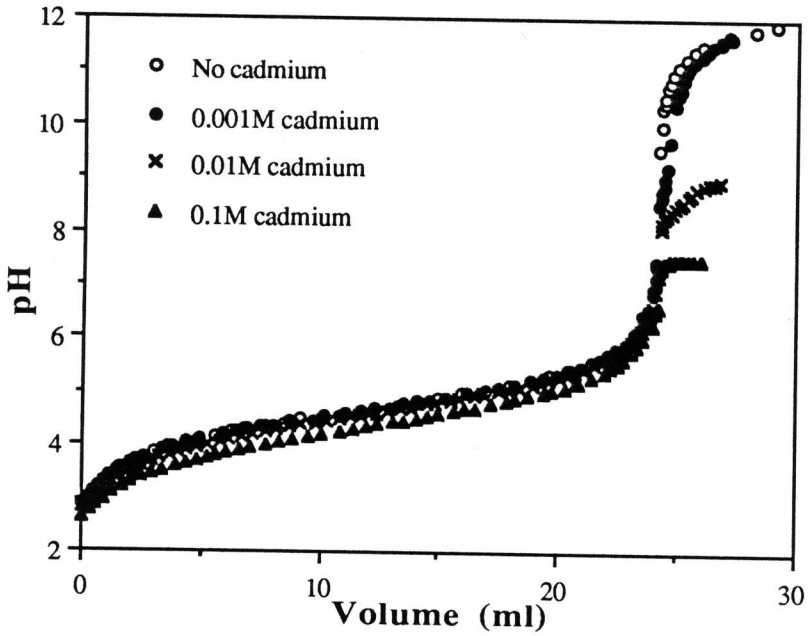

Figure 45. Titration of 0.1M acetic acid with 0.1M NaOH in the absence and presence various concentrations of $CdCl_2$.

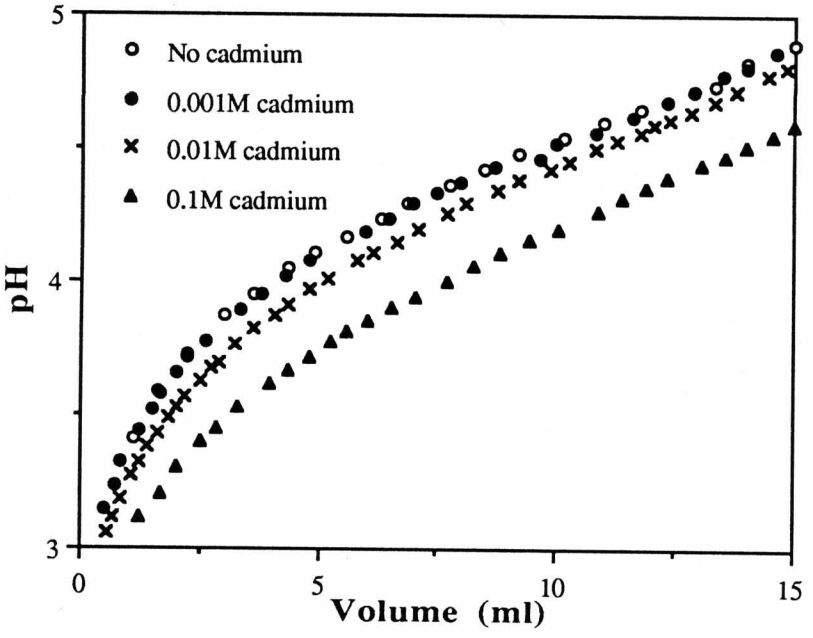

Figure 46. Enlarged portion of the early part of the titration curve of 0.1M acetic acid with 0.1M NaOH in the absence and presence various concentrations of $CdCl_2$.

Chloride salt	concentration(M)	μ(M)	pK_a	pK_a'
No Salt	-	0	4.73	-
Sodium	0.03	0.03	4.77	
	0.3	0.3	4.65	-
Barium	0.01	0.03	-	4.69
	0.1	0.3	-	4.64
Cadmium	0.001M	0.003	-	4.68
	0.01M	0.03	-	4.59
	0.1M	0.3	-	4.40
Lead	0.001M	0.003	-	4.69
	0.01M	0.03	-	4.56

Table VIII. The change in pK_a and pK_a' of acetic acid with change in the type and concentration of the salt solutions.

The various equilibrium constants for these processes can thus be defined as

$$K_1=\frac{[MA^+]}{[M^{2+}][A^-]} \qquad (55)$$

$$K_2=\frac{[MA_2]}{[MA^+][A^-]} \qquad (56)$$

$$K_a=\frac{[H^+][A^-]}{[HA]} \qquad (57)$$

where M^{2+}, MA^+, and MA_2 are the metal ion, the 1:1 metal-acid complex, and the 1:2 metal-acid complex, respectively.

The equations for the conservation of metal and acid are

$$T_M = [M^{2+}]+[MA^+]+[MA_2] \qquad (58)$$

$$T_{HA} = [HA]+[A^-]+[MA^+]+2[MA_2] \qquad (59)$$

where T_M and T_{HA} designate total metal ion and total acid present. Electroneutrality requires that

$$2[M^{2+}]+[MA^+]+[Na^+]+[H^+]=[OH^-]+[A^-]+[Cl^-] \qquad (60)$$

and since the metal ion is added as the chloride then

$$[Cl^-]=2T_M \qquad (61)$$

By combining equations 58-61, ñ, the average number of ligands bound per total metal ion, and $[A^-]$ are obtained as

$$\tilde{n} = \frac{[Na^+]+[H^+]-[OH^-]-[A^-]}{T_M} \qquad (62)$$

and

$$[A^-] = (\frac{K_a}{[H^+]})(T_{HA}-[Na^+]-[H^+]+[OH^-]) \qquad (63)$$

In the region of $pH \leq pK_a$ (Datta and Rabin, 1956), the stability constants can be calculated by the equation of Irving and Rossotti (Irving and Rossotti, 1953)

$$\frac{\tilde{n}}{(\tilde{n}-1)[A^-]} = \frac{(2-\tilde{n})[A^-]}{(\tilde{n}-1)} K_1K_2 - K_1 \qquad (64)$$

In the region of $\tilde{n}=1$, this equation becomes indeterminate, therefore data for which $1.1>\tilde{n}>0.9$ were rejected.

The stability constants were calculated from equation 64 for 0.01M cadmium and lead solutions in two ways: i) by graphically determining K_1 and K_2 from the slope and the intercept of least square fit linear plots, and ii) by rearranging equation 64 to

$$\tilde{n} = (2-\tilde{n})[A^-]^2K_1K_2 - (1-\tilde{n})[A^-]K_1 \qquad (65)$$

and using nonlinear regression of $\tilde{n}$ on $[A^-]$ using the SYSTAT (System for statistics, version 3.0, SYSTAT Inc., Evanston, Ill.) program. The linear plots for determining the stability constants for these two ions are shown in Figures 47-48, and the results from these plots along with the nonlinear regression results are tabulated in Table IX. It can be seen that Cd^{2+} and Pb^{2+} can form both 1:1 and 1:2 complexes with acetic acid and the numerical values obtained from both methods of determinations are in good agreement. Pb^{2+} appears to have relatively similar K_1 and K_2

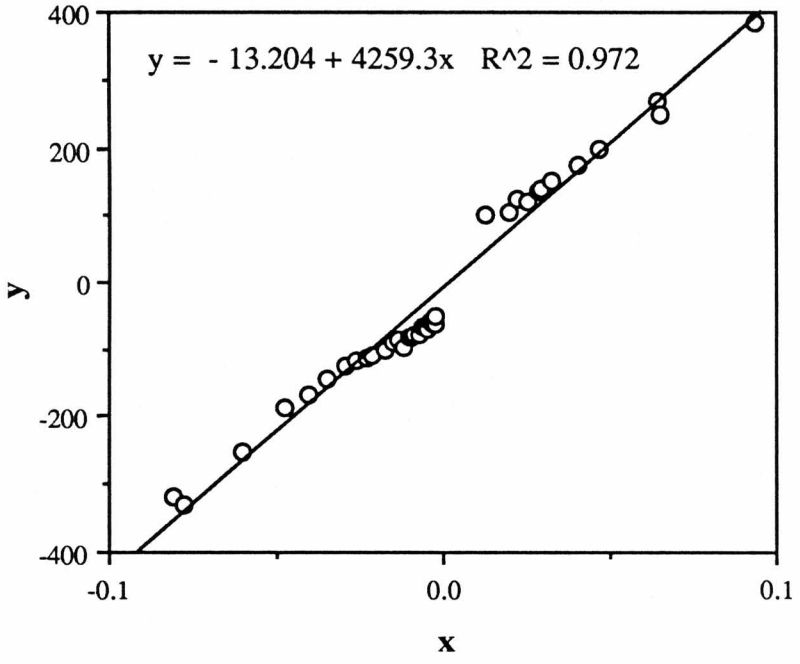

Figure 47. The linear plot from equation 64 for the calculation of the stability constants in the presence of 0.01M $CdCl_2$, where $x=\frac{(2-\tilde{n})[A^-]}{(\tilde{n}-1)}$ and $y=\frac{\tilde{n}}{(\tilde{n}-1)[A^-]}$. The equation of the line from the least square fit is also given, where R^2 represents the correlation coefficient for the fit.

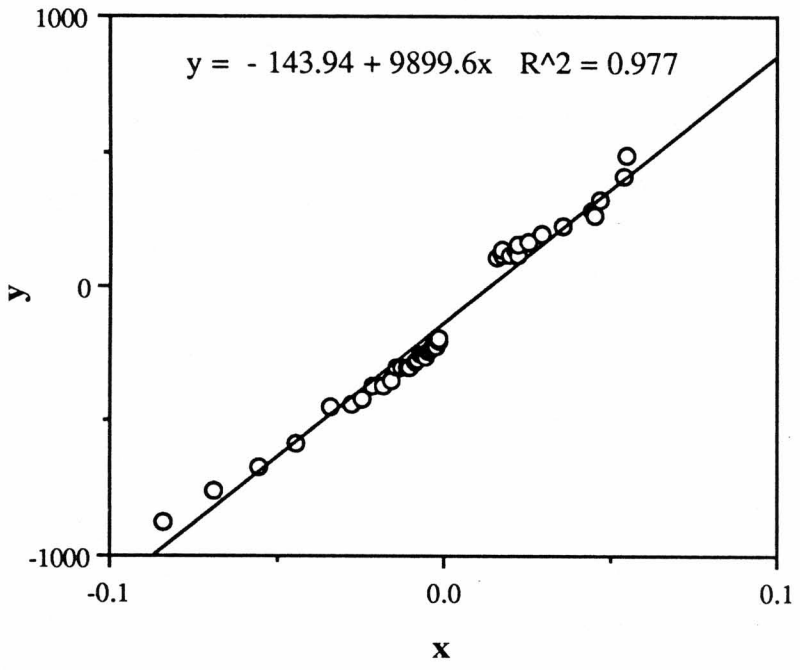

Figure 48. The linear plot from equation 64 for the calculation of the stability constants in the presence of 0.01M $PbCl_2$, where $x=\frac{(2-\tilde{n})[A^-]}{(\tilde{n}-1)}$ and $y=\frac{\tilde{n}}{(\tilde{n}-1)[A^-]}$. The equation of the line from the least square fit is also given, where R^2 represents the correlation coefficient for the fit.

	Least square fit		Non-linear regression	
Metal ion	K_1	K_2	K_1	K_2
Cadmium	13	323	13±4	328±114
Lead	129	77	121±12	79±11

Table IX. The stability constants of acetic acid , K_1 and K_2 in units 1/M, with 0.01M $CdCl_2$ and $PbCl_2$ calculated by the least square linear fit and nonlinear regression.

values, whereas, K_2 values are much larger than K_1 values for Cd^{2+}. Therefore, it is likely that there is an equal probability of having both 1:1 and 1:2 complexes for Pb^{2+}, whereas, Cd^{2+} tends to form mostly 1:2 complexes with carboxylates. The stability constants at 0.001M concentrations of cadmium and lead ions and for barium ions at all concentrations could not be calculated due to the absence of a discernible shift in the titration curves. At 0.1M cadmium concentration, stability constants could not be calculated since the metal ion concentration was much higher than the acid concentration, i.e. there was not enough ligand present to bond with the metal.

Measurements of Rheological Properties

The spatial capillary wave vector, k, and the spatial capillary wave damping coefficient, β, obtained from the ECWD measurements were used in the Lucassen-Reynders dispersion equation (equation 26) to calculate longitudinal surface elasticity, ε_l, and longitudinal surface viscosity, κ, of stearic acid monolayers under a variety of experimental conditions. The basic assumptions for these calculations are that the transverse viscosity, μ_v, is negligible and that $\gamma^*=\gamma$. The first assumption has been shown to be valid from surface light scattering studies of small amphiphiles and polymers (Chen, 1986). The second assumption, in this case, may result in some uncertainty since γ could not be measured simultaneously in these experiments, and γ values for a given area were taken from the Π-A measurements and used in the dispersion equation. The error associated with the uncertainty in γ in estimating the viscoelastic parameters from the

dispersion equation affects the calculation of κ more drastically than ε_l. For example, varying the static surface tension by 5 dyn/cm changes ε_l by 1 dyn/cm, whereas, it can change κ as much as two orders of magnitude.

The ECWD data are presented in terms of plots of ε_l, κ, and viscous loss modulus, $\omega\kappa$, all as a function of frequency. ε_l and $\omega\kappa$ have the same dimensions and allow comparisons between elastic and viscous contributions to the overall surface modulus (see equation 27). The error bars in the plots represent the standard deviations from the mean of at least three independent measurements.

Preliminary studies were done with stearic acid at pH 2.0 to determine the viscoelastic parameters at different surface concentrations (areas per molecule). Figures 49-51 show ε_l, κ, and $\omega\kappa$ values at 20.0Å^2/molecule and 20.5Å^2/molecule, and indicate that there are no significant differences in the rheological parameters for monolayers at these two areas. This is in good agreement with $\delta\Delta$ and ΔV measurements that also reach a constant value at areas <24Å^2/molecule, thus allowing the comparison of the ECWD results with these other techniques. Also, it can be seen that both ε_l and $\omega\kappa$ are essentially frequency independent. In physical terms, this means that the time scale for the molecular motion and relaxation at these two areas is much faster than the time scale covered in the range of the frequencies studied, i.e. 100 to 5000Hz. A more detailed discussion and analysis of the frequency dependence of the viscoelastic parameters is given later in this section.

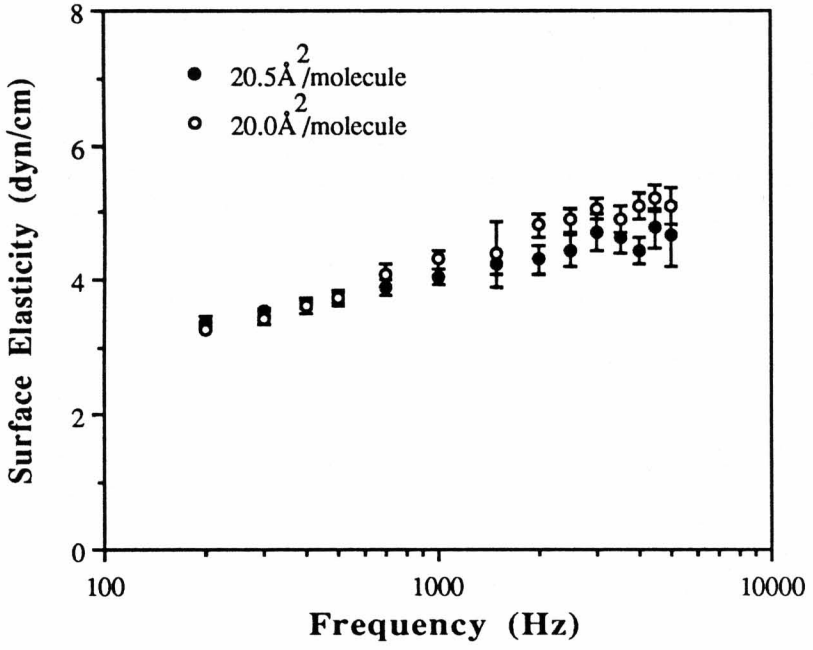

Figure 49. Surface elasticity vs. frequency for stearic acid in the presence of 0.01M HCl at pH 2.0 and different areas occupied per molecule.

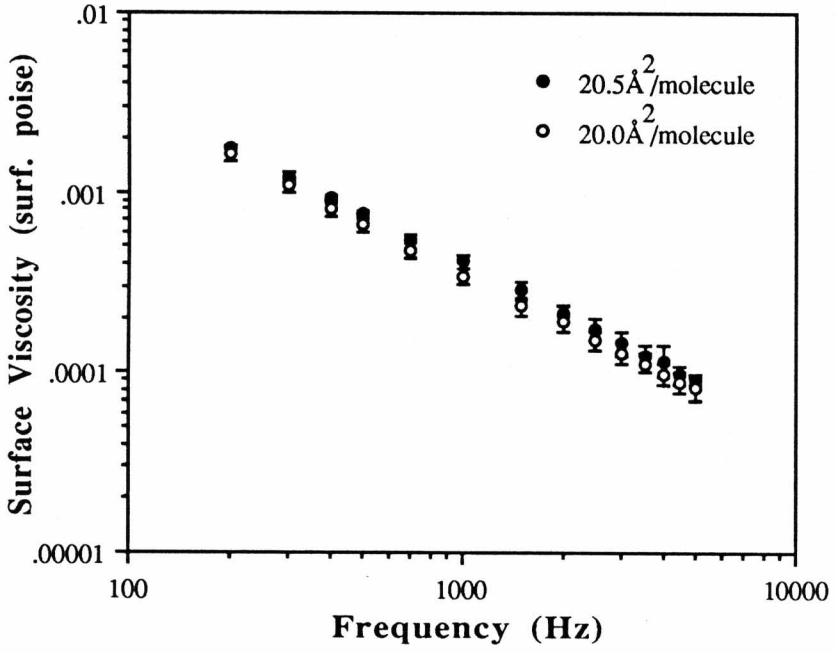

Figure 50. Surface viscosity vs. frequency for stearic acid in the presence of 0.01M HCl at pH 2.0 and different areas occupied per molecule.

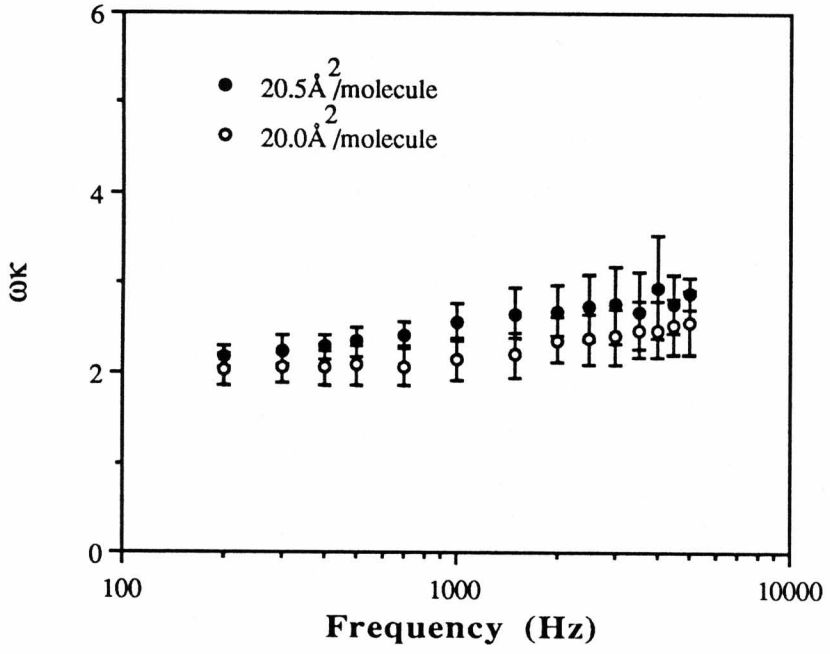

Figure 51. Viscous loss modulus vs. frequency for stearic acid in the presence of 0.01M HCl at pH 2.0 and different areas occupied per molecule.

The Effect of pH

ε_l, κ, and $\omega\kappa$ for stearic acid at 20.5Å^2/molecule from 0.01M HCl at pH 2.0 to 0.01M NaCl at pH 6.0 are shown in Figures 52-54. It can be seen that as the pH is increased from 2.0 to 6.0; ε_l, κ, and $\omega\kappa$ appear to slightly decrease. This decrease in each case can be attributed to the change in the degree of the ionization of the monolayer from one that is completely unionized at pH 2.0 to one that is partially ionized at pH 6.0. Again it can be seen that both ε_l and $\omega\kappa$ are frequency independent.

The Effect of Divalent Cations

The introduction of 1mM salts of alkaline earth ions at pH 6.0 slightly increases the overall magnitude of ε_l, κ, and $\omega\kappa$ (Figures 55-57). Moreover, ε_l exhibits slightly higher values with an increase in frequency, whereas, $\omega\kappa$ is frequency independent. The presence of Co^{2+} results in exactly the same changes in ε_l, κ, and $\omega\kappa$ as those seen with alkaline earth ions (Figures 58-60). However, The presence of Cd^{2+} results in slightly higher ε_l values than those in the presence of alkaline earth ions and Co^{2+} and lower κ values than those obtained with all other ions including Na^+. Similar to alkaline earth ions, ε_l for Cd^{2+} and Co^{2+} is slightly frequency dependent and $\omega\kappa$ is frequency independent.

In the presence of Pb^{2+} the stearic acid monolayer exhibits much higher values for ε_l, κ, and $\omega\kappa$ than those obtained with all other ions including Na^+ (Figures 61-63). Here, ε_l is clearly frequency dependent and $\omega\kappa$ is frequency independent.

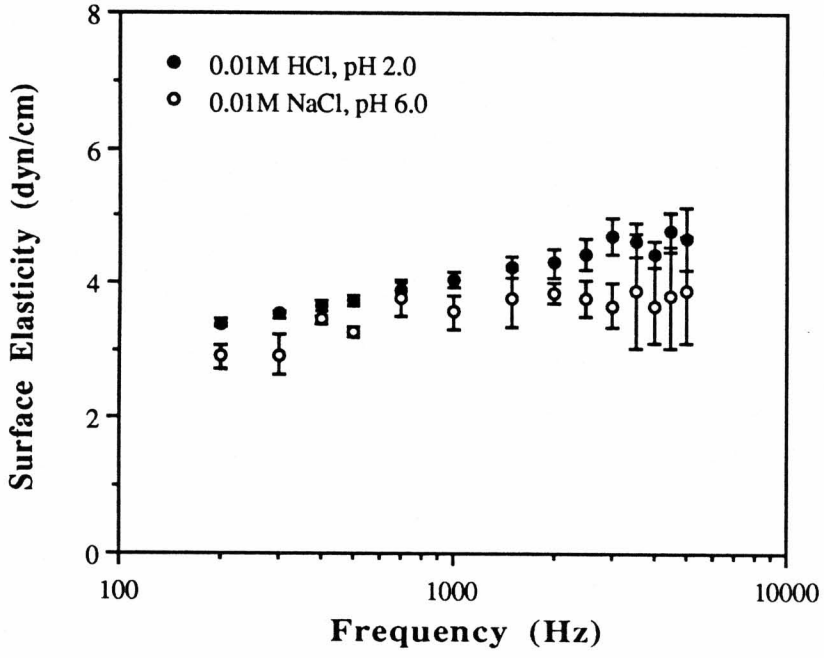

Figure 52. Surface elasticity vs. frequency for stearic acid in the presence of 0.01M HCl at pH 2.0 and 0.01M NaCl at pH 6.0 at 20.5Å^2/molecule.

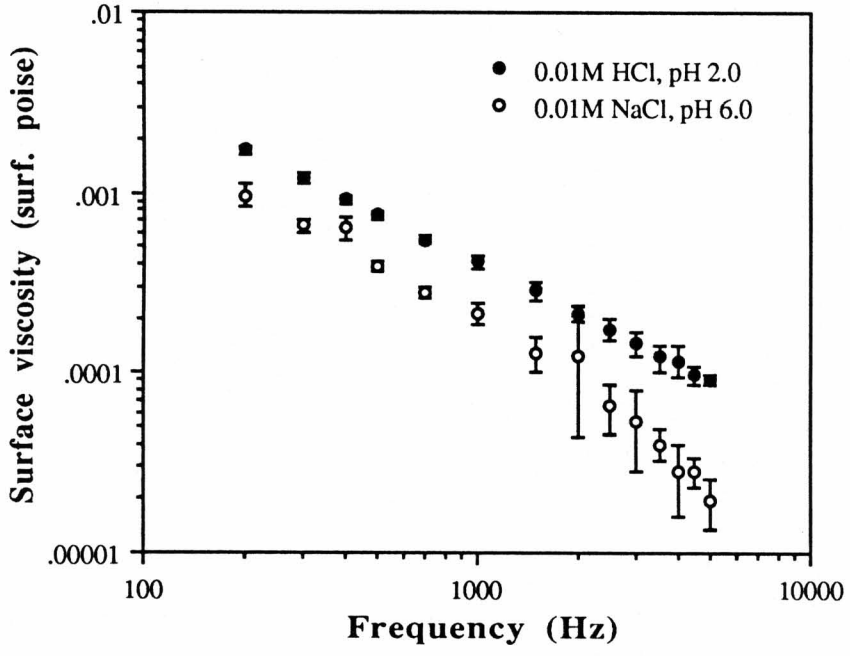

Figure 53. Surface viscosity vs. frequency for stearic acid in the presence of 0.01M HCl at pH 2.0 and 0.01M NaCl at pH 6.0 at 20.5Å^2/molecule.

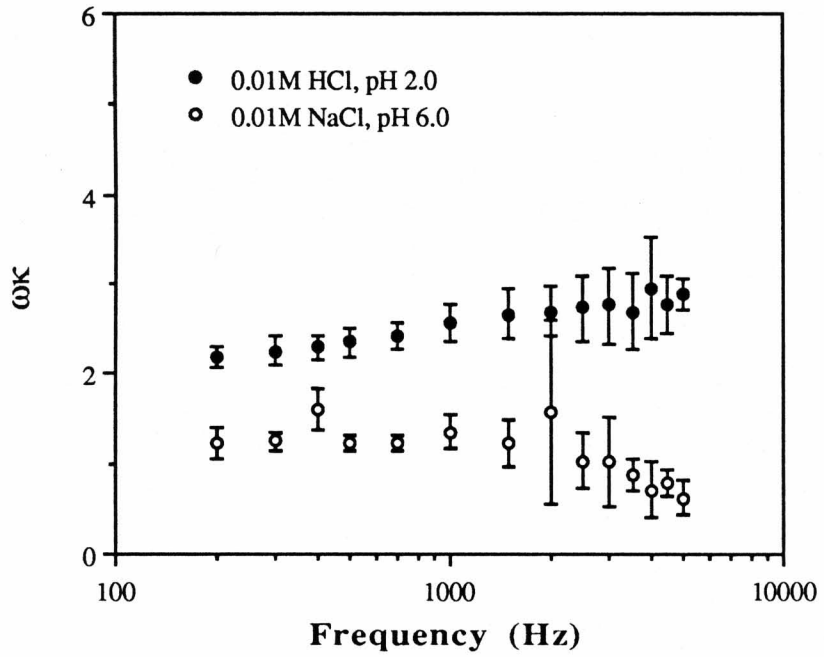

Figure 54. Viscous loss modulus vs. frequency for stearic acid in the presence of 0.01M HCl at pH 2.0 and 0.01M NaCl at pH 6.0 at 20.5Å^2/molecule.

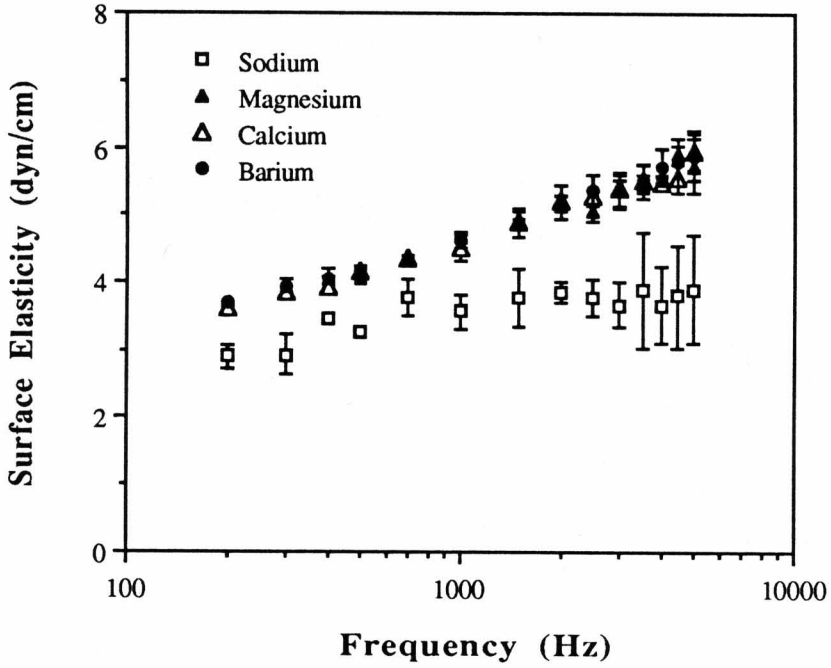

Figure 55. Surface elasticity vs. frequency for stearic acid in the presence of 1mM of chloride salts of magnesium, calcium, and barium relative to that of 0.01M sodium chloride at pH 6.0 and μ=0.01M.

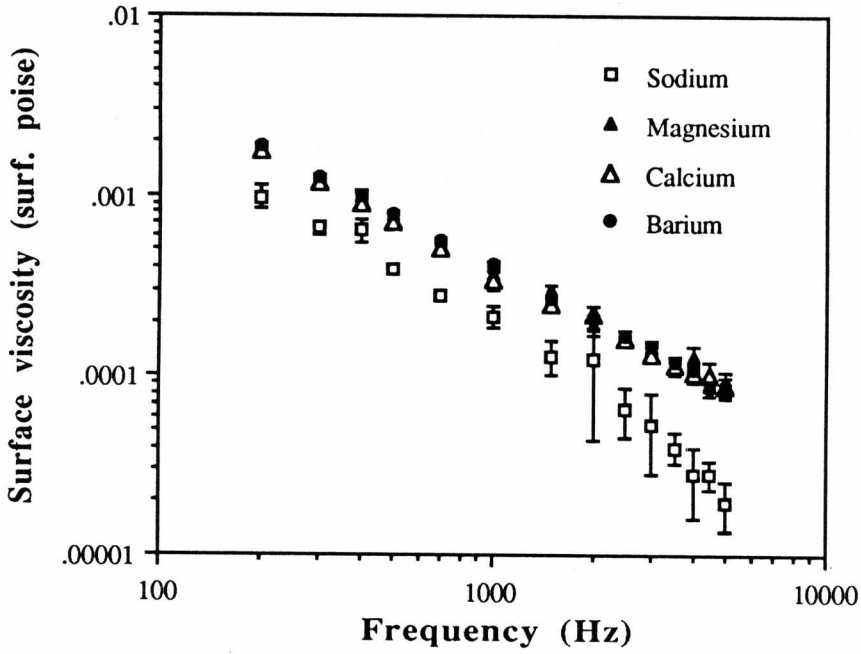

Figure 56. Surface viscosity vs. frequency for stearic acid in the presence of 1mM of chloride salts of magnesium, calcium, and barium relative to that of 0.01M sodium chloride at pH 6.0 and μ=0.01M.

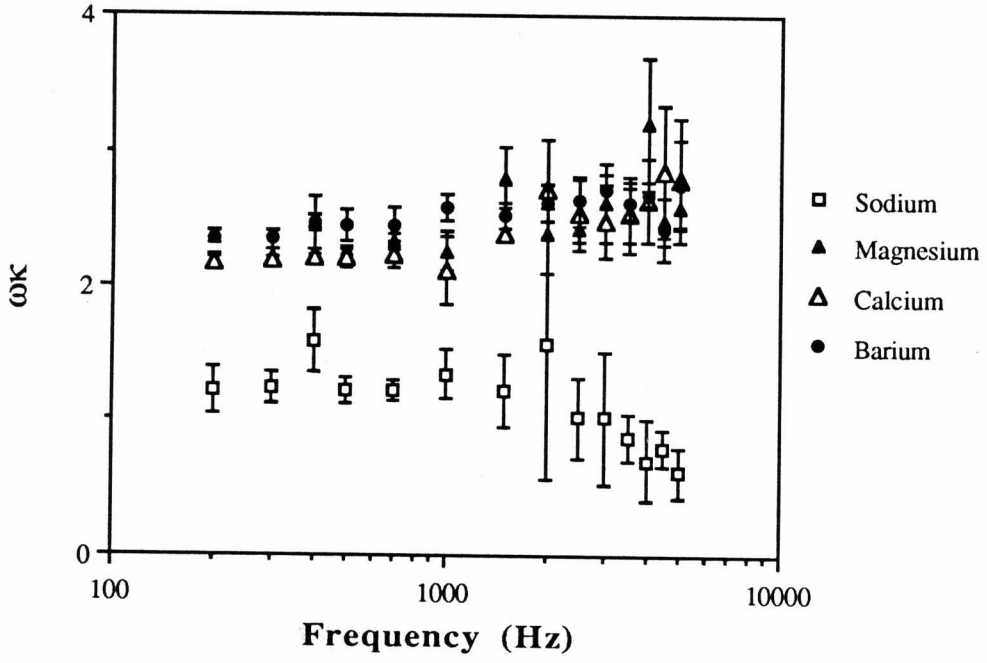

Figure 57. Viscous loss modulus vs. frequency for stearic acid in the presence of 1mM of chloride salts of magnesium, calcium, and barium relative to that of 0.01M sodium chloride at pH 6.0 and μ=0.01M.

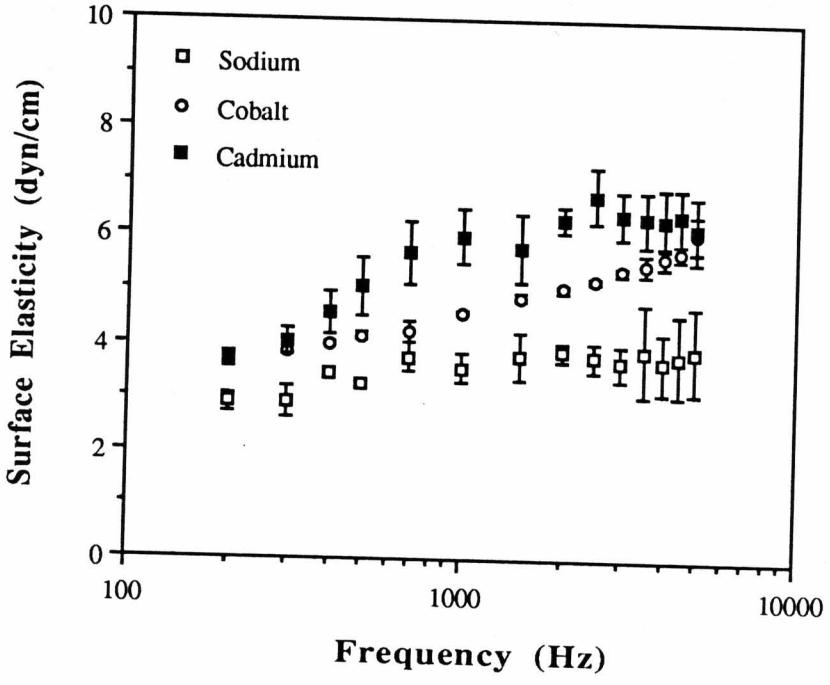

Figure 58. Surface elasticity vs. frequency for stearic acid in the presence of 1mM of chloride salts of cobalt and cadmium relative to that of 0.01M sodium chloride at pH 6.0 and μ=0.01M.

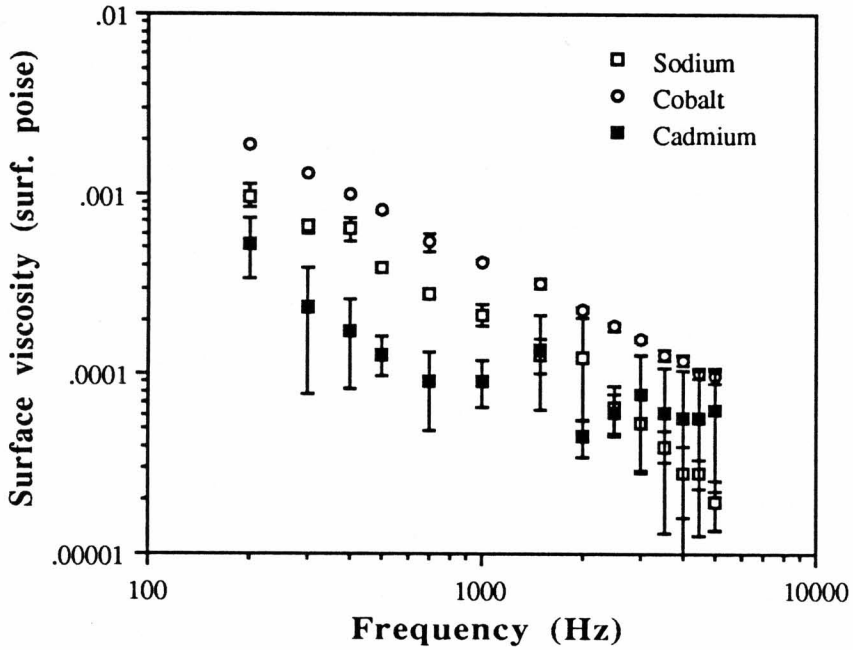

Figure 59. Surface viscosity vs. frequency for stearic acid in the presence of 1mM of chloride salts of cobalt and cadmium relative to that of 0.01M sodium chloride at pH 6.0 and μ=0.01M.

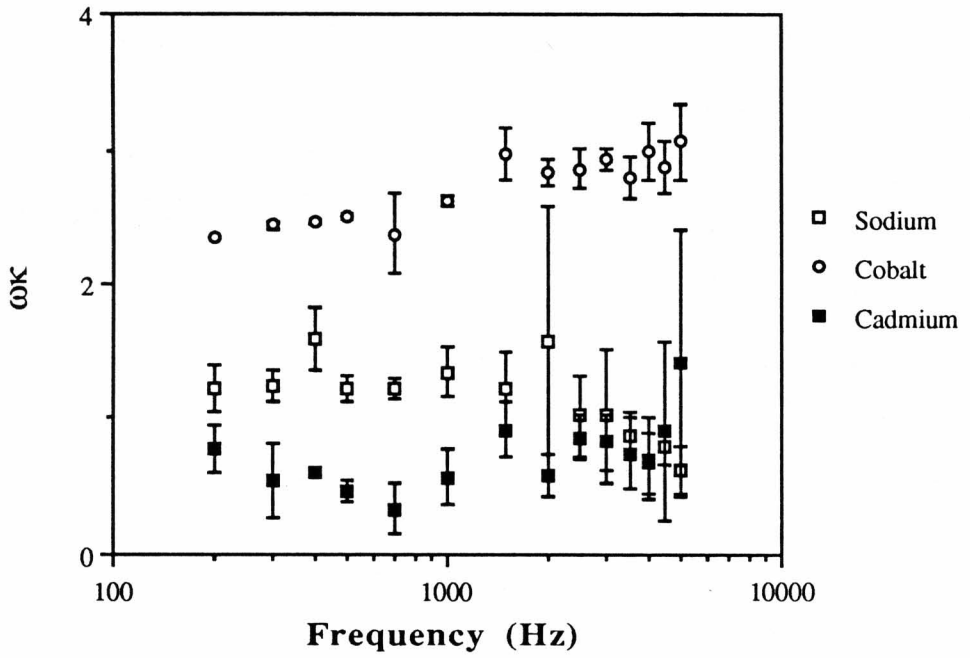

Figure 60. Viscous loss modulus vs. frequency for stearic acid in the presence of 1mM of chloride salts of cobalt and cadmium relative to that of 0.01M sodium chloride at pH 6.0 and μ=0.01M.

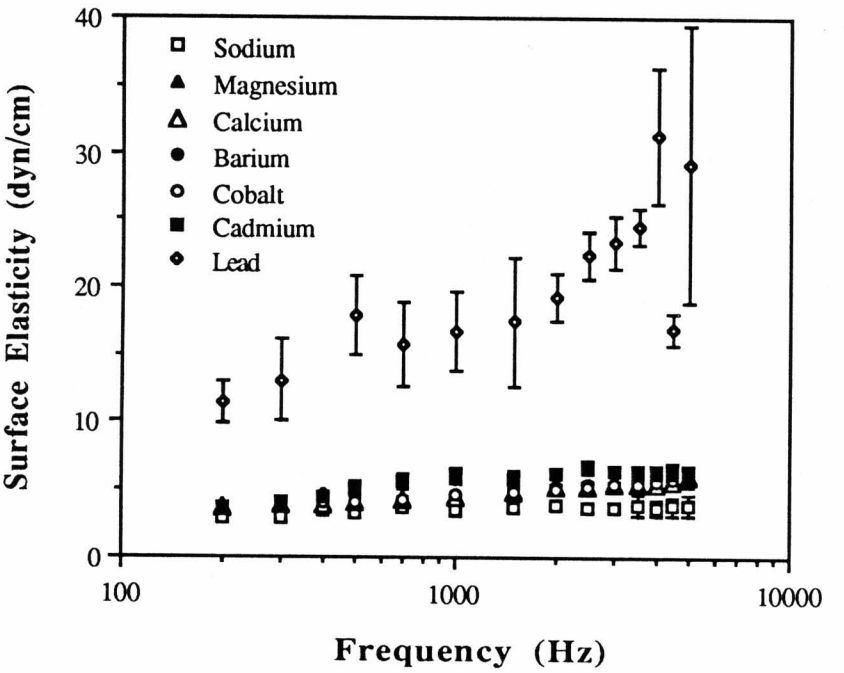

Figure 61. Surface elasticity vs. frequency for stearic acid in the presence of 1mM salts of all divalent ions realtive to that of 0.01M NaCl at pH 6.0 and μ=0.01M.

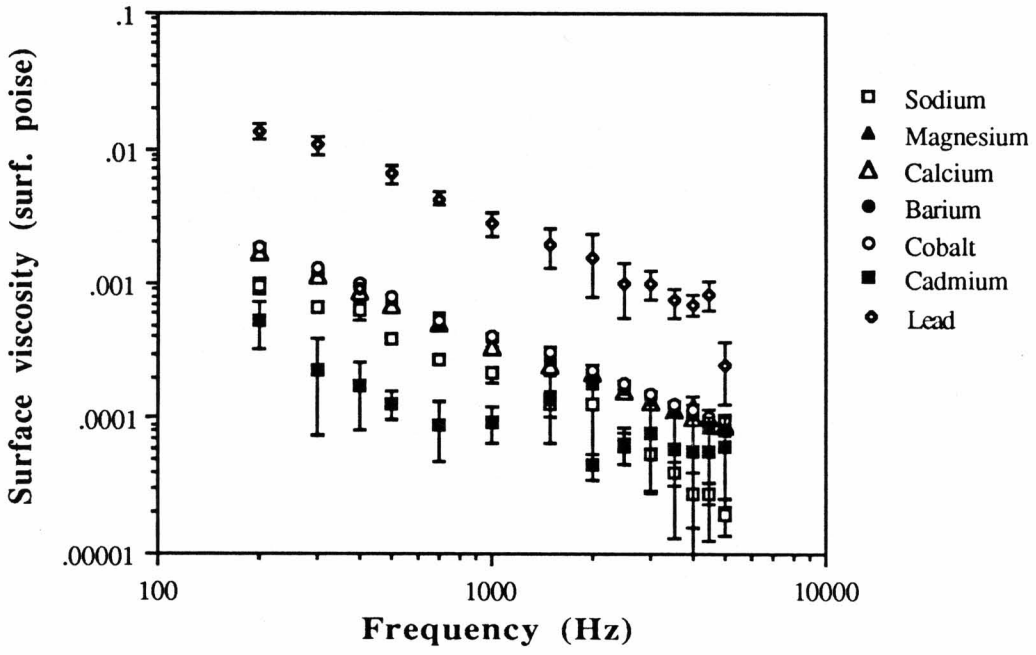

Figure 62. Surface viscosity vs. frequency for stearic acid in the presence of 1mM salts of all divalent ions realtive to that of 0.01M NaCl at pH 6.0 and μ=0.01M.

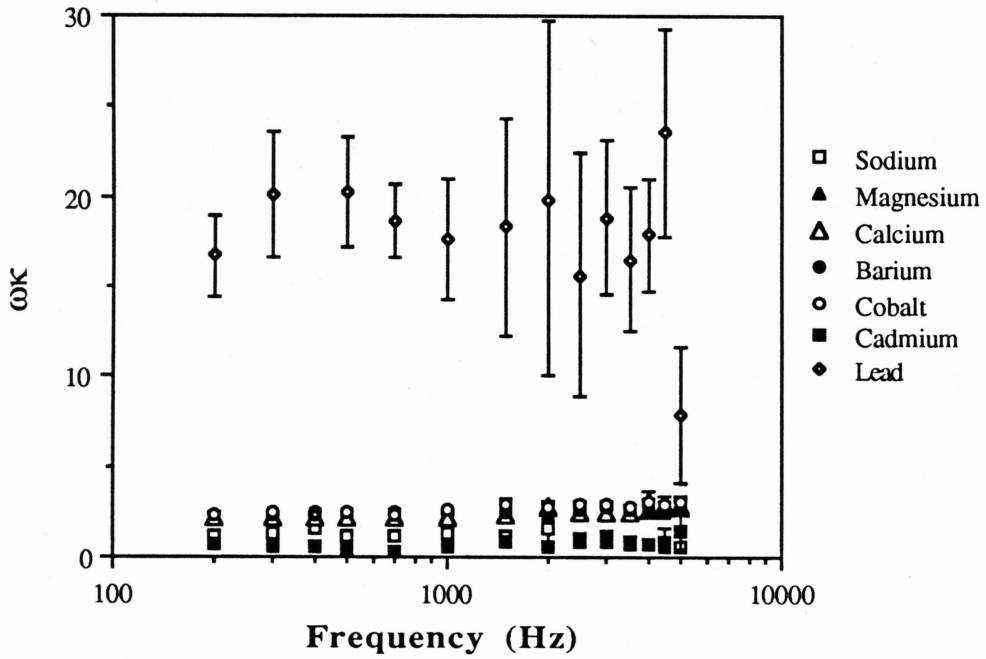

Figure 63. Viscous loss modulus vs. frequency for stearic acid in the presence of 1mM salts of all divalent ions realtive to that of 0.01M NaCl at pH 6.0 and μ=0.01M.

pH dependence in the Presence of Pb^{2+}

The pH dependence of ε_l, κ, and $\omega\kappa$ in the presence of Pb^{2+} is shown in Figures 64-66. It can be seen that the monolayer exhibits much higher values for ε_l, κ, and $\omega\kappa$ at pH 4.0 to 6.0 than those obtained at pH 3.0. Moreover, there appears to be a trend; as the pH of the subphase solution is lowered from 6.0 to 3.0, ε_l, κ, and $\omega\kappa$ also decrease. In the pH range 4.0 to 6.0, ε_l is frequency dependent, whereas, $\omega\kappa$ is frequency independent. At pH 3.0, both ε_l and $\omega\kappa$ are frequency independent and similar to those in the presence of Na^+ at pH 2.0.

The Dependence of ε_l and $\omega\kappa$ on frequency

In principle, ε_l and $\omega\kappa$ can be defined as two dimensional analogues of three dimensional storage, $G'(\omega)$, and loss, $G''(\omega)$, moduli (equations 28 and 29). Since there are no molecular theories for the description of viscoelastic properties of spread monolayers, such as those for polymer solutions, simple linear viscoelastic models generally are considered in an attempt to interpret and understand the rheological results. The basic models for linear viscoelasticity are the Maxwell model with a single relaxation time and the Voigt model having one retardation time. A complete summary for the derivation of the viscoelastic functions exhibited by these models are given by Ferry (Ferry, 1970).

The Maxwell element is comprised of a spring and a dashpot connected in series, where the time required for stress relaxation, (relaxation time, τ_i), is defined as the ratio of the shear rigidity of the spring, G_i, and the viscosity of the dashpot, η_i. In this model $G'(\omega)$ and $G''(\omega)$ are functions of the frequency, reflecting relaxation processes for

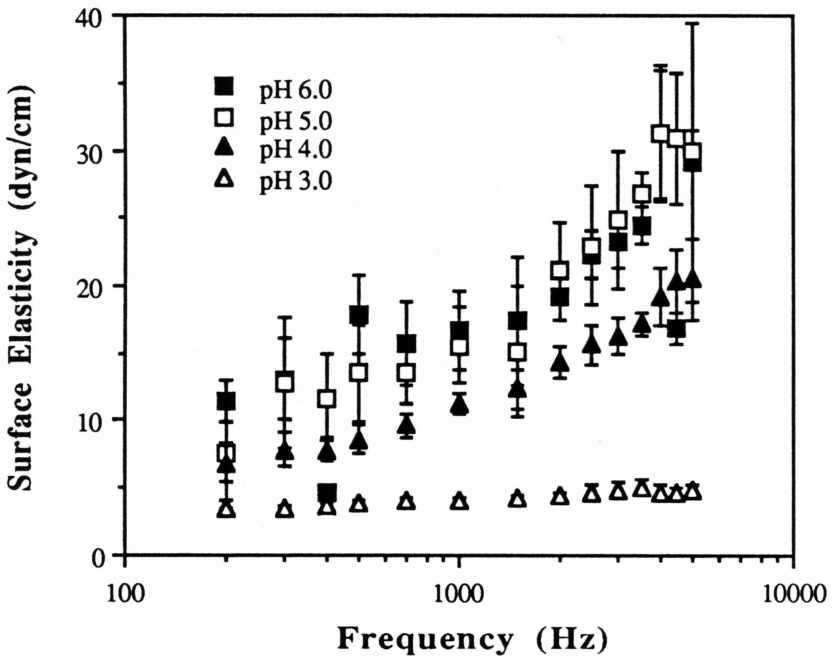

Figure 64. Surface elasticity vs. frequency for stearic acid in the presence of 1mM of lead chloride at various pH values and μ=0.01M.

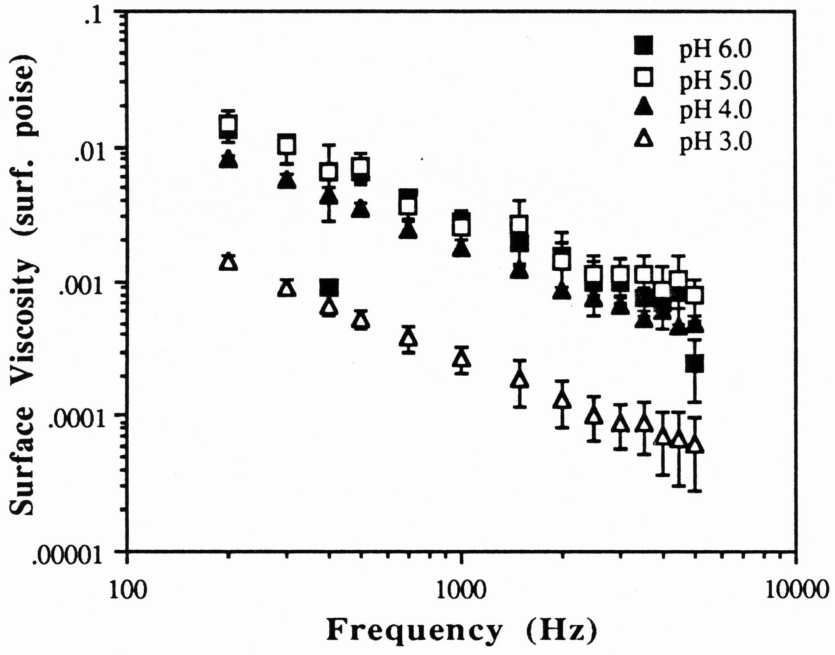

Figure 65. Surface viscosity vs. frequency for stearic acid in the presence of 1mM of lead chloride at various pH values and μ=0.01M.

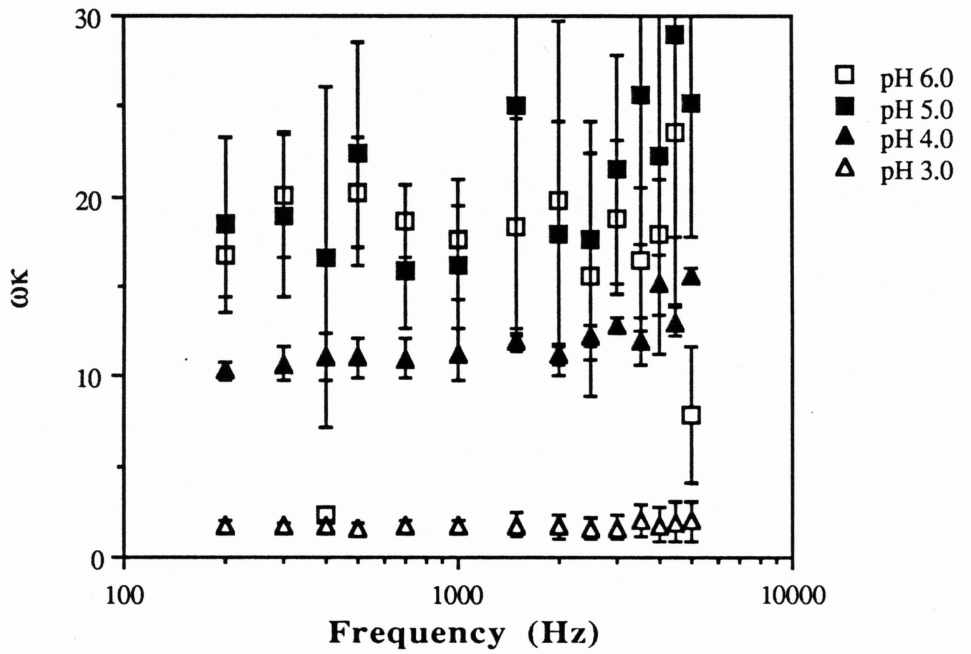

Figure 66. Viscous loss modulus vs.frequency for stearic acid in the presence of 1mM of lead chloride at various pH values and μ=0.01M.

the Maxwell element. They are given as (Ferry, 1970)

$$G'(\omega)=G_i\omega^2\tau_i^2/(1+\omega^2\tau_i^2) \quad (66)$$
$$G''(\omega)=G_i\omega\tau_i/(1+\omega\tau_i) \quad (67)$$

In principle then in the Maxwell element, $G'(\omega)$ should vary with ω^2 whereas $G''(\omega)$ should linearly increase with frequency.

The Voigt element is comprised of a spring and a dashpot connected in parallel. The retardation time, τ_i, is defined as "the time required for the extension of the spring to its equilibrium length while retarded by the dashpot" (Ferry, 1970). In this model $G'(\omega)$ and $G''(\omega)$ are given as

$$G'(\omega)=G_i \quad (68)$$
$$G''(\omega)=G_i\omega\tau_i \quad (69)$$

In the Voigt element, $G'(\omega)$ is constant and independent of the frequency whereas $G''(\omega)$ should linearly increase with frequency.

The values for ε_l and $\omega\kappa$ in the presence of NaCl at different pH values appear to be constant and frequency independent. According to Maxwell and Voigt models this is possible in the limits of very large and very small relaxation or retardation times. Frequency independence due to small relaxation or retardation times is the most likely reason since the process of diffusion and reorientation of the molecules at the interface is extremely fast (Lucassen and Hansen, 1966). The viscosity of the monolayers in all cases was found to be small, which makes the possibility of very large relaxation or retardation times negligible. The presence of all the divalent ions at pH 6.0, with the exception of Pb^{2+}, resulted in a slight

increase in ε_l with frequency while $\omega\kappa$ remained frequency independent. This is in contrast to the Voigt model which predicts frequency independence with ε_l and frequency dependence with $\omega\kappa$. The results are not consistent with the Maxwell model either since ε_l does not vary with the second power of frequency and $\omega\kappa$ is frequency independent. Pb^{2+} which showed a significant change in ε_l with frequency does not satisfy the Maxwell model either; ε_l varies with frequency to the power of 0.6 and $\omega\kappa$ is again frequency independent. In summary, it can be seen that the application of simple linear viscoelastic models to interpret the data does not seem to be appropriate. The results are perhaps better analyzed by more complicated linear or non-linear viscoelastic relationships to describe the viscoelastic relationships for the monolayers spread at the air/water interface.

Static Elasticity

Equation 32 was used to calculate the static elasticity, ε_{st}, values for different systems from the Π-A isotherms of stearic acid. The isotherms were fitted to a polynomial function using a nonlinear least square method and the slopes of the curves were obtained by taking the derivative of the polynomial function with respect to A. Table X lists the ε_{st} values along with those estimated from ε_l vs. frequency plots by extrapolating to zero frequency, ε^0, for various systems. ε^0 in principle should be equivalent to ε_{st}, since the latter represents the elasticity of the film at essentially zero frequency. In the presence of Cd^{2+} and Pb^{2+}, ε_{st} cannot be calculated since the isotherms are extremely condensed and have almost infinite slope. For the other systems it can be seen that ε_{st} and ε^0 values

are quite different, the latter being as much as two orders of magnitude lower. However, the trend with respect to change with pH and the effect due to the presence of various ions appears to be the same.

The reason for the large discrepancy between these results is not clear at this time. Previous measurements of dynamic elasticity of small amphiphiles and polymers have been shown to be in good agreement with static elasticity at low surface concentrations and low surface pressures and to deviate at high surface concentrations and high surface pressures (Lucassen and Hansen, 1966, Hård and Löfgren, 1976, Chen, 1986, Chen et al., 1986, Sauer et al., 1986). For example, pentadecanoic acid at low concentrations, 40 to 50$Å^2$/molecule, shows very similar dynamic and static elasticities (Chen, 1986). However, the dynamic elasticity became much larger than static elasticity at higher surface concentrations from 40 to 31$Å^2$/molecule. Studies at lower areas or higher concentrations were not carried out due to the instability of the pentadecanoic acid monolayer. In a study of propyl stearate monolayers, however, dynamic elasticity was shown to become much smaller than static elasticity at high concentrations and surface pressures (Hård and Löfgren, 1976). Our data appears to be similar to these results in terms of the discrepancy between the static and dynamic elasticities. The reason for this discrepancy is not clear at this time. It may be attributed to the inability of the Lucassen-Reynders dispersion equation to describe the viscoelastic nature of this very closely packed monolayer, wherein the monolayer may not behave as a fluid phase but rather as a "condensed" solid like phase. This may also be due to possible (albeit unlikely) structural changes in the monolayer with a characteristic

time larger than 0.01 msec (100Hz), which might occur in the monolayer in response to the monolayer compression in the Π-A measurements.

It is important to note that despite the discrepancy between the static and dynamic elasticities, the surface viscosity, κ, values in the limit of zero frequency are within the range of the values reported by other investigators for the shear viscosity, η_S. These values are tabulated in Table XI. Such a comparison appears to be reasonable since it is believed that the contribution of shear component to κ is more important than the dilational component.

Salt	pH	Area	ε_{st} (dyn/cm)	ε^0 (dyn/cm)
NaCl	2.0	20.5	211	3.2
NaCl	2.0	20.0	259	3.2
NaCl	6.0	20.5	127	2.8
$MgCl_2$	6.0	20.5	124	3.3
$CaCl_2$	6.0	20.5	195	3.3
$BaCl_2$	6.0	20.5	221	3.3
$CoCl_2$	6.0	20.5	191	3.3
$CdCl_2$	6.0	20.5	-	3.7
$PbCl_2$	6.0	20.5	-	~8
$PbCl_2$	5.0	20.5	-	~7
$PbCl_2$	4.0	20.5	-	~5
$PbCl_2$	3.0	20.5	142	3.3

Table X. ε_{st} and ε^0 in the presence of various metal ions at different pH values.

Compound	surface viscosity	Experimental conditions	Reference
Stearic acid	≈0.002 s.p.	ECWD, 0.01M HCl 20Å^2/molecule, Π=20.5dyn.cm T=25±0.1°C	This Work
Stearic acid	0.004-0.005 s.p.	Torsion pendulum oscillation 0.01M HCl Π=15-20 dyn/cm Room Temperature	Boyd and Harkins, 1940
Stearic acid	0.0008-0.001 s.p.	Canal Viscometer 0.01M, H_2SO_4 Π=15-20 dyn/cm T=20±0.2°C	Jarvis, 1965
Stearic acid	0.0002 s.p.	Torsion pendulum oscillation 30Å^2/molecule Triple distilled water T=25°C, pH=5.2	Enever and Pilpel, 1967
Stearic acid	<0.0005 s.p.	Canal Viscometer Π=31dyn/cm 0.0001M $CaCl_2$ pH=6.0	Neuman, 1975
Arachidic acid	≈0.008 s.p.	Resonance Rheometry Water, pH =5.6 T=22°C	Buhaenko et al., 1988

Table X. The surface shear viscosity, η_s, values measured by different experimental methods in comparison to κ from ECWD. s.p. is surface poise, g/sec.

DISCUSSION

Surface Pressure, Surface Potential, and Surface Ellipsometry

The results of this study indicate that significant qualitative and quantitative differences exist in the manner in which divalent cations affect fatty acid monolayers under identical conditions of pH, ionic strength, temperature, and divalent ion concentration. Surface pressure studies have confirmed the known tendency of these ions to condense partially ionized fatty acid monolayers; for all ions except Pb^{2+} the critical pH range appears to be between 5.0 to 6.0. Pb^{2+}, however, affects the monolayer starting at pH 4.0. Using an intrinsic pK_a of 5.4 for stearic acid and the Guoy-Chapman model for the electrical double layer leads to rough estimates of 5% dissociation in the absence of divalent ions and as much as 25% in their presence at 20Å^2/molecule and pH 6.0 (Figure 24). However, Pb^{2+} clearly appears to interact with the monolayer to produce changes at even lower pH values than might be expected theoretically. Moreover, Pb^{2+} and Cd^{2+}, under all conditions, are much more effective than other cations studied in condensing the monolayer.

The changes in the surface potential at 20Å^2/molecule and pH 6.0, due to the presence of divalent cations, and particularly the differences in the direction of change seen with Pb^{2+}, Cd^{2+}, and Co^{2+}, relative to that with Mg^{2+}, Ca^{2+}, and Ba^{2+}, provide a basis for probing the underlying mechanisms involved and the various models proposed. In Figure 34, it can be seen that the effect of each divalent cation on ΔV is concentration dependent up to a limiting concentration. Thus, it can be assumed that

these changes in ΔV are reflecting some cation dependent type of interaction with the fatty acid. Most significant is the fact that Pb^{2+}, Cd^{2+}, and Co^{2+}, in that order, cause ΔV to become more negative, whereas Mg^{2+}, Ca^{2+}, and Ba^{2+}, in that order, cause ΔV to become more positive. In both cases the effects within each group, i.e. more positive or negative, follow the order of expected degree of hydration, and in the case of Pb^{2+}, Cd^{2+}, and Co^{2+}, the order of covalent complexing tendencies. Thus it can be concluded that the differences in direction of change between these two groups is most likely reflecting a major difference in the underlying mechanisms of how divalent cations interact with fatty acid monolayers.

It is generally believed that the measured value of ΔV obtained with spread monolayers is proportional to an overall effective surface dipole moment, μ, associated with the water-air-monolayer interface (Schulman and Hughes, 1932, Demchak and Fort, 1974). For this discussion it is prefered to simply divide μ into two parts, μ_α and μ^ω, as suggested by Vogel and Möbius (Vogel and Möbius, 1988), (See Introduction). For closely packed monolayers of fatty acids, μ^ω has been estimated to be +0.35D (Vogel and Möbius, 1988).

In the present case, we may assume to a first approximation that monolayers closely packed at $20Å^2$/molecule undergo changes in ΔV under various conditions primarily because of an effect on μ_α, with μ^ω remaining essentially constant. For example, the decrease in ΔV noted going from pH 2.0 to 6.0 with stearic and arachidic acids at $20Å^2$/molecule (Table I) would appear to primarily reflect the increasing

ionization of the carboxyl group (Betts and Pethica, 1956). The surface potential changes brought about by divalent cations may be attributed to at least two major changes taking place in the polar region; screening of negative charges and direct covalent interaction with the carboxyl group. The small, but significant, increases noted for ΔV at pH 6.0 with Ba^{2+}, and Ca^{2+} are consistent with the tendency of alkaline earth metals to screen the charges of carboxylate ions in solution (Kohn, 1987, Cesàro et al., 1988); while the order of effect $Ba^{2+}>Ca^{2+}>Mg^{2+}$ is consistent with the degree of ion hydration (Pashely and Israelachvili, 1984). The order of change in ΔV to give increasingly lower values, $Pb^{2+}>Cd^{2+}>Co^{2+}$, also follows inversely with the degree of ion hydration. However, this order of effect is also directly proportional to the ability of these ions to covalently complex with carboxylate ions (Kohn, 1987, Campbell and Tessier, 1987, Cesàro et al., 1988). Exactly why the values of ΔV should assume increasingly smaller values of ΔV with increasing amounts of Pb^{2+}, Cd^{2+}, or Co^{2+} interaction with the carboxylate group is not easily proven because the various effects on the polar groups are hard to uncouple For example, it can be expected that the major effect of direct covalent binding of these cations would cause a shift in the electronic distribution of the polar group. However, such an effect cannot be uncoupled from those possibly due to the ordering of surrounding water dipoles or to changes in the degree of ionization of the monolayer. Indeed the fact that Pb^{2+} appears to be effective in altering the properties of the monolayer at pH values as low as 4.0, indicates that it simply may be lowering the effective pK_a of the carboxylic acid group through its covalent interaction. This would be

consistent with the findings of Kobayashi et al., 1988, with fatty acid LB films, where 100% of carboxylic acid groups were shown to have interacted with Pb^{2+} at pH 4.0, with Cd^{2+} at pH 6.5, and with Ba^{2+} at pH 8.5. Hence Pb^{2+} and Cd^{2+},in effect, appear to be able to alter the ionization of the carboxylate group through specific interactions, while Ba^{2+} and presumably other alkaline earth metal ions cannot.

In this context, it is interesting to consider the results of the experiments which were designed to see if any effects on ΔV could be caused by simply changing the metal ion counter-ion, as shown in Table III. Some type of effect on ΔV might be expected if the counter-ion had a tendency to complex with divalent cation either in the solution or at the interface. For example, adding an excess amount of anions which complex with the divalent cations in solution could reduce the available free cation for interaction with the carboxyl group and thus cause the value of ΔV to become more positive, while a tendency to complex at the interface might strengthen the interaction and cause ΔV to become more negative. Our results appear to be consistent with the first possibility, since two ions, iodide and thiocyanate, both with strong complexing tendencies with Pb^{2+} and Cd^{2+} in aqueous solution (Sillen, 1971, Högfeldt, 1982) caused an increase in ΔV. On the other hand, those anions which have no tendency to complex with Ba^{2+} (Sillen, 1971, Högfeldt, 1982), correspondingly appear to produce no change in ΔV. This, therefore, seems to support the model wherein ions like Pb^{2+}, Cd^{2+}, and Co^{2+} interact directly with the fatty acid in a fairly specific manner, rather than just nonspecifically screening electrostatic charges, as in the case of Ba^{2+}, Ca^{2+}, and Mg^{2+}. Such

nonspecific electrostatic interactions also are inferred by the results with polyamines such as spermine and spermidine, which like alkaline earth ions, slightly condense the monolayer at pH 6.0 but do not appear to change the electrical properties of the monolayer as measured by surface potential. It appears that the presence of more than one charge on a cation does not necessarily result in significant condensation and closer packing of the monolayer. Rather, more specific interactions for such effects are needed.

Similarly to surface pressure and surface potential measurements, surface ellipsometric studies showed that Pb^{2+} and Cd^{2+} have the most significant effects on surface properties of the fatty acid monolayers. In particular, Pb^{2+} appears to have a significant effect on the fatty acid monolayers at unusually low concentrations and low pH values. The results obtained here are another manifestation of the anomalous characteristics of Pb^{2+} which appear to lower the effective pK_a of the carboxylic acid group through perhaps strong covalent or complex interactions in order to be effective at these concentrations and pH values. In Table XII the number of Pb^{2+} ions in the subphase solution relative to the number of fatty acid molecules spread at the air/water interface for a typical experiment are tabulated. It can be seen that at 0.00125mM where the effect of Pb^{2+} on $\delta\Delta$ and the Π-A isotherms starts to diminish (Figure 38) the number of Pb^{2+} ions in the bulk is almost equivalent to the number of fatty acid molecules at the surface. Thus, although the monolayer is only partially ionized and not all the lead ions are at the surface, the lead ions are able to exert some condensing effect. At the lowest concentration

(0.000025mM) where the number of Pb^{2+} in the bulk is about two orders of magnitude lower than the number of fatty acids in the monolayer, there appears to be no effect on $\delta\Delta$ whereas the Π-A isotherm still is very slightly condensed. Thus, lead ions have a high affinity for fatty acids and this interaction appears to be a very strong and specific one. A comparison of the effect of Pb^{2+} concentration on $\delta\Delta$ and ΔV is shown in Figure 67. The concentration at which the lead ions start to exert some effect on both $\delta\Delta$ and ΔV values is roughly the same. Moreover, $\delta\Delta$ and ΔV values appear to reach some level of saturation at roughly the same concentration.

Based on surface potential measurements some anionic counter-ions, i.e. iodide and thiocyanate, were shown to have an effect on the interaction of divalent ions with the carboxylic acid perhaps by complexing with them in solution and effectively reducing their concentration at the surface. However, from the surface ellipsometric studies, these counter-ions appear to have no major detectable effects on $\delta\Delta$ values in the presence of the divalent cations studied. This may simply be due to the insensitivity of $\delta\Delta$ to any changes in the ionic composition at the surface that may occur due to complexation of divalent cations with counter-ions in the bulk. For example, looking at Table III and Figure 67, it can be seen that in the presence of Pb^{2+} changing the counter-ion from Cl^- to SCN^- increased ΔV by 40mV. This is equivalent to a change in ΔV caused by a change in the concentration of $PbCl_2$ in the subphase solution from 1.0 to 0.01mM. $\delta\Delta$, on the other hand, only changes from $1.25\pm0.03°$ to $1.15\pm0.11°$ over the same concentration range. This can explain the lack

Concentration of $PbCl_2$ (mM)	Number of Pb^{2+} in the subphase	ratio of stearic acid to Pb^{2+}
0.000025	7.525×10^{15}	0.05
0.0005	1.505×10^{17}	0.91
0.00125	3.763×10^{17}	2.27
0.0025	7.525×10^{17}	4.53
0.005	1.505×10^{18}	9.10
0.1	3.010×10^{19}	181.3
1.0	3.010×10^{20}	1813

Table XII. Number of Pb^{2+} ions in the subphase at different concentrations relative to number of stearic acid molecules (1.660×10^{17}) spread at 20$Å^2$/molecule.

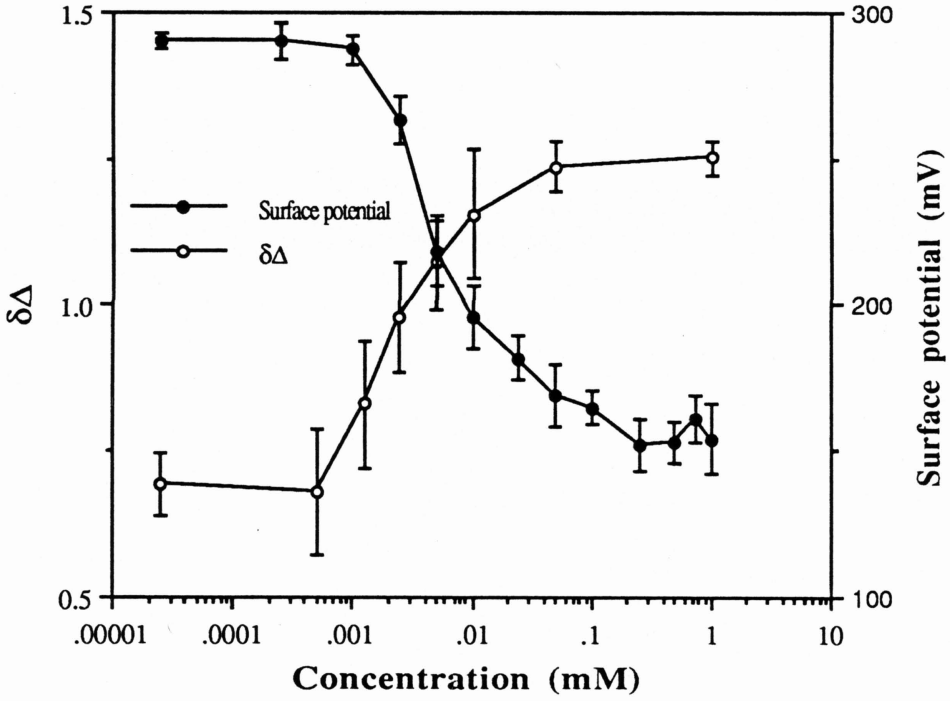

Figure 67. Lead concentration dependence of $\delta\Delta$ and ΔV, at pH 6.0 and μ=0.01M. Error bars represent 95% confidence limit intervals as calculated from Student's t-distribution.

of sensitivity of ellipsometry to changes caused by the anionic counter-ions.

A central issue associated with divalent cation effects on fatty acid LB films, and monolayers at the air/water interface,in general, is whether or not a 1:1 relationship exists between each carboxylic acid group within a layer and ions like Pb^{2+} and Cd^{2+}, as opposed to a more nonspecific 1:2 relationship with alkaline earth ions (Vogel et al., 1979b, 1980, Outka et al, 1987). For monolayers and multilayers transferred to solid substrates there is good direct evidence to support this model (Vogel et al., 1979b, 1980, Outka et al, 1987). For monolayers at the air/water interface no such direct evidence exists, but there certainly appears to be good evidence from this study that the major differences which exist between these ions are consistent with such a model. The much greater degree of condensation for Pb^{2+} and Cd^{2+} and the very significant change in ΔV and $\delta\Delta$ at low Pb^{2+} concentrations, for example, suggest a much tighter packing within the monolayer that could be facilitated by having each fatty acid associated with one Pb^{2+} or Cd^{2+}. Indeed, the titration of acetic acid with sodium hydroxide in the presence of Pb^{2+} and Cd^{2+} yields stability constants for the formation of 1:1 and 1:2 complexes between these ions and acetate ions, whereas for alkaline earth ions such as Ba^{2+} no such complexes occur. Moreover, the magnitude of the stability constants for lead ions are about the same for both 1:1 and 1:2 complexes, whereas cadmium ions show a greater stability constant for the 1:2 complex than the 1:1 complex(Table IX). This could explain the greater effect of Pb^{2+} on ΔV and $\delta\Delta$ at lower concentrations and lower pH values. Whether the

counter-ion effects noted in ΔV are in any way reflecting the process of complex formation, at the present, is not clear, and certainly more direct observations of other monolayer properties will be necessary to test these ideas further.

Rheological Measurements

As was described in the Introduction, the control of the rheological properties of the monolayers at the air/water interface, namely surface elasticity, ε_l, and surface viscosity, κ, appears to be important in transferring the monolayer to form LB films. At a constant surface pressure during such a transfer, the monolayer will experience deformations due to both tangential shearing and compressional stresses along with deformations caused by drainage of water from the monolayer. In the monolayer state, however, the most significant stress the monolayer experiences is the shear stress. For example, measurements of the shear viscosity along with dilational elasticity have shown that when viscosity becomes too high relative to elasticity the monolayer cannot be deposited effectively because of a lack of sufficient rate of stress relaxation. Similarly, when the elasticity becomes too high relative to viscosity, the monolayer becomes rigid and brittle leading to "cracks on insertion" during the transfer process (Buhaenko et al., 1985). In this context, it appears that an effective transfer process requires contributions from both ε_l and κ. The presence of those divalent ions which increase the overall contribution of both ε_l and κ to the overall viscoelastic modulus, ε^*, (see

equation 27) should, in principle, result in more effective deposition of LB films.

The viscoelastic properties of the monolayers in the presence of various metal ions are best compared in terms of loss tangent, tanδ, values. Tanδ is a measure of viscous ($\omega\kappa$) to elastic (ε_l) contribution to the overall viscoelastic modulus of the monolayer (see equation 31). The calculated values of tanδ in the presence of sodium and alkaline earth ions at pH 6.0 are listed in Table XIII and plotted in Figure 68. It can be seen that the presence of all the alkaline earth ions slightly increased tanδ over that due to sodium ions. The δ values, which can be used to categorize the overall viscoelastic behaviour of the monolayer (See Introduction), in the presence of alkaline earth ions are calculated to be ≈30° relative to ≈15-20° in the presence of sodium ions. Thus, it appears that the monolayer in the presence of alkaline earth ions becomes slightly more viscoelastic in nature. The calculated values of tanδ in the presence of Na^+, Co^{2+}, Cd^{2+}, and Pb^{2+} at pH 6.0 are plotted against the frequency in Figure 69 and listed in Table XIV. The presence of Pb^{2+} significantly increased tanδ while a significant decrease occurred in the presence of Cd^{2+}. The increase in tanδ in the presence of Co^{2+} was similar to that due to alkaline earth ions. The δ values in the presence of Pb^{2+}, Co^{2+}, and Cd^{2+} are calculated to be ≈50-60°, ≈30°, and ≈10°, respectively. Hence, the monolayer can be classified as being very viscoelastic in the presence of Pb^{2+} to being somewhat elastic in the presence of Cd^{2+}. The significant change in the presence of Pb^{2+} appears to be pH dependent as is shown in Figure 70 and listed in Table XV. Here tanδ values at pH 4.0 to 6.0 are

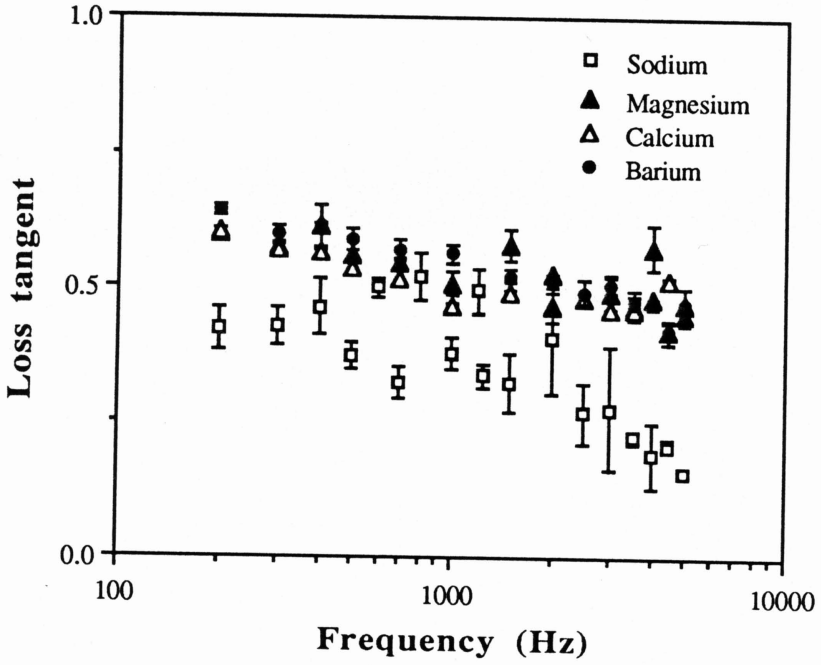

Figure 68. Loss tangent vs. frequency for for stearic acid in the presence of sodium and alkaline earth ions at pH 6.0 and μ=0.01M.

Frequency (Hz)	Loss tangent			
	Sodium	Magnesium	Calcium	Barium
200	0.42±0.04	0.60±0.01	0.60±0.00	0.64±0.01
300	0.43±0.03	0.57±0.01	0.57±0.00	0.59±0.02
400	0.46±0.05	0.61±0.04	0.56±0.00	0.61±0.01
500	0.37±0.02	0.56±0.01	0.53±0.00	0.59±0.02
700	0.33±0.03	0.54±0.01	0.51±0.00	0.57±0.02
1000	0.38±0.03	0.51±0.02	0.47±0.00	0.56±0.02
1500	0.32±0.05	0.58±0.03	0.49±0.00	0.52±0.01
2000	0.41±0.10	0.47±0.03	0.52±0.00	0.51±0.02
2500	0.27±0.06	0.48±0.01	0.48±0.00	0.49±0.02
3000	0.28±0.12	0.49±0.03	0.46±0.00	0.51±0.02
3500	0.23±0.01	0.47±0.03	0.46±0.00	0.47±0.01
4000	0.19±0.06	0.58±0.04	0.48±0.00	0.47±0.01
4500	0.21±0.01	0.42±0.01	0.51±0.00	0.42±0.02
5000	0.16±0.01	0.45±0.02	0.47±0.00	0.47±0.03

Table XIII. Loss tangent values as a function of frequency for stearic acid in the presence of sodium and alkaline earth ions at pH 6.0 and μ=0.01M.

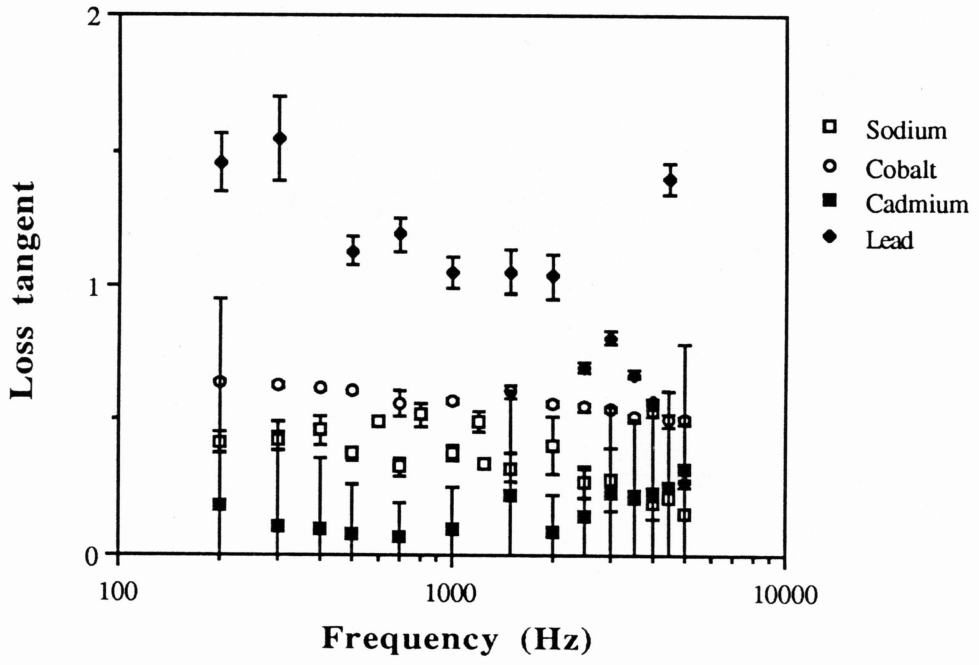

Figure 69. Loss tangent vs. frequency for for stearic acid in the presence of Na^{+}, Co^{2+}, Cd^{2+}, and Pb^{2+} at pH 6.0 and μ=0.01M.

Frequency (Hz)	Loss tangent			
	Sodium	Cobalt	Cadmium	Lead
200	0.42±0.04	0.64±0.00	0.18±.077	1.46±0.11
300	0.43±0.03	0.63±0.01	0.11±0.38	1.54±0.16
400	0.46±0.05	0.62±0.00	0.10±0.27	0.51±0.01
500	0.37±0.02	0.61±0.01	0.08±0.18	1.13±0.05
700	0.33±0.03	0.56±0.05	0.07±0.12	1.19±0.06
1000	0.38±0.03	0.57±0.01	0.10±0.16	1.05±0.06
1500	0.32±0.05	0.61±0.02	0.23±0.38	1.05±0.08
2000	0.41±0.10	0.56±0.01	0.09±0.13	1.03±0.08
2500	0.27±0.06	0.55±0.02	0.14±0.18	0.70±0.02
3000	0.28±0.12	0.55±0.01	0.23±0.32	0.81±0.03
3500	0.23±0.01	0.51±0.01	0.21±0.30	0.67±0.01
4000	0.19±0.06	0.53±0.02	0.23±0.32	0.57±0.01
4500	0.21±0.01	0.50±0.02	0.26±0.36	1.40±0.06
5000	0.16±0.01	0.50±0.02	0.32±0.47	0.27±0.01

Table XIV. Loss tangent values as a function of frequency for stearic acid in the presence of Na^{+}, Co^{2+}, Cd^{2+}, and Pb^{2+} at pH 6.0 and μ=0.01M.

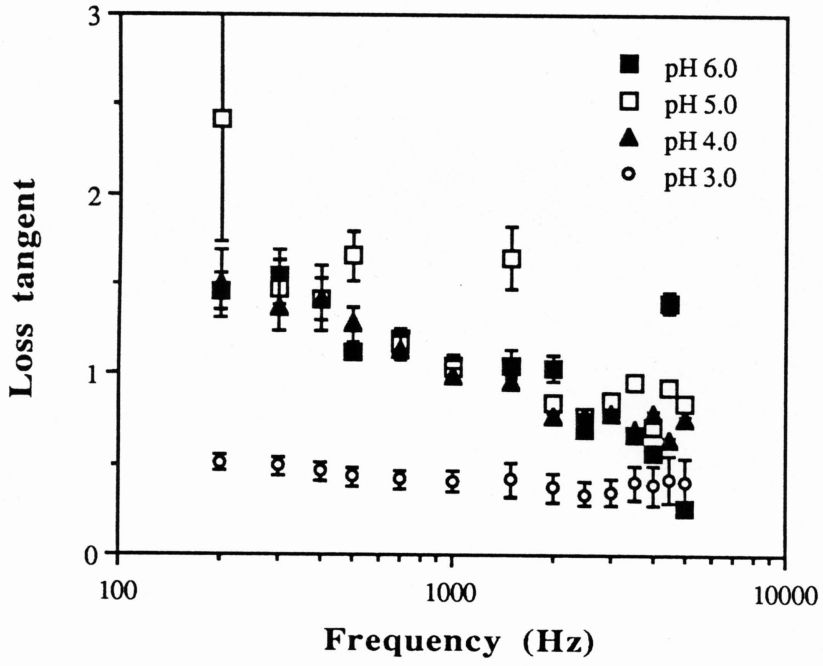

Figure 70. Loss tangent vs. frequency for stearic acid in the presence of 1mM $PbCl_2$, μ=0.01M, at various pH values.

Frequency (Hz)	Loss tangent			
	pH 6.0	pH 5.0	pH 4.0	pH 3.0
200	1.46±0.11	2.42±0.69	1.49±0.19	0.51±0.05
300	1.54±0.16	1.48±0.15	1.37±0.14	0.49±0.05
400	0.51±0.01	1.42±0.18	1.41±0.12	0.46±0.05
500	1.13±0.05	1.66±0.14	1.28±0.09	0.43±0.05
700	1.19±0.06	1.16±0.05	1.14±0.06	0.42±0.06
1000	1.05±0.06	1.03±0.04	1.00±0.04	0.41±0.06
1500	1.05±0.08	1.64±0.17	0.96±0.03	0.42±0.09
2000	1.03±0.08	0.85±0.03	0.78±0.01	0.37±0.08
2500	0.70±0.02	0.77±0.03	0.78±0.01	0.34±0.07
3000	0.81±0.03	0.86±0.03	0.79±0.01	0.35±0.07
3500	0.67±0.01	0.96±0.02	0.69±0.01	0.40±0.10
4000	0.57±0.01	0.71±0.02	0.79±0.02	0.39±0.11
4500	1.40±0.06	0.94±0.03	0.64±0.01	0.42±0.13
5000	0.27±0.01	0.84±0.02	0.76±0.01	0.41±0.13

Table XV. Loss tangent values as a function of frequency for stearic acid in the presence of 1mM $PbCl_2$, μ=0.01M, at various pH values.

strikingly similar and significantly higher than those at pH 3.0, the latter being similar to the values at pH 2.0 in the presence of sodium ions. δ values at pH 4.0 to 6.0 are $\approx$40-60° and at pH 3.0 are $\approx$20-30°. The order of diminished effect of lead ions in terms of altering ε_l, κ, $\omega\kappa$, and tanδ with change in the pH of the subphase solution, follow exactly the same order of effect as was observed in Π, $\delta\Delta$ and to some extent ΔV (Figures 12, 34, and Tables IV, XV). Moreover, despite the uncertainties of ε_l relative to ε_{st}, Pb^{2+} clearly has the most dramatic effects on the viscoelastic parameters relative to the rest of the ions.

The very low surface viscosity values observed for Cd^{2+} are somewhat surprising since the earlier results had shown the effects of this ion to be intermediate between Pb^{2+} and the other divalent cations. This appears to be a particularly interesting observation since the surface elasticity values for Cd^{2+} are still intermediate between Pb^{2+} and the other divalent cations. Clearly, Cd^{2+} can produce a fairly elastic monolayer that has an unusually short relaxation time, while the extreme effectiveness of Pb^{2+} in forming condensed monolayers leads to a highly elastic monolayer with significantly longer relaxation times. Two questions arise from this observation: 1) why does Cd^{2+} produce such low surface viscosities while enhancing surface elasticities, whereas Pb^{2+} exhibits marked increases in both surface elasticity and surface viscosity, and 2) is this lower viscosity with higher elasticity important in establishing Cd^{2+} as a promoter of optimal fatty acid LB film formation? In essence, is the key to LB film formation the need to have a critical level of elasticity along with a sufficiently short relaxation time to overcome mechanical stresses?

With regard to the first question, it has been shown that fatty acid LB films formed from aqueous subphases in the presence of these ions at pH 6.0 are 100% associatted with Pb^{2+} and only about 75% with Cd^{2+} (Kobayashi et al., 1988). Therefore, with Cd^{2+} in the monolayer state, likewise, some significant proportion of the fatty acids may still exist in the unionized state, whereas in the presence of Pb^{2+} the fatty acids are completely ionized and associated with Pb^{2+}. Thus with Cd^{2+} very close packing may occur so as to produce higher surface elasticity, but the mixture of unionized and salt forms of the fatty acid may provide the means for more rapid realignment of the molecules when the monolayer is stressed.

To answer the second question it will be necessary to directly compare stearic acid LB films prepared under these conditions using Pb^{2+} and Cd^{2+}, and to see whether the overall order and perfection of such films is greater with Cd^{2+} than with Pb^{2+} because of the differences in the surface viscosity.

CONCLUSIONS

1. The effect of various metal ions with stearic and arachidic acid monolayers at various pH values and concentrations of divalent metal ions were studied using surface pressure, surface potential and surface ellipsometric measurements. In the range of pH 5.0 to 6.0 the extent of ionization of the fatty acids studied was sufficient for all the divalent cations to interact with the fatty acid and to alter its monolayer properties significantly. Such effects due to Pb^{2+} and Cd^{2+} were found to be distinctly different than the other divalent ions, depending on the concentration and the pH of the subphase solution. In particular, whereas with other divalent ions effects occur between pH 5.0 and 6.0, effects with Pb^{2+} were noted at pH values as low as 4.0 and at concentrations as low as 0.0005mM where the stoichiometry of the interaction approaches 1:1 between the fatty acid and lead ions.

2. Alkaline earth metals; magnesium, calcium, and barium, appear to interact with fatty acids electrostatically by screening the negative charges, as demonstrated by an increase in the surface potential as the concentration of these ions in the subphase is increased. Cadmium, cobalt, and lead ions significantly decrease surface potential and appear to interact more strongly via covalent bonding. Changing the type of anion present and possibly causing complexes to form with Pb^{2+} and Cd^{2+} appears to reduce the interaction between these ions and the fatty acid monolayer, as

demonstrated by a positive shift in the surface potential. In contrast, in the presence of alkaline earth metal ions no counter ion effects were noted.

3. Surface ellipsometric experiments were sensitive in determining the extent and the specificity of fatty acid-divalent ion interactions as a function of pH and concentration. These measurement correlate strongly with the surface potential measurements with regard to divalent ion effects.

4. The much greater degree of condensation of the monolayer in the presence of Pb^{2+} and Cd^{2+} relative to other divalent ions and the very significant changes in $\delta\Delta$ and ΔV at very low Pb^{2+} concentrations, suggest a much tighter packing in the the monolayer where a 1:1 stoichiometry, rather than 1:2, between these ions and fatty acids is possible. The stability constants from the potentiometric titrations support the 1:1 stoichiometry for Pb^{2+} and Cd^{2+}. A more non-specific 1:2 relationship between the fatty acids and alkaline earth ions appears more likely.

5. Electrocapillary wave diffraction measurements of stearic acid spread as monolayer allowed estimation of the viscoelastic parameters in the presence of various metal ions and at various pH values. Pb^{2+} and Cd^{2+} were found to be significantly different than the other ions in altering the viscoelastic properties of the monolayer. Whereas, Pb^{2+} increased substantially both surface elasticity, ε_l, and surface viscosity, κ, relative

to Na^+, Cd^{2+} increased ε_l and decreased κ. All the other divalent ions slightly increased both ε_l and κ. Despite uncertainties of dynamic elasticity, ε_l, relative to static elasticity, ε_{st}, Pb^{2+} clearly has the most dramatic effect on the viscoelastic parameters from pH 4.0 to 6.0. This is in agreement with the effect of this ion at this pH range on the surface properties measured with the other techniques. The measured values of κ with Cd^{2+} were most surprising and may have important implications for the formation of stable LB films.

REFERENCES

Abraham, B.M., Ketterson, J.B., Miyano, K., and Kueny, A., Shear rigidity of stearic acid monolayers on water, *J. Chem. Phys.*, **75**, 3137-3141 (1981)

Adamson, A.W., *Physical Chemistry of Surfaces*, John Wiley & Sons, Inc., New York, 4th Edn, 1982.

Azzam, R.M.A. and Bashara, N.M., *Ellipsometry and Polarized Light*, North Holland, New York, 1977.

Baes, C.F. Jr. and Mesmer, R.E., *The Hydrolysis of Cations*, John Wiley & Sons, Inc., New York, 1976.

Bagg, J., Abramson, M.B., Fichman, M., Haber, M.D., and Gregor, H.P., Composition of stearic acid monolayers from calcium-containing substrates, *J. Am. Chem. Soc.*, **86**, 2759-2763 (1964)

Bagg, J., Haber, M.D., and Gregor, H.P., Composition of stearic and behenic acid monolayers from sodium-containing substrates, *J. Colloid Interface Sci.*, **22**, 138-143 (1966)

Barraud, A., Rosilio, C., and Ruaudel-Teixier, A., Polymerized monomolecular layers: A new class of ultrathin resins for microlithography, *Thin Solid Films*, **68**, 91-98 (1980)

Barraud, A., L.B. films: A 2D approach for molecular electronics, *J. Chim. Phys.*, **85**, 1121-1123 (1988)

Berejich, N. In *New Methods of Polymer Characterization*, Ke, B., Ed., Interscience, New York, 1964.

Berg, J.M. and Claesson, P.M., Forces between carboxylic acid layers in divalent solutions, *Thin Solid Films*, **178**, 261-270 (1989)

Betts, J.J., and Pethica, B.A., The ionization characteristics of monolayers of weak acid and bases, *Trans. Faraday Soc.*, **52**, 1581-1589 (1956)

Biddle, M.B., Rickert, S.E., and Lando, J.B., Constructing a processing window for a Langmuir-Blodgett film, *Thin Solid Films*, **134**, 121-134 (1985)

Blodgett, K.B., Monomolecular films of fatty acids on glass, *J. Am. Chem. Soc.*, **56**, 495 (1934)

Blodgett, K.B., Films built by depositing successive monomolecular layers on a solid surface, *J. Am. Chem. Soc.*, **57**, 1007-1022 (1935).

Blodgett, K.B., and Langmuir, I., Built-up films of barium stearate and their optical properties, *Phys. Rev.*, **51**, 964-982 (1937)

Blum. L., Theory of electrified interfaces, *J. Phys. Chem.*, **81**, 136-147 (1977)

Bolt, G.H., Analysis of the validity of the Gouy-Chapman theory of the electric double layer, *J.Colloid Interface Sci.*, **10**, 206-218 (1955)

Bootsma, G.A., and Meyer, F., Ellipsometry in the sub-monolayer region, *Surf. Sci.*, **14**, 52-76 (1968)

Boyd, E. and Harkins, Molecular interactions in monolayers: Viscosity of two dimensional liquids and plastic solids. V. Long chain fatty acids, *J. Am. Chem. Soc.*, **61**, 1188-1195 (1939)

Buhaenko, M.R., Goodwin, J.W., Richardson, R.M., and Daniel, M.F, The influence of shear viscosity of spread monolayers on the Langmuir-Blodgett process, *Thin Solid Films*, , **134**, 217-226 (1985)

Buhaenko, M.R., Goodwin, J.W., and Richardson, R.M., Surface rheology of spread monolayers, *Thin Solid Films*, , **159**, 171-189 (1988)

Buhaenko, M.R., Grundy, M.J., Richardson, R.M., and Roser, S.J., Structure and temperature dependence of fatty acid Langmuir-Blodgett films studied by neutron and X-ray scatterring, *Thin Solid Films*, **159**, 253-263 (1988)

Calvin, M. and Wilson, K.W., Stability of chelate compounds, *J. Am. Chem. Soc.*, **67**, 2003-2007 (1945)

Campbell, P.G.C. and Tessier, A., In *Sources and Fates of Aquatic Pollutants*, Ch. 7., Metal speciation in natural waters: Influence of environmental acidification, pp. 185-207, 1987.

Carnie, S.L., Chan, D.Y.C., Mitchel, D.J., and Ninham, B.W., The structure of electrolytes at charged surfaces: The primitive model, *J. Chem. Phys.*, **74**, 1472-1478 (1981)

Cesàro, A., Delben, F., and Paoletti, S., Interaction of divalent cations with polyuronates, *J. Chem. Soc., Faraday Trans. 1.*, **84**, 2573-2584 (1988)

Chapman, D.L., A contribution to the theory of electrocapillarity, *Phil. Mag.*, **25**, 475-481 (1913)

Chen, Y-L., Surface light scattering at the air/water and oil/water interfaces, Ph.D. Thesis, University of Wisconsin-Madison, 1986.

Chen, Y-L., Sano, M., Kawaguchi, M., Yu, H., and Zografi, G., Static and dynamic properties of pentadecanoic acid monolayers at the air-water interface, *Langmuir*, **2**, 349-354 (1986)

Cheesman, D.F. and Davies, J.T., Physiochemical and biological aspects of proteins at interfaces, *Adv. Protein Chem.*, **9**, 439-501 (1954)

Datta, S.P. and Rabin, B.R., The chelation of metal ions by dipeptides and related substances. Part 1. Cobaltous and manganous complexes, *Trans. Faraday Soc.*, **52**, 1117-1122 (1956)

Davies, J.T. and Rideal, E.K., *Interfacial Phenomena*, Academic Press, New York, 2nd Edn. 1963.

De Feijter. J.A., Benjamins, J., and Veer, F.A., Ellipsometry as a tool to study the adsorption behavior of synthetic and biopolymers at the air-water interface, *Biopolymers*, **17**, 1759-1772 (1978)

Demchak, R.J. and Fort, T.Jr., Surface dipole moments of close packed un-ionized monolayers at the air-water interface, *J. Colloid Interface Sci.*, **46**, 191-202 (1974)

den Engelsen, D. and de Koning, B., Ellipsometric study of organic monolayers, Part 1.-Condensed monolayers, *J. Chem. Soc. Faraday 1.*, **70**, 1603-1614 (1974a)

den Engelsen, D. and de Koning, B., Ellipsometry of spread monolayers, Part 2.-Coloured systems: Chlorophyll a, carotenoic acid, rhodamine 6G, and a cyanine dye, *J. Chem. Soc. Faraday 1.*, **70**, 2100-2112 (1974b)

Dervichian, D.G. in *Surface Phenomena in Chemistry and Biology*, Danielli, J.F., Pankhurst, K.G.A., Riddiford, A.C., Eds., Pergamon, New York, 1958.

Devaux, H., Les lames d'huile étendues sur l'eau et sur le mercure, *Revue Général des Sciences*, février 1913.

Drexhage, K.H., Zwick, M.M., and Kuhn, H., Sensibilisierte Fluoreszenz nach Strahlungslosem Energieübergang durch dünne Schichten, *Ber. Bunsenges. Phys. Chem.*, **67**, 62-74 (1963)

Drude, P., Ueber Oberflächenschichten. I. Theil, *Ann. Physik*, **272**, 532-560 (1889a)

Drude, P., Ueber Oberflächenschichten. II. Theil, *Ann. Physik*, **272**, 865-897 (1889b)

Egert-Charlier, M., Sanson, A., Ptak, M., and Bouloussa, O., Ionisation of fatty acids at the lipid-water interface, *FEBS Lett.*, **89**, 313-316 (1978)

Elliassen, J.D., Ph.D. Dissertation, University of Minnesota, Minneapolis, MN, 1963.

Ellis, J.W. and Pauley, J.L., The infrared determination of the composition of stearic acid multilayers deposited from salt substrata of varying pH, *J. Colloid Sci.*, **19**, 755-764 (1964)

Enever, R.P. and Pilpel, N., Reaction between stearic acid and caclium ions at the air-water interface using surface viscometry, *Trans. Faraday Soc.*, **63**, 781-792 (1967)

Ferry, J.D., *Viscoelastic Properties of Polymers*, 2nd Ed., John Wiley & Sons, Inc., New York, 2nd Edn., 1970.

Franklin, B., Of the stilling of waves by means of oil, *Phil. Trans. Roy. Soc. London*, **64**, 445-460 (1774)

Gaines, G.L.Jr., *Insoluble Monolayers at Liquid-Gas Interfaces*, Wiley-Interscience, New York, 1st Edn., 1966.

Gaines, G.L.Jr., Precise differential measurements of monolayer surface potentials, *J. Colloid Interface Sci.*, **23**, 292-294 (1967)

Gaines, G.L.Jr., On the use of filter paper Wilhelmy plates with insoluble monolayers, *J. Colloid Interface Sci.*, **62**, 191-192 (1977)

Gaines, G.L.Jr., From monolayer to multilayer: Some unanswered questions, *Thin Solid Films*, **68**, 1-5 (1980)

Gaines, G.L.Jr., On the history of Langmuir-Blodgett films, *Thin Solid Films*, **99**, ix-xiii (1983)

Gibbs, J.W., *Collected Works*, Longmans, Green and Co., New York, Vol. I, p. 301, 1928.

Giles, C.H. and Forrester, S.D., The origins of surface film balance: Studies in the early history of surface chemistry, part 3, *Chem. & Ind.*, 43-53 (1971)

Goodrich, F.C., On the damping of water waves by monomolecular films, *J. Phys. Chem.*, **66**, 1858-1863 (1963)

Gordziel, S.A., Flanagan, D.R., and Swarbrick, J., Interaction of monomolecular films of biological significance with heavy metals and complexes at the air-water interface, *J. Colloid Interface Sci.*, **86**, 178-184 (1982)

Gouy, M., Sur la constitution de la charge électrique à la surface d'un électrolyte, *J. Phys. Radium*, **9**, 457-468 (1910)

Grahame, D.C., Effects of dielectric saturation upon diffuse double layer and the free energy of hydration of ions, *J. Chem. Phys.*, **18**, 903-909 (1950)

Grundy, M. J., Richardson, R.M., Roser, S.J., Penfold, J., and Ward, R.C., X-ray and neutron reflectivity from spread monolayers, *Thin Solid Films*, **159**, 43-52, (1988)

Hård, S. and Löfgren, H., Elasticity and viscosity measurements of monomolecular propyl stearate films at air-water interfaces using laser light scattering techniques, *J. Colloid Interface Sci.*, **60**, 529-539 (1977)

Hardy, W.B., The tension of composite fluid surfaces and the mechanical stability of films of fluid, *Proc. Roy. Soc.*, **A86**, 610-635 (1912)

Hardy, W.B., The influence of chemical constitution upon interfacial tension, .*Proc. Roy. Soc.*, **A87**, 303-313 (1913)

Harkins, W.D., Davies, E.C.H., and Clark, G.L., The orientation of molecules in the surface of liquids, the energy relations at surfaces, solubility, adsorption, emulsification, molecular association, and the effect of acids and bases on the interfacial tension. (Surface Energy VI), *J. Am. Chem. Soc.*, **39**, 541-596 (1917)

Hasmonay, H., Vincent, M., and Dupeyrat, M., Composition and transfer mechanism of Langmuir-Blodgett multilayers of stearates, *Thin Solid Films*, **68**, 21-31 (1980)

Henderson, D. and Blum, L., Some exact results and the application of the mean spherical approximation to charged hard spheres near a charged hard wall, *J. Chem. Phys.*, **69**, 5441-5449 (1978)

Hiemenz, P., *Principles of Colloid and Surface Chemistry*, Marcel Dekker, Inc., New York, 2nd Edn. 1986.

Högfeldt, E., In *Stability Constants of Metal-Ion Complexes, Part A: Inorganic Ligands*, IUPAC Chemical Data Series, No. 21, Pergamon Press: Oxford, 1982.

Irving, H.M. and Rossotti, H.S., Methods for computing successive stability constants from experimental formation curves, *J. Chem. Soc.* 3397-3405 (1953)

Irving, H.M. and Rossotti, H.S., The calculation of formation curves of metal complexes from pH titration curves, *J. Chem. Soc.* 2904-2910 (1954)

Irving, H.M. and Rossotti, H.S., The stabilities of some metal complexes of 8-hydroxylquinoline and related substances, *J. Chem. Soc.* 2910-2918 (1954)

Itaya, A., Van der Auweraer, M., and De Schryver, F.C., Preparation of monolayers and stacked layers of 1-octadecanethiol, *Langmuir*, **5**, 1123-1126 (1989)

Ito, K., Sauer, B.B., Skarlupka, R.J., Sano, M., and Yu, H., Dynamic interfacial properties of poly(ethylene oxide and polystyrene at Toluene/water interface, *Langmuir*, In press (1990)

Jackson, J.D., In *Classical Thermodynamics*, Wiley, New York, pp. 123-125, 1962.

Jarvis, N.L., Surface viscosity of monomolecular films of long chain aliphatic amides, amines, alcohols, and carboxylic acids, *J. Phys. Chem.*, **69**, 1789-1797 (1965)

Joly, M., In *Recent Progress in Surface Science*, Danielli, J.F., Pankhurst, K.G.A., and Riddiford, A.C., Eds., Academic Press, New York, **2**, 1-50 (1964)

Joly, M., In *Surface and Colloid Science*, Matijevic, E., Ed., Wiley, New York, **5**, 80-188 (1972)

Joos, P., Effect of the pH on the collapse pressure of fatty acid monolayers evaluation of the surface dissociation constant, *Bull. Soc. Chim. Belges*, **80**, 277-281 (1971)

Karplus, M. and Porter, R.N., *Atoms and Molecules*, Benjamin Inc., Philipines, p. 374, 1976.

Kim, M.W., Sauer, B.B., Yu., H., Yazdanian, M., and Zografi, G., Ionic interactions of fatty acid monolayers studied by ellipsometry, *Langmuir*, **6**, 236-240 (1990)

Kjaer, K., Als-Nielsen, J., Helm, C.A., Tippman-Krayer, P., and Möhwald, H., An X-ray scattering study of lipid monolayers at the air-water interface and on solid supports, *Thin Solid Films*, **159**, 17-28 (1988)

Kjaer, K., Als-Nielsen, J., Helm, C.A., Tippman-Krayer, P., and Möhwald, H., Synchrotron X-ray diffraction and reflection studies of arachidic acid monolayers at the air-water interface, *J. Phys. Chem.*, **93**, 3200-3206 (1989)

Kobayashi, K., Takaoka, K., and Ochiai, S., Application of X-ray photoelectron spectroscopy and Fourier transform IR reflection absorption spectroscopy to studies of the composition of Langmuir Blodgett films, *Thin Solid Films*, **159**, 267-273 (1989)

Kohn, R., Binding of divalent cations to oligomeric fragments of pectin, *Carbohyd. Res.*, **160**, 343-353, (1987)

Kuhn, H., On possible ways of assembling simple organized systems of molecules, In *Structural Chemistry and Molecular Biology*, Rich, A., and Davidson, N., Eds., W.H. Freeman and Comp., San Francisco and London, pp. 566-572, 1968.

Kuhn, H., Spectroscopy of monolayer assemblies: Part I. Principles and applications, In *Physical Methods of Chemistry*, Weissberger and Rossiter, Eds., Vol. I, Wiley-Interscience, New York, pp. 577-650, 1972.

Kuhn, H., Present status and future prospects of Langmuir-Blodgett film research, *Thin Solid Films*, **178**, 1-16 (1989)

Langmuir, I., The constitution and fundamental properties of solids and liquids. II. Liquids. , *J. Am. Chem. Soc.*, **39**, 1848-1906 (1917)

Langmuir, I., The mechanism of the surface phenomena of flotation, *Trans. Farad. Soc.*, **15**, 62-74 (1920)

Langmuir, I. and Schaefer, V.J., Composition of fatty acid films on water containing calcium and barium salts, *J. Am. Chem. Soc.*, **58**, 284-287 (1936)

Langmuir, I. and Schaefer, V.J., The effect of dissolved salts on insoluble monolayers, *J. Am. Chem. Soc.*, **59**, 2400-2414 (1937)

Laxhuber, L. and Möhwald, H., Secondary ion mass spectroscopy of the selective ion binding to fatty acid monolayers, *Colloids Surfaces*, **10**, 225-231, (1984)

Leiderer, P., Charged interface of 3He-4He mixtures. Softening of interfacial waves, *Phys. Rev. B.*, **20**, 4511-4517 (1979)

Levine, S. and Outhwaite, C.W., Comparisons of the aqueous electric double layer at a charged plane interface, *J. Chem. Soc. Faraday Trans. II*, **74**, 1670-1689 (1978)

Lord Rayleigh, Measurement of the amount of oil necessary in order to check the motions of camphor upon water, *Proc. Roy. Soc.*, **47**, 364-367 (1890)

Lord Rayleigh, The tension of contaminated water-surfaces, *Phil. Mag.*, **48**, 331-337 (1899)

Lucassen, J. and Hansen, R.S., Damping of waves on monolayer-covered surfaces, I. Systems with negligible surface dilational viscosity, *J. Colloid Interface Sci.*, **22**, 32-44 (1966)

Lucassen, J., Longitudinal capillary waves, *Trans. Faraday Soc.*, **64**, 2221-2235 (1968)

Lucassen-Reynders, E.H. and Lucassen, J., Properties of capillary waves, *Adv. Colloid Interface Sci.*, **2**, 347-395 (1969)

Lucassen-Reynders, E.H., In *Anionic Surfactants*, Lucassen-Reynders, E.H., Ed., Marcell Decker, New York, **11**, 173-216 (1981)

Magerlein, J.H. and Sanders, T.M.Jr., Surface tension of He^4 near T_λ, *Phys. Rev. Lett.*, **36**, 258-261 (1976)

Mann, J.A., Jr. and Hansen, R.S., Propagation characteristics of capillary ripples, II. Instrumentation for measurement of ripple velocity and amplitude, *J. Colloid Sci.*, **18**, 757-771 (1968)

Mann, J.A, Jr, Dynamics, structure, and function of interfacial regions, *Langmuir*, **1**, 10-23 (1985)

Mann, J.A., Tjatjopoulos, G.J., Azzam, M.J., Boggs, K.E., Robinson, K.M., and Sanders, J.N., Pre-Langmuir-Blodgett monolayers, *Thin Solid Films*, **152**, 29-48 (1987)

Marcelin, A., Épaisseur des couches très minces à la surface de l'eau (huiles, résines et camphre), *Ann. Phys.*, **1**, 19-34 (1914)

Matsubara, A., Martsumara, R., and Kimisuka, H., A study of the interaction between the stearic acid monolayers and the calcium ions by the radiotracer method, *Bull. Chem. Soc. Japan* , **38**, 369-373 (1965)

Mingins, J. and Owens, N.F., Experimental considerations in insoluble spread monolayers, *Thin Solid Films*, **152**, 9-28 (1987)

Miyano, J.D., Abraham, B.M., Xu, S.Q., and Ketterson, J.B., The effect of heavy metallic ions on fatty acid monolayers at the air-water interface, *J. Chem. Phys.*, **77**, 2190-2192 (1982)

Miyano, K., Abraham, B.M., Ting, L., and Wasan, D.T., Longitudinal surface waves for the study of dynamic properties of surfactant systems, *J. Colloid Interface Sci.*, **92**, 297-302 (1983)

Motomura, K. and Matuura, R., Physiochemical studies of stearic acid monolayer-aluminum ion interaction. II. The surface viscoelasticity, *Bull. Chem. Soc. Japan*, **35**, 289-295 (1962)

Myers, R.J. and Harkins, W.D., Effect of traces of metalic ions on films at interfaces and on the surface of water, *Nature*, **139**, 367-368 (1937)

Mysels, K.J., *Introduction to Colloid Chemistry*, Interscience, Inc. Fourth Ed., pp. 372-375, 1967.

Nagarajan, N., Webb, W.W., and Widom, B., Surface tension of a two component liquid mixture near its crtical solution point, *J. Chem. Phys.*, **77**, 5771-5783 (1982)

Neuman, R.D., Calcium binding in stearic acid monomolecular films, *J. Colloid Interface Sci.*, **53**, 161-171 (1975)

Okahata, Y., Tsuruta, T., Ijiro, K., and Ariga, K., Langmuir-Blodgett films of an enzyme-lipid complex for sensor membranes, *Langmuir*, **4**, 1373-1375 (1988)

Oliveira, O.N., Taylor, D.M., Lewis, T.J., Salvagno, S., and Sterling, C.J.M., Estimation of group dipole moments from surface potential measurements on Langmuir monolayers, *J. Chem. Soc., Faraday Trans. 1.*, **85**, 1009-1018 (1989)

Outka, D.A., Stöhr, J., Rabe, J.P., Swalen, J.D., and Rotermund, H.H., Orientation of arachidic chains in Langmuir-Blodgett monolayers on Si(111), *Phys. Rev. Lett.*, **59**, 1321-1324 (1987)

Pallas, N.R. and Pethica, B.A., The surface tension of water, *Colloids Surfaces*, **6**, 221-227 (1983)

Pallas, N.R. and Pethica, B.A., The surface tension of water, *Colloids Surfaces*, **36**, 369-372 (1989)

Pashley, R.M. and Israelachvili, J.N., DLVO and hydration forces between mica surfaces in Mg^{2+}, Ca^{2+}, Sr^{2+}, and Ba^{2+} chloride solutions, *J. Colloid Interface Sci.*, **97** 446-455 (1984)

Pearson, R.G., Hard and soft acid and bases, *J. Am. Chem. Soc.* **85**, 3533-3539 (1963)

Pearson, R.G., Hard and soft acids and bases, *Chem. Britain*, **3**, 103-107 (1967)

Pethica, B.A., Experimental criteria for monolayer studies in relation to the formation of Langmuir-Blodgett films, *Thin Solid Films*, **152**, 3-9 (1987)

Petrov, J.G, Kuleff, I., and Platikanov, D., Neutron activation analysis of metal ions in Langmuir-Blodgett multilayers of arachidic acid, *J. Colloid Interface Sci.*, **88**, 29-35 (1982)

Pilpel, N. and Enever, R.P., Reaction between stearic acid and caclium ions at the air-water interface using surface viscometry, Part 3.-Mechanism, *Trans. Faraday Soc.*, **64**, 231-237 (1968)

Pockels, A., Surface tension, *Nature*, **43**, 437-439 (1891)

Rabe, J.P., Swalen, J.D., Outka, D.A., and Stöhr, J., Near-edge X-ray absorption fine structure studies of oriented molecular chains in polyethylene and Langmuir-Blodgett monolayers on Si(111), *Thin Solid Films*, **159**, 275-283 (1988)

Rasing, Th., Hsuing, H., Shen, Y.R., and Kim, M.W., Ellipsometry of two dimensional phase transitions, *Physical Rev. A.*, **37**, 2732-2735 (1988)

Roberts, G.G., Transducer and other applications of Langmuir-Blodgett films, *Sensor and Actuators*, **4**, 131-145 (1983)

Roberts, G.G., An applied science perspective of Langmuir-Blodgett films, *Adv. Phys.*, **34**,475-512 (1985)

Ruaudel-Teixier, Leloup, J., and Barraud, A., Insertion compounds in LB films, *Mol. Cryst. Liq. Cryst.*, **134**, 347-354 (1986)

Sano, M., Kawaguchi, M., Chen, Y-L, Skarlupka, R.J., Chang, T., Zografi, G., and Yu, H., Technique of surface-wave scattering and calibration with simple liquids, *Rev. Sci. Instrum.*, **57**, 1158-1162 (1986)

Sano, M., Surface light scattering and its application to polymer monolayers, Ph.D. Thesis, University of Wisconsin-Madison, 1987.

Sauer, B.B., Chen, Y-L, Zografi, G., and Yu, H, Static and dynamic interfacial tensions of a phospholipid monolayer at the oil/water interface: Dipalmitoylphosphatidylcholine at heptane/water, *Langmuir*, **2**, 683-685 (1986)

Sauer, B.B., Yu, H., Yazdanian, M., Zografi, G., and Kim, M.W., An ellipsometric study of polymer monolayers at the air/water interface, *Macromolecules*, **22**, 2332-2337 (1989)

Schulman, H., and Hughes, A.H., On the surface potential of unimolecular films of long chain fatty acids. Part IV.- The effect of the underlying solution and transition phenomena in the film., *Proc. Roy. Soc. London, Ser. A.*, **138**, 436-450 (1932)

Shutt, J.D. and Rickert, S.E., Poly(diacetylene) salts as thin-film dielectrics in metal-Langmuir film-semiconductor devices, *Langmuir*, **3**, 460-467 (1987)

Sillen, L.G. and Martell, A.E., In *Stability Constants of Metal-Ion Complexes*, Supplement no. 1. Special Pub. No. 25, The Chemical Society: London, 1971.

Sims, B. and Zografi, G., Time dependent behavior of insoluble monomolecular films: Fatty acids and some drivatives, *J. Colloid Interface Sci.*, **41**, 35-46 (1972)

Skarlupka, R.J., Polymer/polymer interfacial dynamics by electrocapillary waves, Ph.D. Thesis, University of Wisconsin-Madison, 1990.

Sohl, C.H., Miyano, K., and Ketterson, J.B., Novel technique for dynamic surface tension and viscosity measurements at liquid/gas interfaces, *Rev. Sci. Instrum.*, **49**, 1464-1469 (1978)

Spink, J.A. and Sanders, J.V., Soap formation in monomolecular films on aqueous solutions, *Trans. Faraday Soc.*, **51**, 1154-1165 (1955)

Stenvot, C. and Langevin, D., Study of viscoelasticity of soluble monolayers using analysis of propagation of excited capillary waves, *Langmuir*, **4**, 1179-1183 (1988)

Swalen, J.D., Structure of Langmuir-Blodgett films, *Thin solid Films*, **152**, 151-154 (1987)

Tabor, D., Babylonian lecanomancy: An ancient text on the spreading of oil on water, *J. Colloid Interface Sci.*, **75**, 240-245 (1980)

Torrie, G.M. and Valleau, J.P., A Monte Carlo study of an electrical double layer, *Chem. Phys. Lett.*, **65**, 343-346 (1979)

Verwey, E.J.W. and Overbeek, J.Th.G., *Theory of the Stability of Lyophobic Colloids*, Elsevier, p. 32, Amsterdam, 1948.

Vogel, C., Corset, J., Billoudet, F., Vincent, M., and Dupeyrat, M., Proprietes de couches monomoleculaires d'acid stearique en presence de sels de Pb^{++}, ou de Ba^{++} en relation avec la composition et la

structure des multicouches de Langmuir-Blodgett *J. Chim. Phys.*, **77**, 947-951 (1980)

Vogel, C., Corset, J., and Dupeyrat, M., Etude par spectroscopie infrarouge de la structure de couches de Langmuir-Blodgett. I - Couche d'acid stearique et de stearate de plomb, *J. Chim. Phys.*, **76**, 903-908 (1979a)

Vogel, C., Corset, J., and Dupeyrat, M., Etude par spectroscopie infrarouge de la structure de couches de Langmuir-Blodgett. II - Couche de stearate de Na^+, Li^+, Cd^{++}, Pb^{++}, Ba^{++} purs ou en melange avec l'acid stearique, *J. Chim. Phys.*, **76**, 909-917 (1979b)

Vogel, V., Möbius, D., Local surface potentials and electric dipole moments of lipid monolayers: Contributions of the water/lipid and the lipid/air interfaces, *J. Colloid Interface Sci.*, **126**, 408-420 (1988)

Vogel, V., Möbius, D., Resonance of transverse capillary and longitudinal waves as a tool for monolayer investigations at the air/water interface, *Langmuir*, **5**, 129-133 (1989)

Vold, R.D. and Vold, M.J., *Colloid and Interface Chemistry*, Addison-Wesley, Inc., Reading, Mass. 1983.

Wolstenholme, G.A. and Schulman, J.H., Metal-monolayer interactions in aqueous systems, Part I.-The interaction of monolayers of long chain polar compounds with metal ions in the underlying solution, *Trans. Faraday Soc.*, **46**, 475-487 (1950)

Yazdanian, M., Ionic interactions of pentadecanoic acid at the air/water interface, M.S. Thesis, University of Wisconsin-Madison, 1988.

VITA SHEET

Title of thesis	Ionic Interactions of Fatty Acid Monolayers at the Air/Water Interface
Major professor	George Zografi
Major	Pharmacy
Minor	Physical Chemistry
Name	Mehran Yazdanian
Place and date of birth	Teheran, Iran. Nov. 8, 1964
Colleges and universities: years attended and degrees	University of Wisconsin-Madison, 1982-1985, B.S. University of Wisconsin-Madison, 1986-1988, M.S. University of Wisconsin-Madison, 1988-1990, Ph.D.
Memberships in learned or honorary societies	Rho Chi and American Chemical Society.
Publications	Please see next page.
Current date	July 6, 1990

Publications

1. Yazdanian, M., "Ionic Interactions of Pentadecanoic Acid at the Air/Water Interface", M.S. Thesis, University of Wisconsin-Madison, 1988.

2. Sauer, B.B., Yu, H., Yazdanian, M., Zografi, G., and Kim, M.W., "An Ellipsometric Study of Polymer Monolayers at the Air/Water Interface.", *Macromolecules* **22**, 2332-2337 (1989)

3. Kim, M.W., Sauer, B.B., Yu, H., Yazdanian, M.,and Zografi, G., "Ionic Interactions of Fatty Acid Monolayers Studied by Ellipsometry", *Langmuir*, **6**, 236-240 (1990)

4. Kim, M.W., Sauer, B.B., Yu, H., Yazdanian, M.,and Zografi, G., "Influence of Cationic Interactions on Fatty Acid Monolayers Studied by Ellipsometry", *Mat. Res. Soc. Symp. Proc.*, **177**, 405-410 (1990)

5. Yazdanian, M., Yu, H., Zografi, G.,"Ionic Interactions of Fatty Acids at the Air/Water interface", *Langmuir*, **6**, 1093-1098 (1990)